AN EPIFLUORESCENCE MICROSCOPIC SURFACE BALANCE TO OBSERVE MONOLAYERS AT THE AIR-WATER INTERFACE

KAUSHIK NAG

AN EPIFLUORESCENCE MICROSCOPIC SURFACE BALANCE TO OBSERVE MONOLAYERS AT THE AIR - WATER INTERFACE.

by

Kaushik Nag

A Thesis submitted in partial fulfilment
of the requirement for the degree of
Master of Science

Department of Biochemistry,
Memorial University of Newfoundland,
St. John's, Newfoundland A1B 3X9.

ISBN 0-315-65366-3

ABSTRACT

The details of the design and construction of an epifluorescence microscopic surface balance and some preliminary observations on lipid monomolecular layers performed using this balance are discussed. The balance consists of a Teflon trough with a computer - controlled movable barrier mounted on a vibration reducing platform. The balance is equipped with an epifluorescence microscopic attachment by which visual observation of fluorescent probes in the monolayer is possible. Barrier movement can be utilized to give monolayer compression and expansion velocity from 20 mm^2/sec up to 600 mm^2/sec. A Wilhelmy dipping plate connected to a force transducer is used to measure surface tension in the monolayer during compression and expansion. The epifluorescence microscope is coupled to a charge couple device in tandem with a microchannel plate which permits observation of the low light level fluorescence from the monolayer. Images of the monolayer under compression were visualized, stored, digitized and processed using a video unit and operator interactive software.

Using the balance preliminary studies of phase behaviour have been performed for monolayers of dipalmitoyl phosphatidylcholine (DPPC) and other lipids. The phase changes were observed by incorporating 1 mol% of a fluorescent probe,

NBD-PC, into the lipid forming the monolayer. This probe had no appreciable effect on the isotherms and surface tension properties of DPPC in monolayers. DPPC was observed to undergo a number of phase transitions when compressed in monolayers. The liquid - expanded to liquid - condensed phase transition was visualized as the formation of dark patches (domains) from a fluorescent background. The domains increased in average size from 100 μ^2 to 1500 μ^2 in a nonlinear manner as a function of area occupied per molecule of the DPPC, when monolayers were compressed at a rate of 20 mm^2/sec. The size, shape and growth of these domains were quantitatively characterized and found to be dependent on compression rates. At a fast speed of compression (4 $Å^2$/molecule/sec) the domains were smaller in size, more irregularly shaped, and unimodally distributed. At a slow compression speed (0.13 $Å^2$/molecule/sec) the domains were larger in size and more regular in shape. The shapes of the domains were found to change dramatically when a small amount (2 mol %) of cholesterol was incorporated in the monolayer. No domain formation was observed in monolayers for lipids with one or two unsaturated chains.

ACKNOWLEDGEMENT

I would like to extend my sincerest gratitude to my supervisor, Dr.K.M.W.Keough, for his patience, supervision and encouragement during the course of this work.

I am extremely grateful to Dr. N.H. Rich for the initial designing and help in construction of the surface balance, and to Mr. C. Boland for writing the programmes needed to control the instrument. I would also like to extend my sincerest thanks to Dr. D. Pink, St.Francis Xavier University, Nova Scotia for suggesting a method for image analysis and to Dr. P. Davis for constant encouragement, periodical moral boosts and in helpful comments in revision of the thesis.

I appreciate the help received from the Technical Services, MUN especially from Mr. B.Parson, D.Fillier and G.Brown, in construction of the various parts of the instrument. I am specially indebted to Mr. R. Ficken of the Biology department of MUN for initial help in photography and experimentation with different methods of image acquisition. I would also like to thank Dr.M. Morrow of the Physics department, MUN for acquiring the video camera.

I am extremely grateful to my friend Doreen and to Dr. S. Mookerjea for constant motivation and moral support during the course of this work. Finally I would like to express my appreciation to School of Graduate Studies for financial support

in the form of a fellowship, and W.Heckle for some valuable advice concerning visualization of the monolayers.

TABLE OF CONTENTS PAGE

LIST OF ABBREVIATIONS

Å - Angstrom

AOI - Area Of Interest

ARDS - Adult respiratory distress syndrome

DPPC - Dipalmitoylphosphatidylcholine

DMPA - Dimyristoylphosphatidic acid

DOPC - Dioleoylphosphatidylcholine

EMSB - Epifluorescence Microscopic Surface Balance

FT-IR - Fourier Transform Infrared spectroscopy

γ - surface tension

LE/LC - liquid expanded to liquid condensed

MHz - mega Hertz

mN/m - milliNewton per meter

μ - micrometer

NBD - 7- Nitro - 2-1,3- benzodiazol - 4 - yl

π - surface pressure

PC - phosphatidylcholine

PE - phosphatidylethanolamine

PG - phosphatidylglycerol

PI - phosphatidylinositol

RDS - Respiratory Distress Syndrome

SAM - Surface active material

SOPC - 1-stearoyl,2-oleoyl phosphatidylcholine

T_c - gel to liquid - crystalline transition temperature of bilayers

TLC - Thin layer chromatography

LIST OF FIGURES

INTRODUCTION

I. Surface active monolayer

Surface tension of a fluid can be considered as a force acting per unit length at its surface. The molecules at the gas-fluid interface compared to the ones in the bulk phase have a non compensated attractive force acting on them directed towards the bulk phase. This imbalance of forces at the interface causes the surface of the fluid to behave like a stretched film under tension. The force exerted can be measured by dipping an inert thin metal plate into the fluid interface. A clean surface of water would register a force acting on the plate. This force, measured per unit length in milliNewtons/meter or dynes/centimetre, is known as surface tension. At 37°C the surface tension of water is observed to be 70 mN/m.

A large number of biological and synthetic amphiphilic molecules when spread on a clean water surface spontaneously form a monomolecular layer of thickness of several Angstrom units These monolayers can counteract the tensile forces acting on the fluid interface and thus reduce the surface tension. The amphiphilic molecules range from biological membrane constituents such as phospholipids to fatty acids, certain proteins and a number of other organic species.

During the early part of this century an instrumental apparatus, today known as a surface balance, was devised by Langmuir by which the physical properties of monolayers could be studied (reviewed by Gaines 1966). The properties of monolayers were studied by compressing the monolayer laterally at the interface and by monitoring the surface pressure exerted on it (Gaines 1966, Adam 1968). The surface pressure is defined to be the value of the difference between the surface tension of the clean surface of the subphase and that of the interface with the monolayer. Several fatty acids were used to study the area occupied by the molecules at the interface and how this would affect the surface pressure during a decrease of monolayer area (Gaines 1966). Surface balances have been modified in the last five decades, though the basic principle of construction remains the same. The balance consists of a trough, made out of chemically inert material, in which the fluid or water is contained. Using a dipping plate in combination with a force measuring device the surface tension is measured. Other techniques using different types of floats and threads on the surface have been used to measure the surface pressure. A monolayer of the material to be studied is spread at the surface from a solution of known concentration of the substance. The solution is made in a highly evaporative solvent. The evaporative solvent is chosen for quick deposition of the material by spreading the solution at the surface. After evaporation of the solvent the monolayer can be compressed and

the surface pressure monitored as a function of molecular area (Gaines 1966, Adams 1968).

II. Pulmonary Surfactant

A number of workers have shown that the type II cells of the alveoli secrete a surface active material to the alveolar air-fluid interface (Buckingham 1962, King 1972, Clements 1976). The surface active material is found to consist of a number of lipid species and some proteins (King 1972, Hawgood 1985). The surfactant extracted from mammalian lung by lavaging the alveolar fluid was found to consist of about 74 % phosphatidylcholine (PC), 10% phosphatidylglycerol (PG), 5% lyso lecithin and sphingomyelin, 4% phosphatidylethanolamine and 2% phosphatidylserine in % of total phosphorous assayed (King 1972, Van Golde 1988). Some hydrophobic proteins, referred to as SP-B and SP-C (Suzuki 1982), and a hydrophillic protein SP-A were also found later by other workers (King 1973). It has been suggested that these lipids in conjunction with some of the proteins act as the pulmonary surface active material (King 1972, Goerke 1974, Suzuki 1982). The surface active material collectively known as pulmonary surfactant has been suggested to form a monomolecular layer at the air - alveolar fluid interface (Pattle 1960). Figure 1 shows a diagram outlining the process of surfactant secretion by type II cell to form a monolayer at the air alveolar interface. The monolayer of surfactant undergoing compression during expiration reduces the surface tension of the alveolar

Figure 1. Diagrammatic representation of possible route of secretion of pulmonary surfactant to the air alveolar interface indicated by the arrows. The surfactant is synthesized and packaged into lamellar bodies (LB), secreted to the alveolar fluid as tubular myelin (TM) and finally adsorbed to the air alveolar interface as a monolayer. (redrawn from Wright 1988)

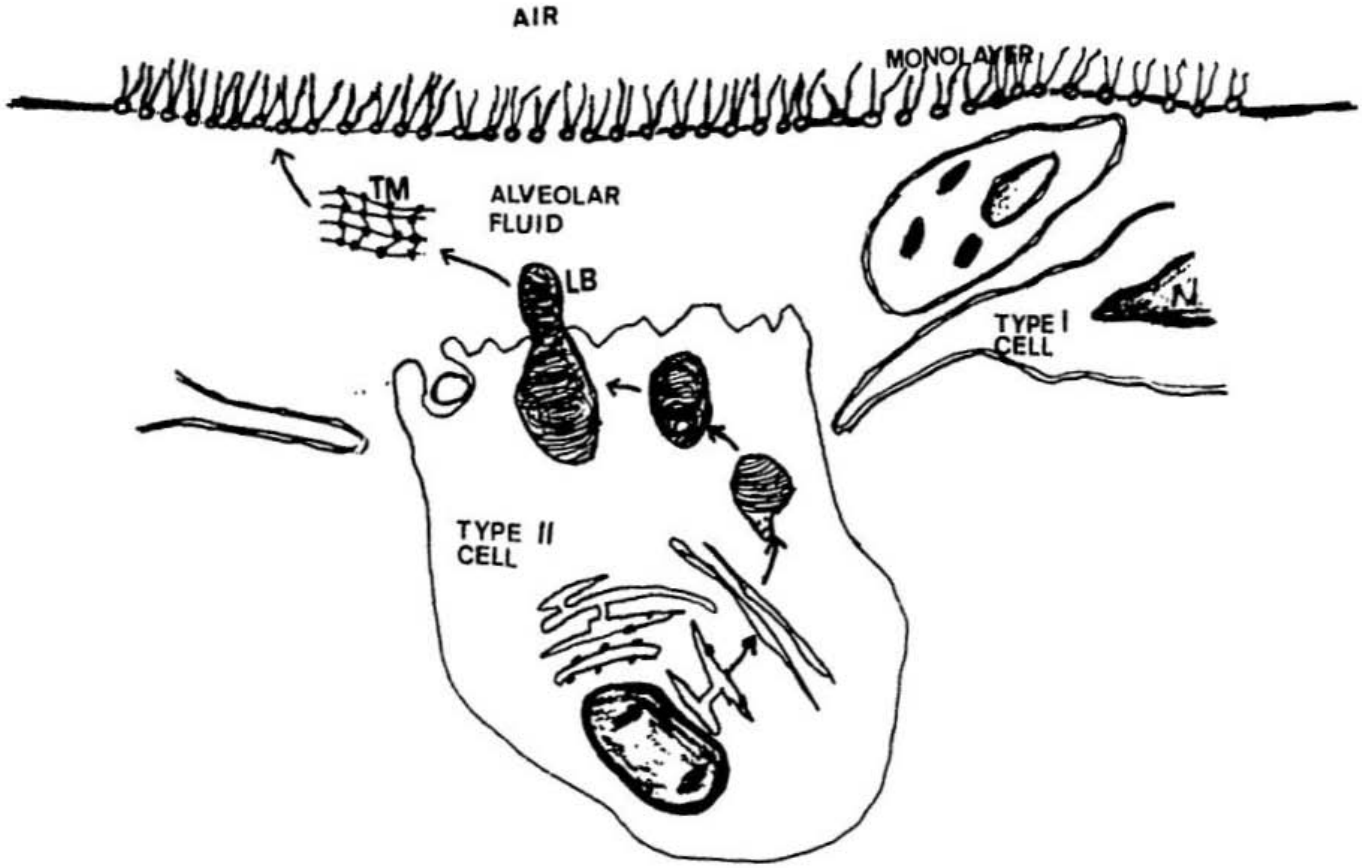

Redrawn from
Wright 1988

fluid (Schurch 1978, Goerke 1974). It was found later that at physiological temperature of 37°C the surface tension at the air alveolar surface at maximal expiration is about 1mN/m (Schurch 1984). This decrease of surface tension in combination with the tensile property of the alveoli reduces lung compliance and thus the work of breathing (Scarpelli 1988).

The major component of the surfactant (about 45% of total weight) was found to be a zwitterionic phospholipid 1,2 dipalmitoyl phosphatidylcholine [DPPC] (King 1972). This amphiphile was also found to spread in a monolayer in vitro and reduce surface tension of water to near 0 mN/m when compressed to the minimal molecular area (Galdstone 1967, Notter 1980). Direct determination of surface tension of the alveolar fluid interface at low lung volume also showed such low values (Schurch 1978). DPPC has been studied extensively in the last thirty years using surface balance techniques, and its surfactant and other biophysical properties characterised (Chapman 1967, Phillips 1968, Notter 1984). Though DPPC seems the ideal material for acting as a surfactant during the respiratory process, it cannot maintain a constant monomolecular layer during respiratory cycles. Due to the materials slow respreading and readsorption properties at the interface, loss of DPPC at the surface during the increase and decrease of alveolar interfacial area would deplete the monolayer of material. Other surfactant components such as mixed acyl chain phosphatidylglycerol, phosphatidylinositol (Notter 1980) and hydrophobic proteins SP-B

and SP-C (Suzuki 1982, Hawgood 1989) have been suggested to play an important role in surfactant monolayer homeostasis (King 1972, Notter 1980, Keough 1984). Though the physical process by which the pulmonary surfactant forms monolayers at the air-alveolar interface is not clear to date the study of its individual components *in vitro* can yield information relevant to normal pulmonary functioning (Goerke 1974, Bangham 1979, Keough 1984).

Absence of surfactant in the alveoli was shown to cause a particular syndrome during which the lungs of premature neonates collapse during cycles of breathing (Avery 1959). In neonates this condition is termed as Respiratory Distress Syndrome [RDS] (Hildebran 1979, Enhorning 1990). Another syndrome known as adult respiratory distress syndrome or ARDS is suggested to occur in adults due to leakage of some plasma proteins into the alveolar fluid causing hinderance in normal surfactant activity (Ashbaugh 1967). Medical research has been intensive in the last decade to find an artificial surface active material (SAM) which could be applied exogenously in patients suffering from RDS (Hallman 1984, Obladem 1990). It is suggested that the composition of such artificial SAM should have the properties of fast respreading and adsorption to the interface, lowering of the surface tension to about 0 mN/m of the alveolar fluid interface during maximal expiration and ability to form a stable film for a significant period of time (Clements 1976, Bachofen 1987). The material should also be easily delivered to the air-alveolar interface from an exogenous source. It is yet

not totally clear which components of SAM are responsible for these biophysical processes in vivo, but a number of clinical trials with different artificial lipid and lipid-protein mixtures have shown a certain degree of success in alleviating patients suffering from the syndrome (Fujiwara 80, Muller 1990). These findings have renewed interest in studying surfactant monolayers in vitro using versions of the classical Langmuir technique, and by current modified methods of visual observation of the monolayer. Other techniques of direct infrared spectroscopy of the monolayer at the interface (Dluhy 1989) have given a new approach to study the surface phenomena of surfactants. These techniques provide information on the molecular organization of the surfactant in the monolayer.

III. Physical properties of insoluble monolayers

Phospholipid and other amphiphilic molecules when spread at the air - water interface form a monomolecular layer, in which the hydrophobic moiety of the molecule orients itself towards the air and the hydrophilic or polar headgroup dissolves in the water (Gaines 1966). When such a molecular layer is compressed laterally the surface shows a non - linear reduction of surface tension or an increase of surface pressure in the monolayer up to the point of monolayer collapse. The surface pressure plotted against the molecular area at the relevant state

of compression and at a fixed temperature, gives indirect information about the physical state and the orientation of the molecules at the interface and is known as a pressure-area isotherm. Such plots are shown schematically in figure. 2.

Isotherms of the phospholipid, DPPC, below 41°C display a "lateral phase transition" or a disordered to an ordered state of molecular packing in the monolayer over a range of molecular areas and surface pressures (Phillips 1968, Gershfeld 1976, Albrecht 1978). As shown by the isotherm II in Figure 2 the surface pressure increases in a nonlinear manner during compression and decrease of the molecular interfacial area of the amphiphiles in the monolayer. The isotherms become horizontal at a particular molecular areas, indicating a change of physical state of the DPPC monolayer. This change of state occurs due to the change of packing and dynamics of the molecules at the interface and is termed as a "phase transition". At large molecular areas and surface pressures near 0 mN/m, the monolayer behaves like a two-dimensional gas (G in isotherm II, Fig.2) in which it is assumed the molecules are separated by large intermolecular distances. With decreasing area per molecule and increasing surface pressure the gas phase changes to a liquid - like phase. For amphiphiles such as DPPC two liquid - like phase, liquid - expanded (LE in Fig.2) and liquid - condensed (LC in Fig.2) may exist (Albrecht 1978). A transition from LE to LC occurs as the area per molecule is decreased. It has been suggested that in the LC phase the chains of the molecules

Figure 2. Examples of surface pressure vs molecular area isotherms showing isothermal phase transitions for four different lipid species compressed in monolayers at room temperature. I. Stearic acid, II. DPPC, III.DOPC and IV. diolein. The individual phases are indicated as gas (G), liquid - expanded (LE), liquid - condensed (LC) and solid (S) on the isotherms. (after Cadenhead 1985)

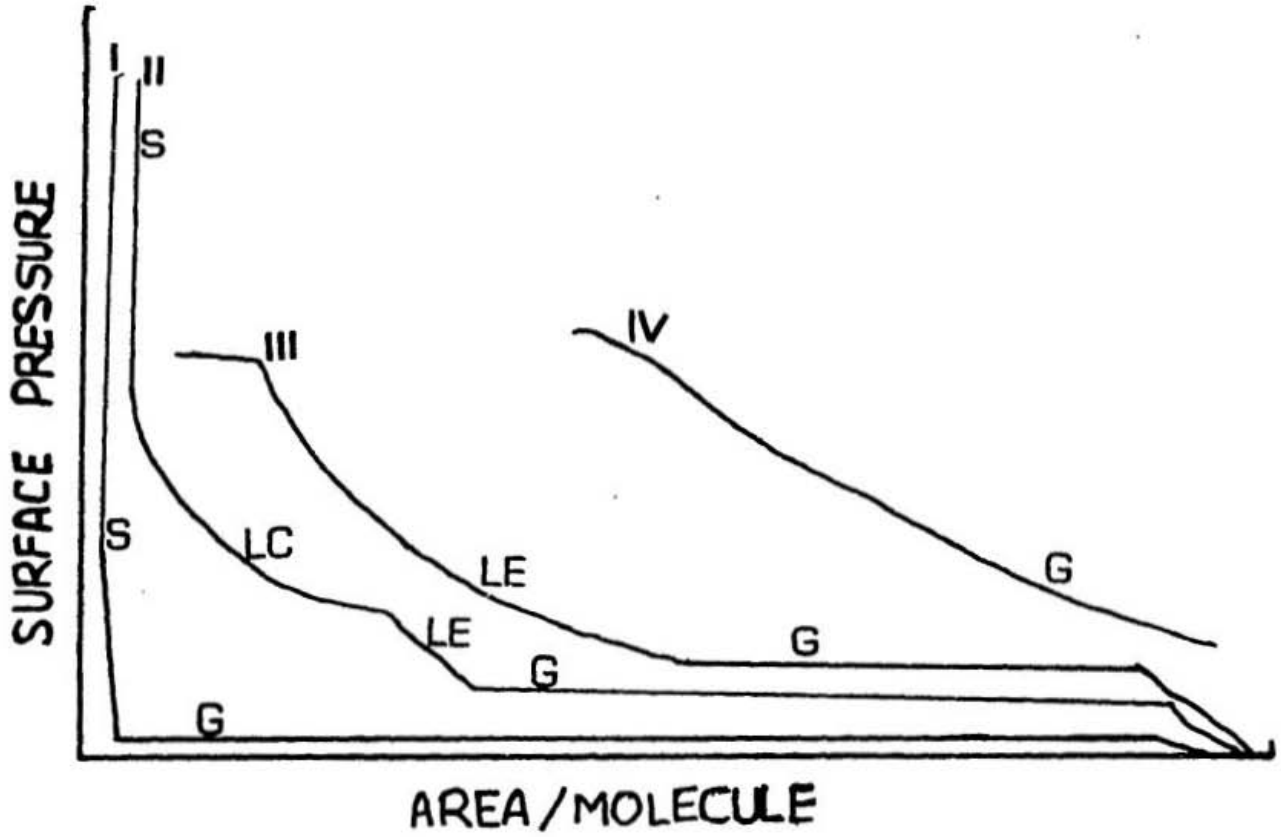

Redrawn from Cadenhead

are oriented more regularly and perpendicular to the interface than in the LE phase (Sackman 1987). Further increase of surface pressure is suggested to form a solid (S in Fig. 2) phase until the monolayer collapses (Gershfeld 1982). The isotherm I in Figure 2 shows a gas to solid transition as seen during compression of various fatty acid monolayers such as stearic and palmitic acids at room temperature. The isotherm III in Figure 2 displays a gas to liquid - expanded transition as observed during compression of phospholipids having unsaturated chains such as DOPC, and isotherm IV shows a continuous gas phase as observed for monolayers of diolein and triolein (Cadenhead 1984). The phase regions for DPPC are also shown in the isotherm in Figure 3a, and the possible molecular conformation in these regions as suggested by a number of workers are shown in figure 3b (Albrecht 1978, Sackman 1987). The molecular details of these transitions are not quite clear at present and several theoretical models for molecular orientation in the different phases of the monolayer have been suggested (Albrecht 1978, Georgallas 1982, Zuckerman 1982). These theoretical models suggest that below their chain melting temperature the conformations (gauche, trans) of the hydrocarbon chains of the saturated phospholipid molecules change during the expanded to condensed phase transition of the monolayer. The change in conformation of the hydrocarbon chains causes an ordering of the molecules in the condensed phase. Infrared spectroscopic data supports this suggestion of acyl chain ordering during the phase transition of DPPC in

Figure 3. Diagram showing the possible molecular arrangement of phospholipid molecules (b) in the different phases of the monolayer during compression. The phases are pointed on the DPPC isotherm (a) as G (gas), LC ←LE (liquid expanded to liquid condensed) and S (solid). (after Cadenhead 1985)

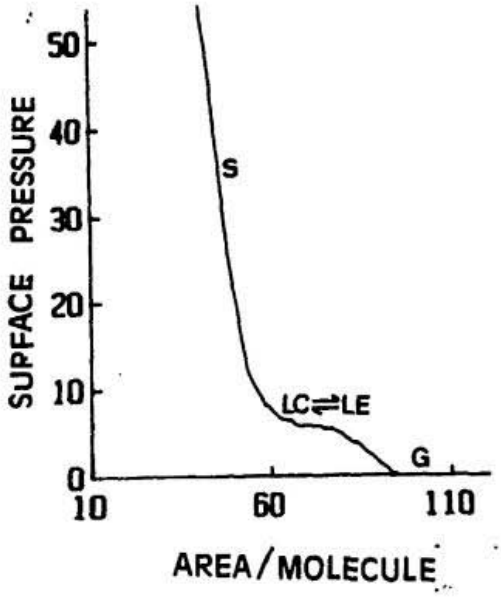

a

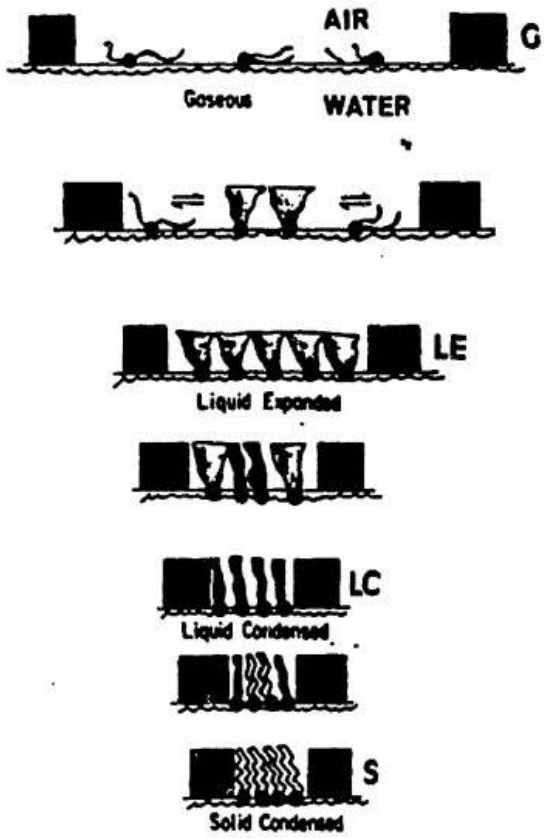

b

Redrawn from
Cadenhead 1985

monolayers (Dluhy 1989).

Most of the biophysical studies of phospholipids have been conducted in relation to the fact that a monolayer is a simple model of a biological membrane (Daneilli 1934). The external surface area of a set of erythrocytes, and the area obtained from extracted lipid materials when spread and compressed in a monolayer were compared by some workers (Gorter 1935). They found that the surface area of the lipid monolayer was close to twice that of the erythrocyte and hence proposed a bilayer structure for cell membrane. The early models of the bilayer membrane were flawed by not assuming that proteins are an integral part of biomembrane, and were later modified by others. The currently accepted bilayer model of the cell membrane (Singer 1972) is in fact designed partly from initial data of the earlier studies. Research on monolayers as a model for biological membranes has provided useful biophysical information, especially on the potential lipid orientation (Cadenhead 1980, 1985), lipid - lipid (Cadenhead 1984), and lipid - protein interactions (Nakagaki 1982, Mohwald 1990) in biomembranes. Information from monolayer studies also shed light on the nature of bilayer organization of molecules such as chain ordering (Birdi 1988), headgroup electrostatic interaction, electrical properties (Korenbrot 1980, El Mashak 1982) and some immunological processes such as cell surface antigen binding (Subramanium 1986) and receptor-substrate coupling (Krull 1990).

IV. Instrumental design and development

In the last few decades monolayer physical properties have been studied using several modified versions of Wilhelmy balances (Gaines 1966), by bubble and balance types of surfactometers (Enhorning 1977) and through transfer of the molecular layer onto a solid substrate by the Langmuir-Blodgett technique (Fischer 1985). The studies conducted using either the surface balance or the bubble method have furnished a great amount of information on pulmonary surfactant dynamics. These methods simulate the respiratory process *in vitro* as the monolayers can be compressed and expanded rapidly and their dynamic properties studied with ease. Individual components of the pulmonary surfactant and their binary and ternary mixtures have been characterized using these methods (Notter 1980), although the reliability of the surface balance technique to study pulmonary surfactant has been questioned by others (Bangham 1987).

Though the bubble surfactometer technique may apply the most relevant conditions to surfactants as found in alveoli it has certain disadvantages. The technique can create conditions that best simulate a breathing lung such as 100% humidity for the monolayer environment, the monolayers have interfacial curvature in the bubble similar to that expected in the alveoli, and the cycling speeds performed are reflective of the respiratory process. The orientation of the monolayer in the

surface balance and the bubble are shown in Figure 4a and 4b respectively. The process by which the surface tension of the interface is measured in the bubble is shown in Figure 4b. The pressure P measured to hold the bubble open is related to surface tension by the Laplace equation discussed in the legend of Figure 4b, and should not be confused with surface pressure (π). Disadvantages of the bubble technique are that it can only yield minimal information about the concentration of the material on the surface (Enhorning 1977) and it does not allow for separation of processes of adsorption and surface refining very easily. Thus it is difficult to analyze with precision the respreading properties of binary and other mixtures of the surfactant components using this method (Notter 1984). The Wilhelmy technique does give information about specific concentration of the material in the monolayer, and also surface pressure - area, surface pressure - time dependency of the monolayer. The major disadvantage of the technique is found to be monolayer leakage around the barriers at high surface pressure. A combination of information from both techniques is best suited for analyzing pulmonary surfactant and its biophysical properties.

The basic design of a Langmuir type surface balance consists of a trough made from solid Teflon block in which a subphase with a surface monolayer is contained. A movable barrier with tapered edges is used to compress the monolayer. A continuous Teflon strip or a rhomboidal frame can also be used to

Figure 4. Shows the possible arrangement of molecules in monolayers in (a) surface balance and (b) a bubble. Surface tension(γ) or surface pressure(π) during compression of the monolayer in the balance can be represented as a function of monolayer area as shown by the graph X. The surface tension (γ) in the bubble interface is measured from the change of the pressure across the bubble interface ($P_2 - P_1$ or ΔP as shown in the inset graph Y) and radius of the bubble (r) during inflation of the bubble by Laplaces equation; $\Delta P = 2\gamma/r$. The arrows indicate direction of compression of the monolayer in (a), and the direction of decreasing pressure to keep the bubble open in (b).

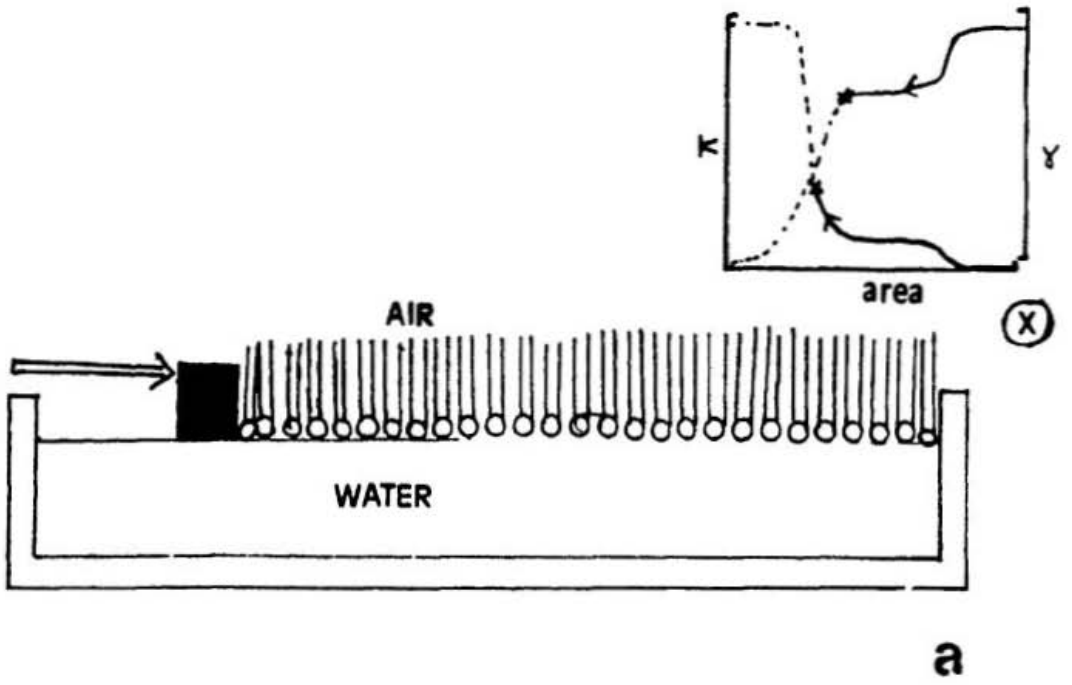
K
γ
area
X
AIR
WATER

a

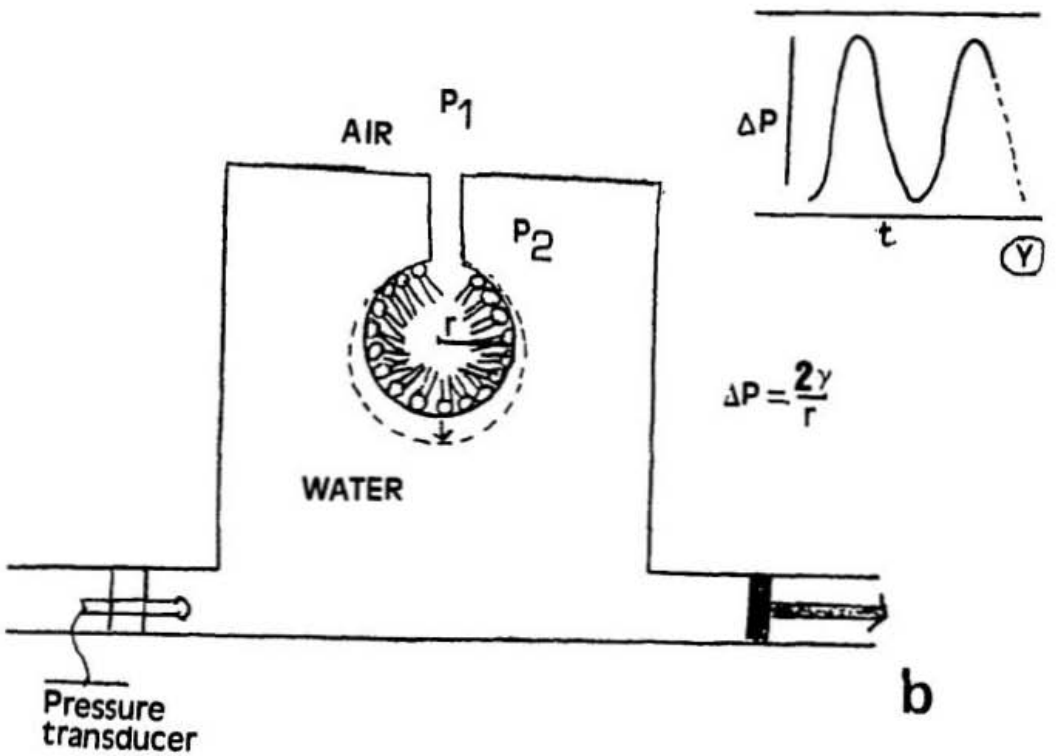
ΔP
t
Y
AIR
P1
P2
r
WATER
ΔP = 2γ/r
Pressure transducer

b

compress the monolayer. By using the latter method monolayer leakage around barriers can be avoided or reduced. Monomolecular films are spread over a water surface from a solution of the material in which the solvent evaporates in a short period of time, leaving behind a metastable or stable monolayer at the air - water interface. The surface tension can be continuously monitored by a dipping plate in combination with strain gage. The outline of the instrumental set up used in this work is shown in Figure 5.

The molecular area can be deduced from the geometric dimensions of the trough and calculated for the particular molecular species using the formula-

Molecular Area ($Å^2$/molecule) = [(length of trough in Å) * (breadth of the trough in Å)] / (Amount of material on the surface in moles * $6.023*10^{23}$).

The surface pressure can be calculated from the force acting on a dipping plate of negligible thickness by the formula-

Surface Pressure Π (mN/m) = [Surface tension of water (mN/m) - Surface tension of water with monolayer (mN/m)]

$\Pi = \Delta\ \gamma = \gamma_0 - \gamma$ where γ_0 - surface tension of distilled water

γ - surface tension of water with monolayer

An alternative method of employing a force transducer in combination with computerized programme which can measure

Figure 5. Diagrammatic outline of a) surface balance and b) horizontal view of the trough. The monolayer is spread on the trough and compressed by a barrier. The surface tension can be monitored by a platinum dipping plate in combination with a force transducer, and displayed with a digital display unit. b) Shows the trough with cylindrical collar attachments to reduce monolayer convective movement. One of the cylindrical hole can be used for visual observation and the other for the dipping plate. The holes are connected to the bulk of the subphase by channels. The cylindrical collar attachment is used in surface balances in which visual observation of the monolayer is possible.

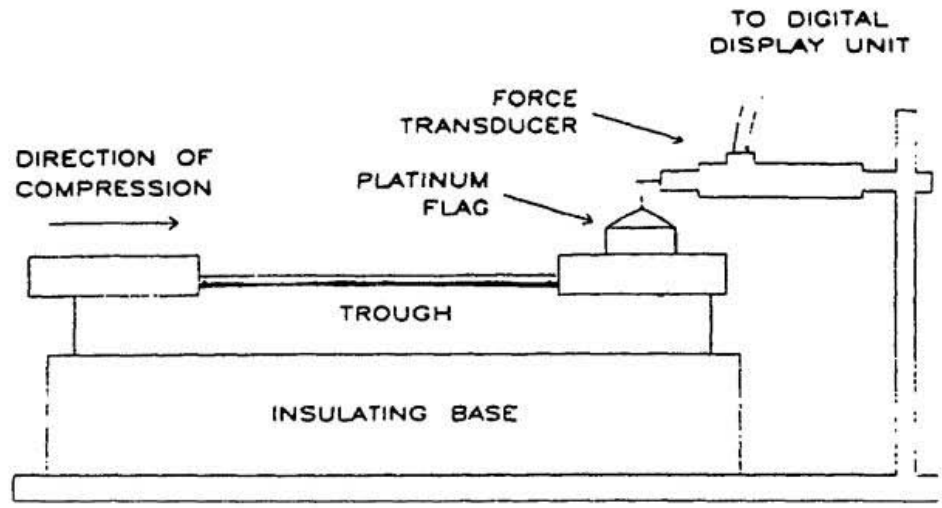

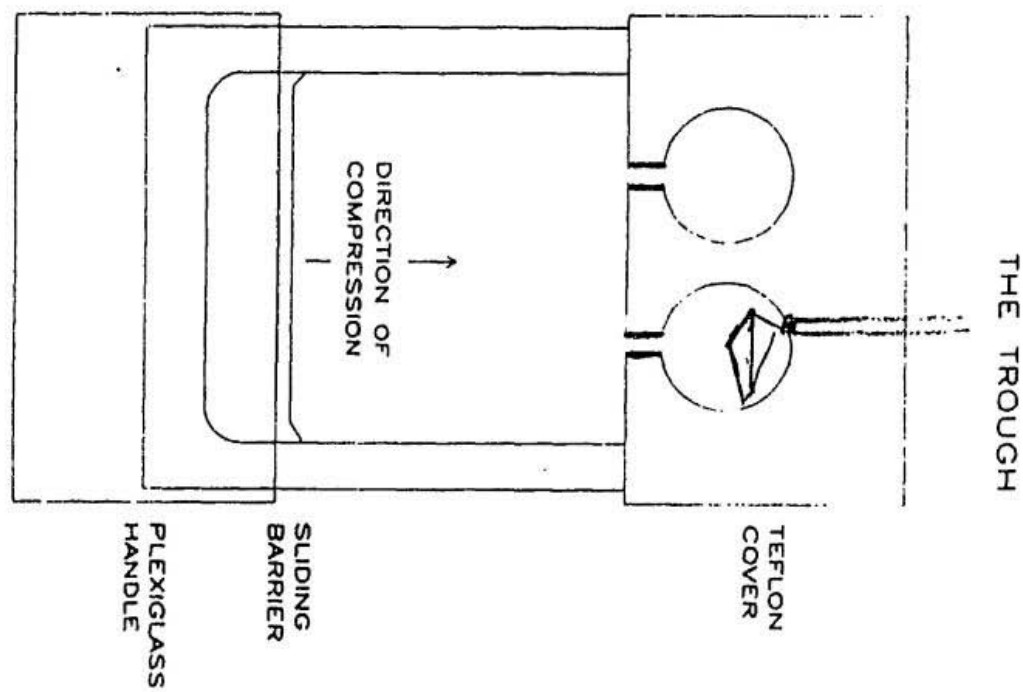

Redrawn from
Folley 1987

differential force (Cadenhead 1984) or surface tension change shown in the equation-

$$\Delta F = \Delta\omega * g = p * \Delta\gamma * \cos\theta$$

where $\Delta\omega$- measured weight change of the plate

g- acceleration due to gravity

p-perimeter of the plate

θ- contact angle of the substrate meniscus on the plate.

can also be used.

When the plate is totally wetted the contact angle θ is equal to 0 and thus $\cos\theta = 1$ and the equation becomes-

$$\Pi = (\Delta\omega * g)/p.$$

For precise measurement of these parameters a microprocessor based system can be used in which the barrier movements, pressure and temperature measurement and time dependent changes can be monitored by a computer (Albrecht 1983).

V. Visualization of Monolayers

Attempts to visualize monolayers transferred onto a solid substrate by electron microscopy lead to conflicting views on monolayer surface architecture (Fischer 1985, Neumann 1984). The major breakthrough in this field came in the early part of this decade when a group of workers reported observing

visually the phase transition region of a DPPC monolayer using fluorescence microscopy (von Tscharner 1981). The technique used a fluorescent lipid analogue in the monolayer and observed the fluorescence from the monolayer during compression. Using an epifluorescence microscope they observed black patches against a fluorescent background at the LE to LC phase transition region of the isotherm. Epifluorescence can be described as a microscopic arrangement of lenses by which using a single objective lens the excitation and observation of fluorescence from the object can be performed. It was suggested that the probe molecules partitioned between the different phases. The dark patches were later considered as liquid - condensed phase and the fluorescent area as liquid - expanded phase (McConnell 1984, Losche 1984).

A number of other workers substantiated the preliminary observations in the years to follow. One group of workers published the first visual images of the phase coexistence region while attempting to measure translational diffusion speeds of DMPC and DPPC in monolayers (Peters 1983). A complete description of the technique was published simultaneously by others (Losche 1984, Burghardt 1984). The technique was extensively modified in the last few years using computer - assisted video microscopy (Meller 1988) and a different type of leak proof trough design (Mojtabai 1989).

Each individual instrumental design was based on the type of information needed to be obtained about the monolayer. Some studies were aimed at visually characterizing the phase

transition of fatty acid monolayers (Moore 1983, Knobler 1990), whereas others have tried to study the effect of ions on the phase transition process of a charged phospholipid monolayer(Eklund 1988). Others, by modifying the technique, could measure the electrostatic interaction between phospholipid molecules at the air - water interface (Thompson 1984,1988). To date a single report exists on the quantitative analysis of the monolayer architecture of DPPC (Florsheimer 1989). These workers (Florsheimer 1989) attempted a quantitative evaluation of the surface architecture in order to determine if the features observed had equilibrium properties and their efforts had met with limited success (Florsheimer 1989). The visual architecture observed by fluorescence technique was also observed by other techniques such as charge decoration electron microscopy and electron diffraction of DMPA and arachidic acid monolayers (Fischer 1986). The architectures observed in electron microcopy of DMPA monolayers were similar to the ones observed by the fluorescence technique of DPPC monolayers. The process of enzymatic degradation of DPPC and DMPC monolayers by hydrolytic action of phospholipase A_2 was also visualized for the first time using the fluorescence technique (Grainger 1989). Lipid - protein interaction (Heckle 1985) and ligand - receptor interactions (Krull 1990) have also been visualized by this technique.

The basic design and construction of surface balances for visual observation of monolayers are similar. The

instruments consist of a rectangular trough with a movable barrier or compression system and an epifluorescence microscopic attachment. The fluorescent probe is excited either from above (von Tscharner 1981, Meller 1988) or from below (Losche 1984) the monolayer using a light source and appropriate filter combination allowing a fixed wavelength(s) of light to be incident on the monolayer. The emission of fluorescence from the monolayer is visualized either using still photography (McConnell 1984) or by using a low light level video camera (Losche 1984, Moore 1986, Meller 1988). The surface pressure - molecular area is simultaneously monitored. This technique allows for visual inspection of each specific region of the isotherm. The visual data is quantified using digital image processing and image analysis systems (Losche 1988, Seul 1990). The surface pressure - molecular area data can accordingly be correlated with quantitative visual information.

The method has been used to observe the phase transition process of various ampiphilic molecules in the monolayers such as stearic acid (Moore 1986), DPPA (Losche 1988), DMPE (Helm 1988) and DPPC (McConnell 1984, Florsheimer 1989). The information obtained by the above mentioned workers is of relevance to modelling molecular packing in biomembranes. None of the studies were aimed at observing the monolayer during dynamic compression - expansion cycles which are relevant to lung surfactant recycling in the alveoli. The various designs discussed above were modified by us to attempt to simulate such

conditions.

VI. Monolayer Architecture

Using the epifluorescence balance different regions of the DPPC isotherm showed distinctly different visual architecture (vonTscharner 1981, Peters 1983, Losche 1984). At large molecular areas where the surface pressure was near 0 mN/m large dark "gaseous" circular areas were observed to coexist with fluorescent "liquid" outlines (Losche 1984). These images resembled foam like structures and were theoretically speculated to be either the coexistence of gas and liquid phases (Losche 1984, Berge 1990) or to be areas in the monolayer devoid of any lipids coexisting with lipid containing areas (McConnell 1984). These patterns were also observed in monolayers of pentadecanoic acid (Berge 1990) and stearic acid (Moore 1983). When the DPPC monolayer was compressed beyond the point of gas phase the surface was observed to be homogenously fluorescent from surface pressures of 2-5 mN/m up to the break point of the isotherm (McConnell 1984). The break point of the isotherm (shown by point B in Figure 2) was observed visually as consisting of " non homogenous black patches or nucleation sites" appearing from the fluorescent background and was regarded as the onset point of the main "lateral phase transition" (von Tscharner 1981, Mohwald 1990). These patchy areas were found to grow to a limited size with lateral compression of the monolayer and to exhibit different shapes (mainly circular or elliptical). They were termed as " condensed phase lipid domains" (McConnell 1984).

These domains were found to have long range electrostatic order and were arranged in the monolayer with periodic symmetry (McConnell 1984). The domains were also found to have certain equilibrium properties and were considered as liquid crystals by a certain group (Mohwald 1990). These domain structures were also observed in DMPC, DMPA (Losche 1988) and in DLPE monolayers (Helm 1988) compressed at very slow speeds below the thermal transition temperature (T_c) of these molecules.

VII. Objectives of this work

The main objectives of this work were to design and construct an epifluorescence microscopic surface balance and studying monolayers visually at the air - water interface using such a balance. The instrument was designed to perform compression and expansion of monolayers with different speeds so that slow and fast processes occurring in the monolayer during phase transition could be studied.

The components of pulmonary surfactants, especially DPPC has been studied in surface balances, and surface pressure - area, pressure - time dependency of such monolayers quite well characterised by a number of workers (reviewed by Notter 1984). Though these studies give us a fair idea of DPPC monolayers physical behaviour at the air - water interface, the actual process by which these behaviours occur could not be directly visualized by earlier techniques. Our second objective was to study DPPC in monolayers using our balance. These studies can

also yield information on the efficiency of our balance to study components of the pulmonary surfactant. As mentioned earlier monolayers need to be compressed and expanded rapidly to relate to respiratory rates and pulmonary surfactant functioning in vivo. We also wanted to observe our instruments capability of performing fast compressions of monolayers, and whether the processes occurring at the interface during such compressions could be visually observed. Checking these capabilities would also yield information on the merits and demerits of the instrument and the limits of its performance.

Our final aim was to visually observe the LE to LC phase transition of DPPC in monolayers, and possibly some higher surface pressure regime of the DPPC isotherm and to characterize quantitatively the features observed during such a transition. The quantitative information of the visual architectures observed during this transition is extremely limited at present. Thus we wanted to study the LE/LC phase visually and analyze the domain structures observed in relation to some other physical properties of the monolayers such as surface tension, surface pressure and molecular areas. We also wanted to visually observe some other lipids in monolayers under compression to gain an understanding molecular mechanism of domain formation in monolayers.

DESIGN AND CONSTRUCTION OF THE APPARATUS

I. Principles of construction

The principles of design and construction were based upon earlier reported designs of epifluorescence microscopic surface balances (Peters 1983, Losche 1984, Meller 1988) and from initial experiments performed by us with a small Teflon trough and a microscope. Each of these experimental systems differ in their functional aspects. The design of a collar, as used by some workers (Peters 1983) to decrease translational motion on the monolayer surface was also employed in our design. A microprocessor and interfacing design was tested and built into the system. A software programme to operate the system was also constructed, modified and used.

The basic mechanical components of the balance are represented in Figure 6. The main components are the Teflon trough, a Wilhelmy plate, a force transducer mounted on a XYZ translator, the microscope and optical system, and the anti-vibration block. A schematic block diagram of the balance with its computer-controlled barrier drive and data acquisition components is represented in Figure 7. The balance portion of the trough is attached to the anti-vibration block separately from the microscope. The motor movements are controlled by a stepper board, and data collected by a data acquisition system.

Figure 6. Diagram outlining the attachments of the epifluorescence microscope to the surface balance. A. Teflon trough, B. aluminum base, C. Teflon collar, D.plastic cover with sealing, E. movable Teflon barrier, F. stepper motor, G. limit switch for motor controls, H. X-Y-Z translator, I. vibration isolation support, J. granite base, K. force transducer, L. fluorescence condenser, M. light source, N. image intensifier, O. CCD camera, P. trinocular tube.

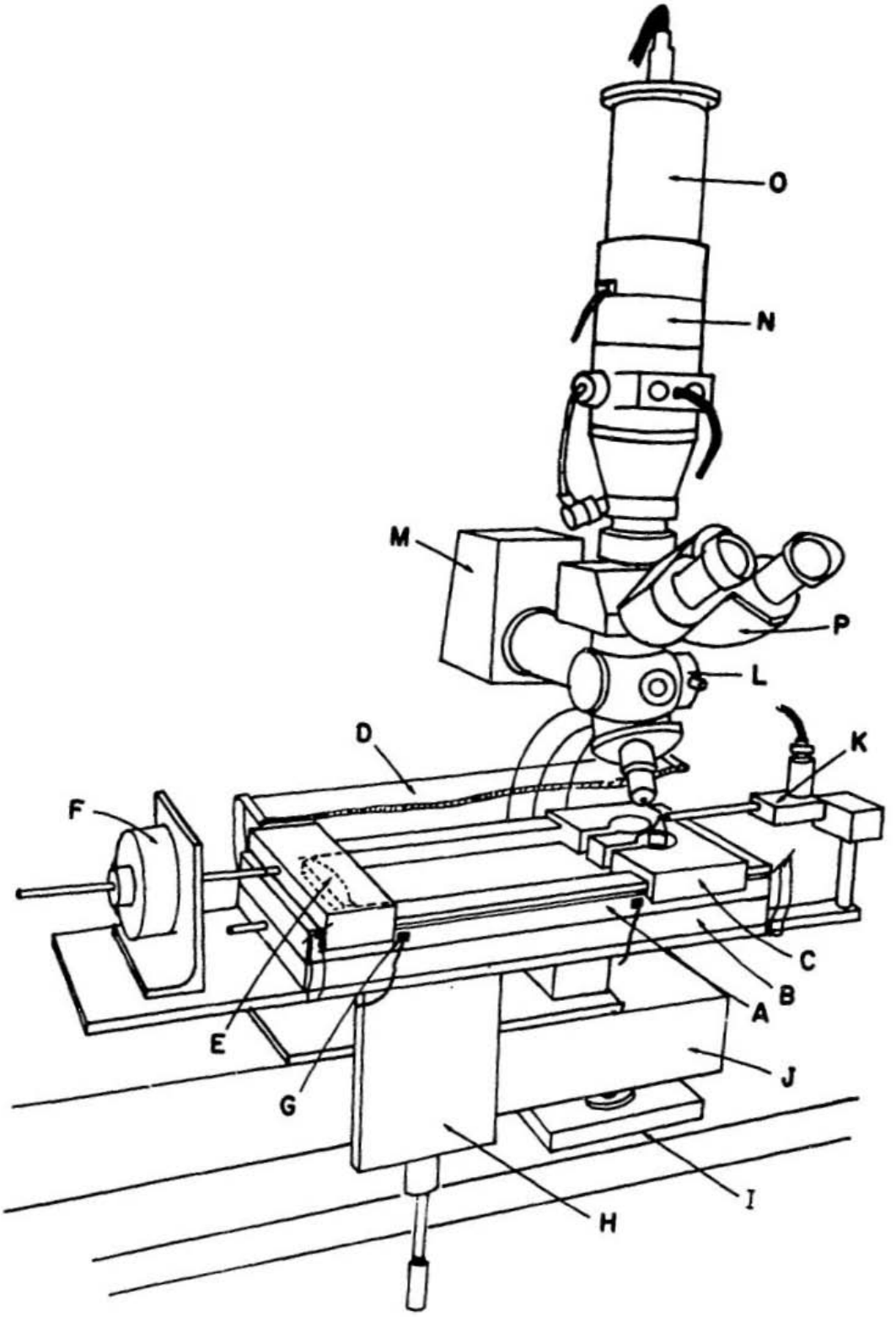
O
N
M
P
L
K
D
F
C
B
A
E
G
J
I
H

Figure 7. Schematic block diagram of the balance showing interface connections of the different parts with the computer. Images are recorded by the camera into the VCR or directly into the computer by the frame grabber board. The computer receives digital information from the pressure transducer via the pressure gauge and data acquisition interface (DAS-8) board. The motor control is performed by signals from the computer converted through the MSTEP-5 interface board.

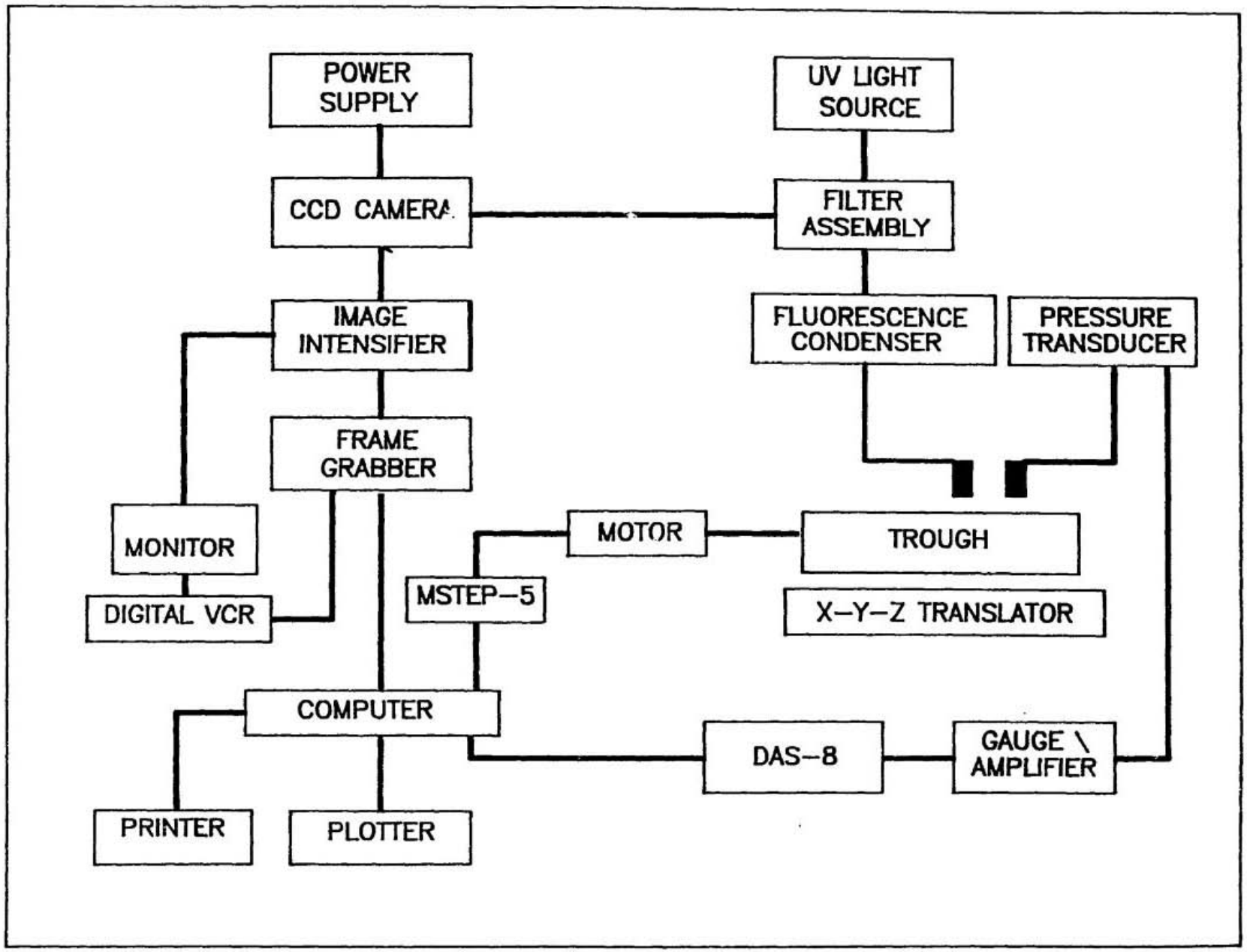
POWER SUPPLY
UV LIGHT SOURCE
CCD CAMERA
FILTER ASSEMBLY
IMAGE INTENSIFIER
FLUORESCENCE CONDENSER
PRESSURE TRANSDUCER
FRAME GRABBER
MONITOR
MOTOR
TROUGH
MSTEP–5
DIGITAL VCR
X–Y–Z TRANSLATOR
COMPUTER
DAS–8
GAUGE \ AMPLIFIER
PRINTER
PLOTTER

These systems are interfaced to the same computer, and the experimental operation controlled by programme written in C language. (Appendix B)

Fluorescent probes are excited by a 50W mercury vapour light source and emission is monitored by using an epifluorescence filter combination. Images are recorded by using a charge coupled device (CCD) chip and microchannel plate intensifier either directly onto video tape or by digitizing and recording directly in the computer by "frame-grabbing". Images from the video tape can be subsequently digitized by "frame-grabbing". The frame - grabbed images can be analyzed by an image analysis system and plotted directly from the memory.

II. Surface Balance

Initial experimentation with various troughs of small area was conducted in our laboratory. To observe monolayers at high surface pressures in these troughs an increased load of material on the surface had to be used. This allowed for a partial construction of the surface pressure - area isotherms. It was also observed that domains in a monolayers could only be visualized when compression was initiated from large area per molecules. Thus to visually observe the monolayer of a complete isotherm from large molecular areas to the point of film collapse a large trough was chosen. The large trough allowed greater

accuracy in measuring the area per molecule and increased the extent to which monolayers could be compressed in the balance.

A solid Teflon block 35 cm x 15 cm was used to construct the trough [Fig. 6 (A)] having cavity dimensions of 22 cm x 7.8 cm x 1.5 cm. An aluminum base [Fig.6 (B)] with milled channels to allow water flow was attached in order to control temperature of the aqueous phase. The whole unit weighed 10 Kg and could not be mounted on a ordinary microscope base. Temperature control with time is within approximately 1°C near room temperature in a given region of the trough, although variations over the whole trough ranged over $\pm$1°C. Thermal conduction through Teflon is low, and some unevenness in milling of the trough base could cause these localized temperature differences. Temperature monitoring was achieved by a thermistor in contact with the water surface. The milliohms output of the thermistor is converted to temperature values in degree kelvin by a formula shown in appendix D. Surface tension and optical observations were made in confined regions as in a "collar" design [Fig.6 (C)] which was suggested earlier to reduce lateral pressure gradients and diffusion gradients in the monolayer (Peters1983). Surface tension measurements of the monolayer were not affected by the collar, as the surface tension values were the same for isotherms constructed in the trough with and without the collar. The trough is enclosed by a plastic cover [Fig. 6(D)] which is about 4 cm above its surface and

contains small openings for the microscope objective, transducer arm and the motor shaft for the movable barrier. The opening for the objective also allows for cleaning the objective during the experiments without changing the focal length. The cover is sealed at the ends to avoid air turbulence, to improve temperature equilibration, and to minimize evaporation. Various designs of movable barriers were constructed and tested. Kalrez a material which, like Teflon, does not wet well, was found to be unsuitable for the movable barrier construction due its high elasticity. A Teflon dam with tapered edges [Fig. 6 (E)] and adjustable tightening attachment was found suitable. At high surface pressures (> 55 mN/m) we observed some evidence suggestive of a small amount leakage of material out of the monolayer. The movable barrier is connected, via a 12 inch threaded shaft, to a bidirectional linear actuator stepper motor (Airpax, L92411-P1, Cheshire, CT) which operates in 0.001 inch increments [Fig.6 (F)]. Its transit is constrained by two roller-type limit switches [Fig.6 (G)] attached to the trough frame. The linear actuator motor is controlled by a stepper motor controller board (MetraByte, MSTEP-5 Taunton, MA) in combination with a accessory board (MetraByte, STA-STEP). The combination provides two independent channel control, bidirectional step movement at constant speed or acceleration or deceleration. The combination also has 5 limit switch inputs and programmable internal and external clock sources. This combination results in a wide range of motor speeds.

For control of the various accessories, an IBM-AT compatible personal computer (TATUNG 7000) with 640 Kbyte RAM and 20 Mbyte hard disc memory is used. The control of the motor movement is performed by modifying the MSTEP-5 software as shown in the programme Temp6 (Appendix B). The operation of the instrument is controlled by a clock setting of 10 MHz.

The trough assembly is mounted on an XYZ translator [Fig.6 (H)] which allows its positioning, including focusing, under the epifluorescence microscope. The translator could withstand a load of maximum 10 kg. To avoid straining the system a ball bearing is attached to the Z arm of the translator. This helps to smoothen the vertical movement during focusing and during other vertical movement of the translator. During an experiment, movement of the trough is restricted to about 3mm in the X and Y direction by the cover of the trough. The restriction occurs because the cover is designed to fit fairly closely around the microscope objective. The trough and the translator are fastened to a large granite base which is in turn mounted on vibration isolation supports [Fig.6 (J)]. The trough can be easily removed for cleaning.

III. Data Collection

A force transducer (GRASS, 5F58P0, Quincy, MA.) of

displacement sensitivity 20 mm/Kg, in combination with a strain gauge DC amplifier (designed and built by Technical Services, Memorial University of Newfoundland) is used to monitor surface tension of the subphase of the monolayer. The surface tension is measured by a rectangular platinum dipping of 2.5 cm in length, 1 cm in breadth and 0.25 mm thickness. This system is interfaced through a data acquisition system (Metra Byte, DAS-8) to the computer. The DAS-8 system has a limitation of reading analog signals in the voltage scale. A 9 volt D.C. amplifier used to boost the millivolt signals from the pressure gauge is connected to the analog to digital (A/D) converter. The 8 channel A/D converter allows data collection efficiency at 4000 data points/sec, which is an advantage during high speed compressions. Compression-expansion cycles are controlled by a high level program,(TEMP-6) combining the signal from the transducer and the motor step information into surface area vs surface pressure (or surface tension) for real-time graphical output (real-time display of, surface pressure vs time is also possible). The programme also contains information about total area of the trough, the area compressed by the barrier and time required for one complete compression expansion cycle. The control of the programme is performed via a mouse and curser. The A/D converter scan rate is set at 1000 conversions/sec and the software averages from 50-250 conversions/data point during compression.

In addition to data file control, the program provides

for input of volume and concentration of the material used for spreading the monolayer which permits calculation of, and direct display of, the area per molecule of the lipid on the X axis of an isotherm. Percentage of total pool area can also be displayed on the abscissa.

Speeds of compression from 20-600 mm^2/sec (7% - 219 % of the maximum monolayer area /min) are attainable. The barrier can be stepped in small or large incremental distances and stopped after any desired increment. This allows for use of pressure jumps followed by real-time monitoring of changes in the surface.

IV. Epifluorescence and Optics

An epifluorescence condenser (Zeiss, type IVF1) [Fig. 1(L)] was attached to a standard Zeiss optical microscope base fixed to the anti-vibration block (a 70 kg granite slab of dimensions 90 cm X 38 cm X 7 cm). The stage of the microscope was removed, and the trough positioned under the objective by the XYZ translator.

Various types of objective lenses were investigated. Zeiss Planar, Neofluar and Epiplanar lenses of magnification 16X, 40X and 60X were tried. The customary objective lenses used for observing fluorescent samples could not be used as these require a coverslip over the sample. The low magnification objective

(16X) had large working distance but was found to have low light gathering efficiency due to the large distance from the monolayer surface. Lenses with magnification of 60X had too short a working distance and were also found unsuitable for observing a moving liquid surface. An 40X objective (Zeiss Epiplan 40/0.85 W) was found appropriate for current applications. This lens does not require a coverslip over the sample and also has a large aperture which enhanced the light collection efficiency of the microscope. The objective and the trinocular tube [Fig. 6 (P)] in combination with the camera and a 12 inch monitor gave visual magnification up to about 5000 times. The high resolution of the instrument has an advantage of allowing observation of any shape or structural changes that occur in individual domains.

A 50 Watt mercury vapour lamp with housing (Zeiss HBO 50W) [Fig.6 (M)] was found suitable for excitation. The low light level decreased photobleaching of the probe and thus allowed an increase in the observation time of the monolayer. An red attenuation filter was used in the condenser of the microscope to block the infrared and red wavelengths of the excitation light. An advantage of low intensity illumination was that surface photoreactions due to high excitation intensity, which might cause fluctuations in domain shape (Seul 1990) could be avoided. For observing epifluorescence from the surface, a fluorescence filter combination (Zeiss, type ES16) suitable for observing fluorescence from NBD-phospholipids was used. The

combination of filters consisted of a band pass 485/20, excitation FT510, wide emission LP520 filters, which were suitable for observation of green fluorescence and compatible with the Zeiss epifluorescence condenser.

V. Image Acquisition

Still photography with a Zeiss camera (Winder M 35 mm)to collect images during growth of domains resulted in inadequate image resolution due to low light levels and monolayer movement during long exposure times. We could successfully apply still photographic techniques using a super fast film (TMZ 5054 Kodak) with maximum clarity only at higher surface pressures, where the monolayer was relatively immobile. A still photograph obtained at 1 second exposure time and film speed of 30,000 ASA at surface pressures of 20mN/m is represented in Figure 8. In order to allow for observation under dynamic compression and under quasi-equilibrium conditions at low and intermediate surface pressures a low light level video camera [Fig. 6 (N)] (Fairchild Corp. CCD 3000, Palo Alto, CA) in tandem with an image intensifier [Fig.(6) O] (Varo, 25 mm MCP, Garland, TX) was used. The intensifier was controlled by a custom built - power source with manual control features. This allowed for amplifying the signals from the camera during observations of low fluorescence intensity from the monolayer surface and improved

Figure 8. Photograph of a DPPC + 2 mol% NBD-PC monolayer taken with a still camera with super fast speed film (30,000 ASA) at a surface pressure where the monolayer is relatively immobile. The fluorescent areas are represented as white in the photograph and the condensed areas as dark spots. Scale bar is 15μ.

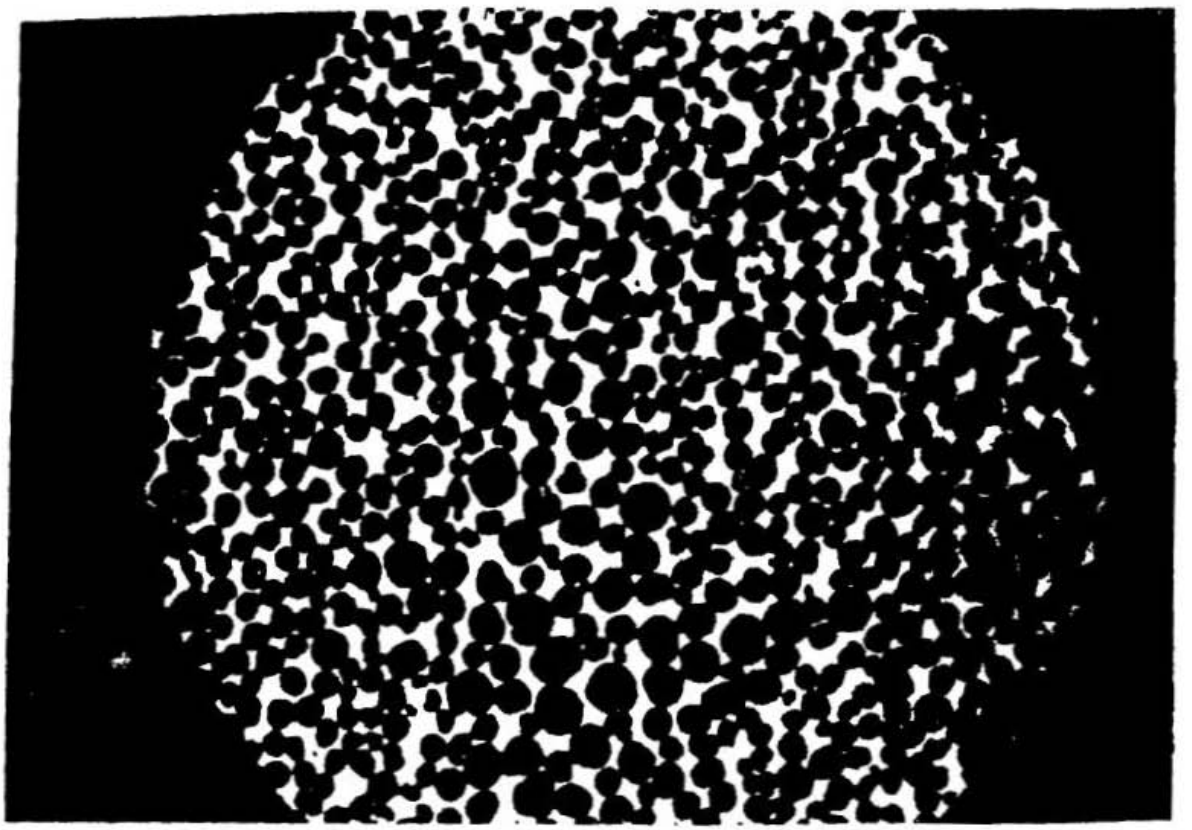

15μ

the quality of the images considerably. The CCD chip of the camera was attached to the eyepiece of the trinocular tube. The silicon chip of the intensifier reduced the noise and was not easily damaged by excessive light. During monolayer compression the fluorescence intensity varied at different regions of the isotherm, but by using automatic gain control the observed fluorescence and quality of images could be controlled. The signal to noise ratio of the images were satisfactory for subsequent image analysis. A photograph of the epifluorescence microscopic surface balance with its various accessories such as the computer, video recorder and power source controls is shown in Figure 9.

VI. Image Processing

Image processing and analysis was controlled by menu - driven software (Jandel Scientific, JAVA, Corte Madera, CA) in conjunction with an image - grabber board (Truevision, TARGA-M8), a digital VHS video cassette recorder (JVC, HR-D700V, Japan) and a monochrome monitor (Panasonic, WV54-10, Yoklohama, Japan). The image capture board featured a spatial resolution of up to 512 by 482 pixels with 8-bit resolution and monochrome input facilities. It also had hardware-implemented zoom and pan features, real-time digitization, and the ability to display 256 colour from a pallet of over 16 million, for false colour if desired.

Figure 9. Photograph of the EMSB showing the various accessory parts needed to control the functioning of the balance.

Images could be either captured directly from the camera through the TARGA board and stored through a specially written macro programme, or recorded with the VCR and digitized from the tape. Initial size calibration was done using a micrometer scale giving 0.2 μm/pixel of spatial resolution.

In routine operation, recording was initially done directly to video tape from the CCD camera. During video recording the surface pressure - area information displayed on the computer screen could be overlaid on the video images, and the combined image recorded. These frame overlays were used during the recording period to distinguish the length of recording time for each individual step of compression. Recorded monochrome images were played back from tape using the digital still-frame and single-frame advance features of the VHS recorder. This allowed the operator to choose from a wide selection of images from the tape. Storage of a large number of digitized images was unnecessary when they were recorded on VHS tape since they could be digitized subsequently from the tape for analysis.

An area of interest (AOI) was defined within the spatial resolution of the display and was maintained constant for all images used in any analysis of a series of images from any given isotherm. Suitable images, randomly chosen at a given surface pressure, were isolated and captured to the display memory of the frame - grabber board. Some preliminary image

processing was usually necessary to enhance the contrast in the AOI. Such operations included contrast enhancement, filtering, and smoothing. An Intensity Range Of Interest (IROI) was chosen so as to define the objects of interest in the AOI and for object area and perimeter determination. Random noise and partial boundary objects were eliminated from the AOI and data for remaining objects transferred to a data spreadsheet. This process was repeated for a number of chosen frames in each of the recording periods and the resulting data and images were stored and analyzed.

MATERIALS AND METHODS

I.Materials

1,2- dipalmitoyl phosphatidylcholine (DPPC), cholesterol, 1- stearoyl,2-oleoyl phosphatidylcholine (SOPC) and stearic acid were purchased from Sigma Chemicals [St.Louis,MO]. The fluorescent lipid analogues N-4-nitrobenzo,2-oxa-1-3 diazole phosphatidylethanolamine(NBD-PE), 1-Palmitoyl-2-(12-[(7-nitro-2-1,3-benzoxadizole-4 yl) amino] dodecanoyl) phosphatidylcholine (NBD-PC), NBD-Stearic acid and 1-palmitoyl,2-parinaroyl phosphatidylcholine(Pa-PC) were purchased from Avanti Polar Lipids (Pelham,AL) and used as probes without further purification.

DPPC and the probes were dissolved in chloroform-methanol (3:1,v/v) and stored in the freezer at -20°C. The concentration of the solutions were checked periodically by a modified Bartlett phosphate assay method (Keough 1987). The lipids were judged to be pure as they showed a single spot on charring with 75 % sulphuric acid after thin layer chromatography using a solvent front of chloroform- methanol- water (65:25:4,v/v). The probes were characterized by their emission and excitation spectra in ethanol and chloroform - methanol (3:1,v/v) using a Shimadzu Spectroflurimeter (RF-540,

Shimadzu Co., Japan).

The subphase on which the monolayer was spread was 0.9% (0.15M) NaCl. The saline was prepared by dissolving NaCl in deionized, double - distilled water, the second distillation being from dilute permanganate solution. The pH of the subphase was adjusted to 6.9 using 0.5N NaOH solution. The saline was further filtered using a Millipore filter system (gvwm 0.22 μm filter, Millipore Co., Missisuaga, Ontario).

One mM stock solution of the probe and DPPC were mixed at various molar ratios. The effect of the probe on isotherms of DPPC was tested on a Kimray surfactometer (Kimray Inc.,Oklahoma City,OL). The trough of the surfactometer was cleaned thoroughly with chloroform methanol (2:1,v/v) and rinsed with double distilled water.

II. System Calibration and Procedures

In the epifluorescence microscopic surface balance prevention of leakage around the barriers was attempted by using a Lanthanum - DSPC coating of the walls and barrier of the trough, as used by another group (Goerke 1981). The Lanthanum DSPC coating is assumed to form a soft coating between the trough and the barrier which somehow reduces leakage (Goerke 1981). We encountered some problems using this technique (discussed in section I of discussion). A number of stearic acid monolayers were tested on the trough to observe any leakage at lower

surface pressures.

The platinum dipping plate was roughened and heated over a oxidizing flame. The flag was attached to the tip of the transducer system and its weight in milligrams adjusted using the strain gauge amplifier. The surface of the saline subphase was cleaned by compression and suction procedures, until a clean surface with surface tension ≥ 70 mN/m was obtained. About 20 nanomols of DPPC + 1 mol% of the probe was spread on the interface using a 25μl Hamilton syringe. The monolayer spread in this way was kept in darkness under the plastic cover for 30 min before any compression was performed.

The monolayers were compressed at speeds ranging between 0.13 $Å^2$/molecule/sec and 4 $Å^2$/molecule/sec in a stepwise manner. The barrier movement was stopped at each step and visual observations were recorded on a VHS video cassette. Any surface tension changes during the visual observation time were also monitored. Isotherms of DPPC were also constructed by compressing monolayers without barrier stoppage. These isotherms of DPPC were compared with the ones constructed for the visual observation experiments.

III. Image analysis

After initial processing of the images the areas and perimeters of the individual domains were measured in square

microns and microns respectively using the JAVA software. The JAVA menu for Object Number was used to count the number of objects in the frame and the information was saved in a data worksheet. Other parameters of the images such as intensity range of the images and number of pixels in the AOI were also saved. A number of images were analyzed (~20) for each of a number of selected surface pressures. The frequency of domains within certain size limits was calculated per frame by dividing the total number of objects in all frames measured by the total number of frames. The frequency distributions of domain size were constructed by using 50 square micron groupings.

To determine the accuracy of the image analysis, computer generated images of domains of known distribution produced by Dr. David Pink, Department of Physics, St.Francis Xavier University, Nova Scotia were digitized and analyzed. The frequency distribution constructed from these images were the ones expected from the functions used to generate the images.

RESULTS

I. Probe Characteristics

The wavelength of maximal excitation(λ_{max}) of the NBD-PC and NBD-PE lipid analogues (probes) in ethanol solution was found to be around 472nm. The excitation and emission spectra of NBD-PC are shown in figure 10. The emission spectrum showed a broad band from 480nm to 580nm with a λ_{max} at 525nm. When observed on a slide in the epifluorescence microscope, the probe in dry powder form showed yellow fluorescence and in ethanol solution a green fluorescence when viewed under blue excitation light. The results agree with other workers who observed emission and excitation characteristics of the probe incorporated in phospholipid vesicles (Struck 1980, Pagano 1981).

The probe NBD-PC was observed to form a monolayer at the air-saline interface and when the monolayer was compressed it reduced surface tension of the subphase to about 10 mN/m as shown in figure 11b. The effects of the probe on the surface tension of DPPC monolayers undergoing compression and expansion are shown in figure 11. In the concentration range of 0.5 to 2 mol % in the monolayer the probe does not substantially effect the surface tension characteristics of DPPC monolayers when they are

Figure 10. Fluorescence excitation (solid line) and emission (dashed line) spectra of NBD-PC in ethanol solution.

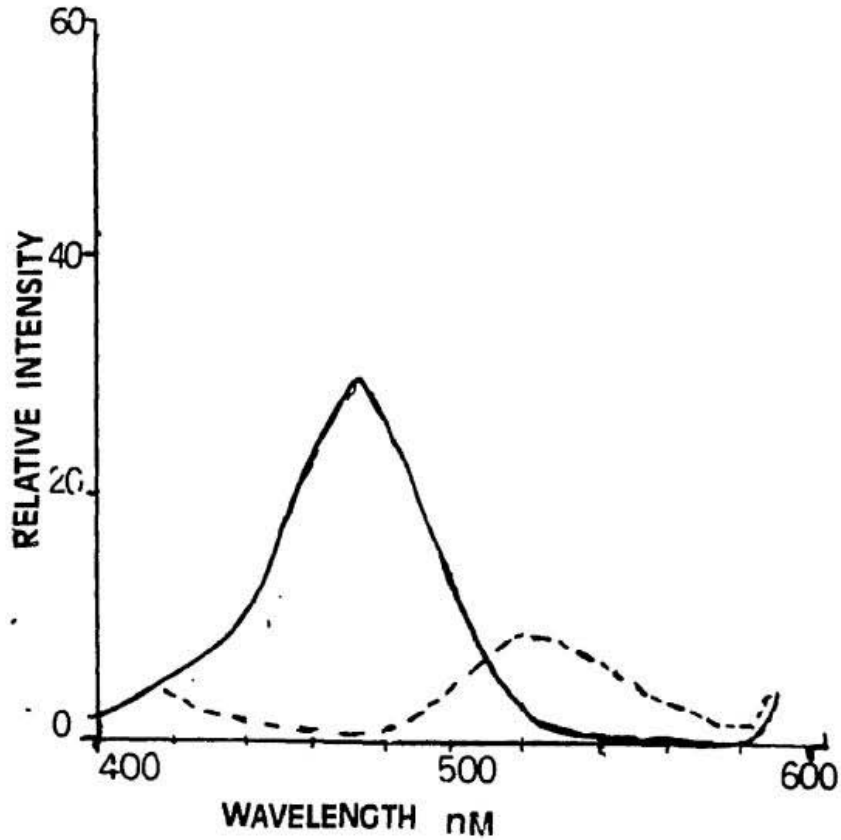
60
40
20
0
RELATIVE INTENSITY
400
500
600
WAVELENGTH nM

Figure 11. Surface tension vs % pool area plots of a) DPPC, b) NBD-PC, x) DPPC + 0.5 mol% of probe, y) DPPC + 2 mol% of probe and z) DPPC + 4 mol% of probe monolayers obtained at 37°C. The arrows pointing left indicate compressions and the ones pointing right, expansions of the monolayer. The plots indicate a collapse of the monolayer at 50% pool area during compression.

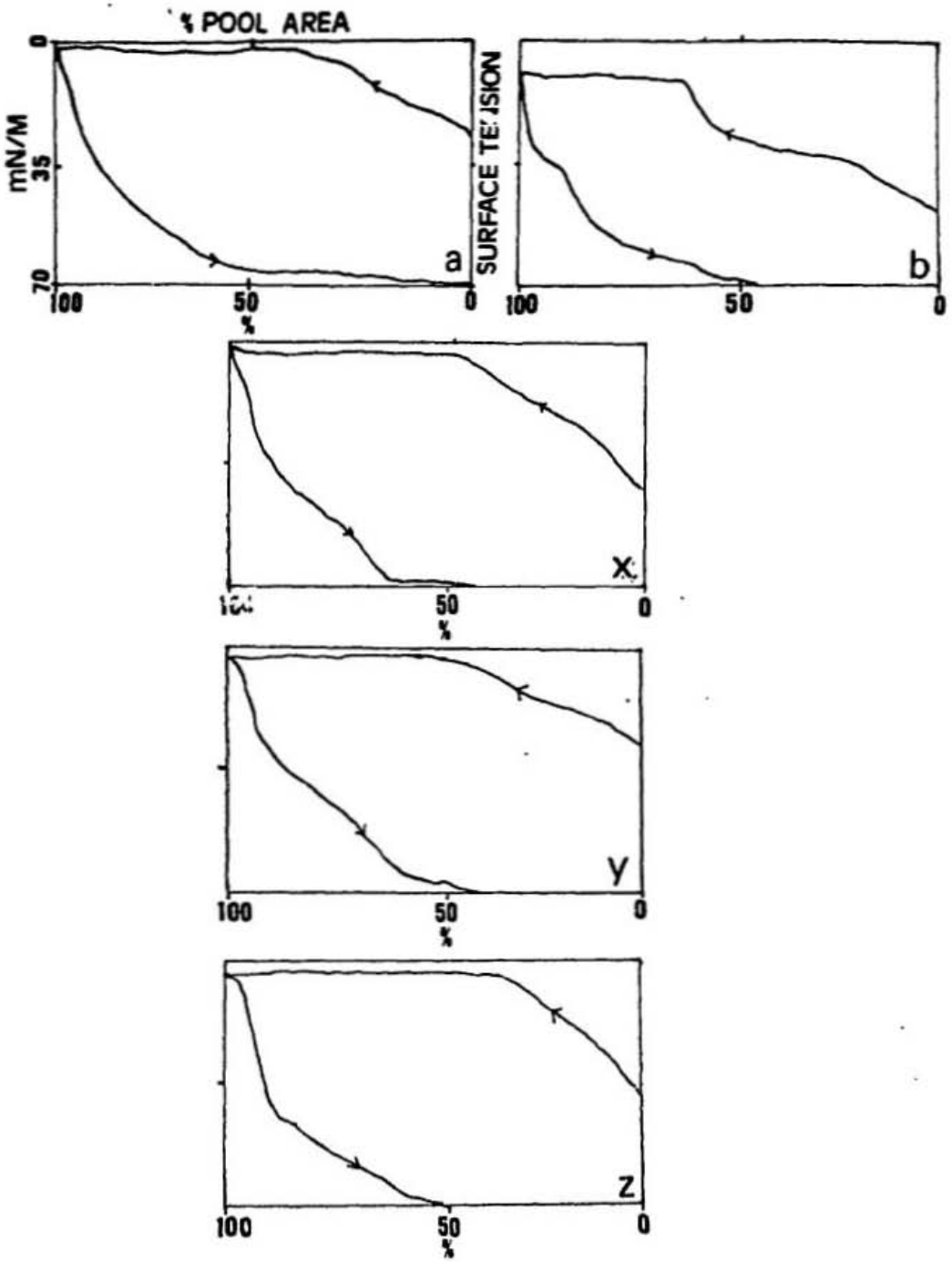
% POOL AREA
mN/M
0
35
70
100
50
0
%
a
SURFACE TE' ISION
b
x
y
z

compressed to a minimum monolayer area at 37°C. The Figures 11 a, x, y and z represent the surface tension vs % pool area plots for DPPC monolayers containing 0 mol%, .5 mol%, 2 mol% and 4 mol% of the probe, respectively. Pool area of the trough indicates the % of the total area of the trough or interface being compressed. These compression - expansion cycles show that a collapse of these monolayers of DPPC, with and without the probe occurred at about 50% of the pool area during compression. The surface tension of the monolayer of DPPC + 4 mol% NBD-PC was observed to be 3 mN/m higher than that of a monolayer of pure DPPC at minimal monolayer area. The isotherm was slightly expanded by 4 mol% of the probe. The probe up to 2 mol% also showed very little effect on the liquid expanded/liquid condensed phase transition region of a DPPC isotherm. The isotherms of DPPC and DPPC plus 2mol% of the probe are shown in figure 12.

The probes were found to migrate on TLC plates like phospholipid species as shown in figure 13. The migration of the fluorescent phospholipids NBD-PC and NBD-PE could be detected as yellow spots on the silica plate even before the charring process. The TLC plate also shows no impurities and breakdown products of the probes NBD-PC and NBD-PE.

Characterization of other fluorescent probes such as NBD-Stearic acid and 1-palmitoyl -2-parinaroyl phosphatidylcholine (PaPC) was attempted with limited success. The PaPC, a conjugated polyene fatty acyl membrane probe, has a long lifetime component in the solid phase and a short lifetime

Figure 12. Isotherms of DPPC (solid line) and DPPC + 2 mol% NBD-PC (dashed line). The monolayers were compressed in steps on 0.15 M NaCl subphase at a temperature of 26°C. A slight effect of the probe on the monolayer can be seen above surface pressures of 10 mN/m as a small deflection in the isotherm of the monolayer containing the probe.

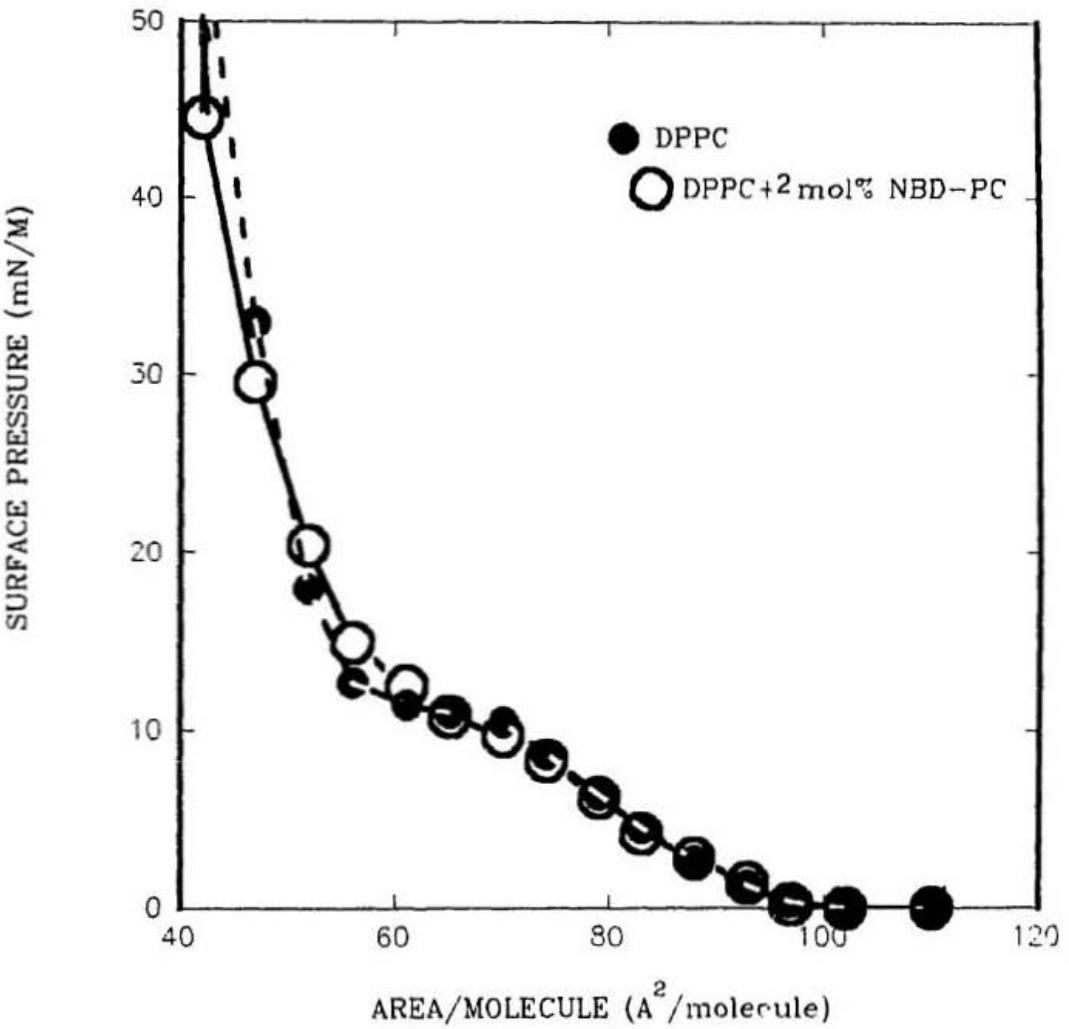
SURFACE PRESSURE (mN/M)
50
40
30
20
10
0
40
60
80
100
120
AREA/MOLECULE (A^2/molecule)
DPPC
DPPC+2 mol% NBD-PC

Figure 13. Photograph of TLC plate showing the migration of DPPC and the probes. The breakdown of PaPC can be seen as two spots in lane six.

K·NAO
A 12//
DPPC
NBD PC
NBD PE
Parn PC

component in the liquid phase of DPPC vesicle membrane (Sklar 1977). The probe was found to breakdown rapidly when in contact with air and thus was considered unsuitable for work at the air - water interface. The fluorescence emission spectra (not shown) of PaPC showed a number of sharp peaks in its emission range of 560 - 590nm in chloroform/methanol(3:1 v/v) solution. The probe in dry powder form also showed weak blue fluorescence when observed under the epifluorescence microscope. The breakdown of the probe was also observed as a second spot on the TLC plate as shown in Figure 13. Another probe, NBD-stearic acid, was used up to 3mol% in DPPC monolayers, but no fluorescence could be observed from the monolayer from the phase transition region of the monolayer. The monolayer could not be clearly focused under the microscope objective due to the lack of any appreciable emission from the probe. The chemical formulas of the various probes are shown in appendix A. These preliminary studies on PaPC and NBD-stearic acid suggests that they are unsuitable for use in visual observation of DPPC monolayers.

II. Observation of the Monolayer

A number of preliminary visual observations were made on monolayers of DPPC, DOPC and DMPE using the probe NBD-PC. Isotherms for these initial experiments could not be constructed because the earlier version of the instrument did not yet have

the surface tension monitoring equipment in place.

For DPPC it was observed that micro domains formed only during compression of the monolayers which were spread at molecular area of ≥ 120 $Å^2$/molecule. No domains were observed when monolayers were compressed from an initial spreading density of less than 100 $Å^2$/molecule. This behaviour was similar to that found by others (Heckle W., personal communication). We also observed that nucleation and growth of domains in DPPC monolayers was dependent on the nature of the probe used. We did not observe a homogenous distribution of the condensed phase domains using the headgroup labelled NBD-PE, whereas circular homogenously distributed dark domains were observed using a fatty acyl NBD labelled analogue 1-Palmitoyl,2-NBD phophatidylcholine. These results are similar to those found by one group of workers (McConnell 1984) but different from those of another, who observed homogenous distribution of domains using the headgroup labelled NBD-PE (Losche 1984). The latter group has also shown that the domains for some phospholipids (DMPE and DPPA) are dependent on pH of the subphase using the headgroup labelled probe. The apparent difference between their observations and ours may be explained by the differences of subphase ionic concentrations or other factors such as compression rates. The condensed DPPC domains were observed as dark patches with a fluorescent background as shown in Figure 14a. Using the same load of material on the surface for DMPE we observed domains of

Figure 14. Photographs of a) DPPC and b) DMPE monolayers with 2 mol% of the probe NBD-PC as seen under the epifluorescence microscope at a temperature of 25 °C. The photographs were taken at high surface pressure where the monolayers were rigid. Note the much larger size of domains for DMPE. The upper left side of the photograph b) is dark as the field under the microscopic objective was out of focus during photography. Scale bar is 15 microns for both images.

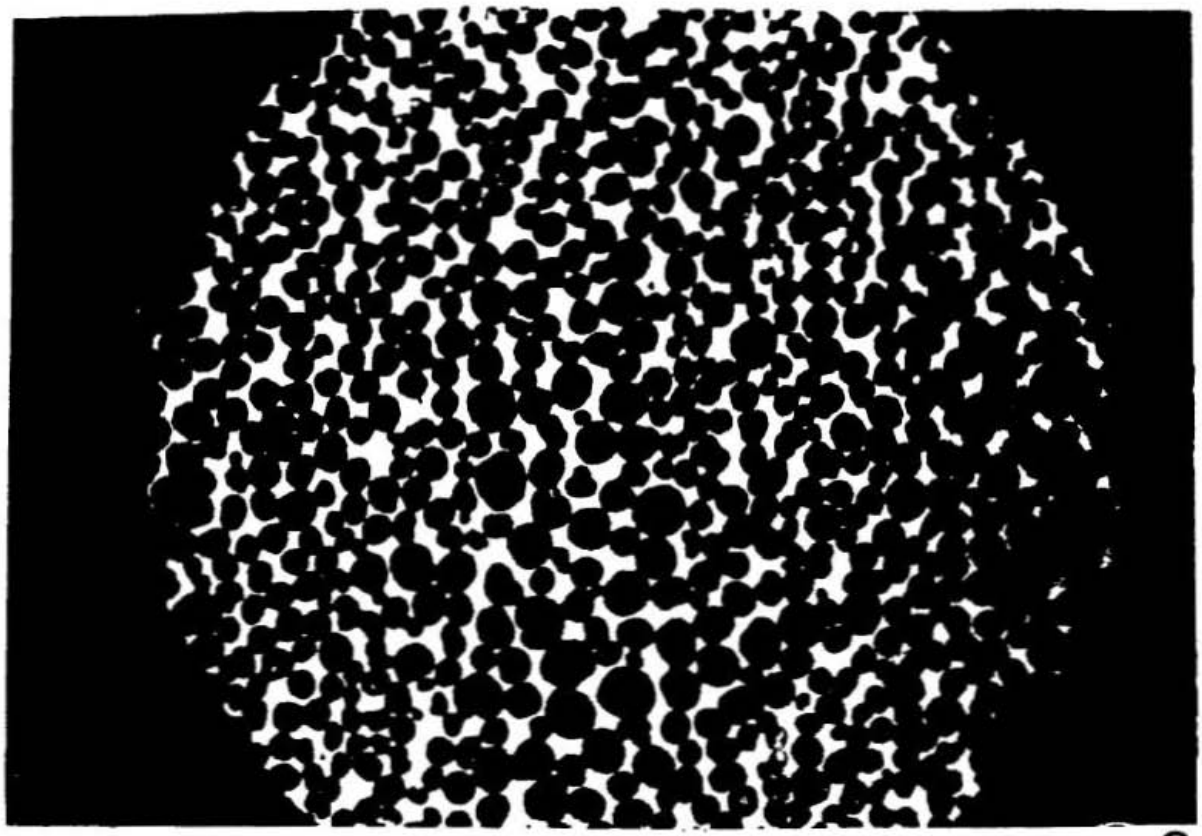

a

15Å

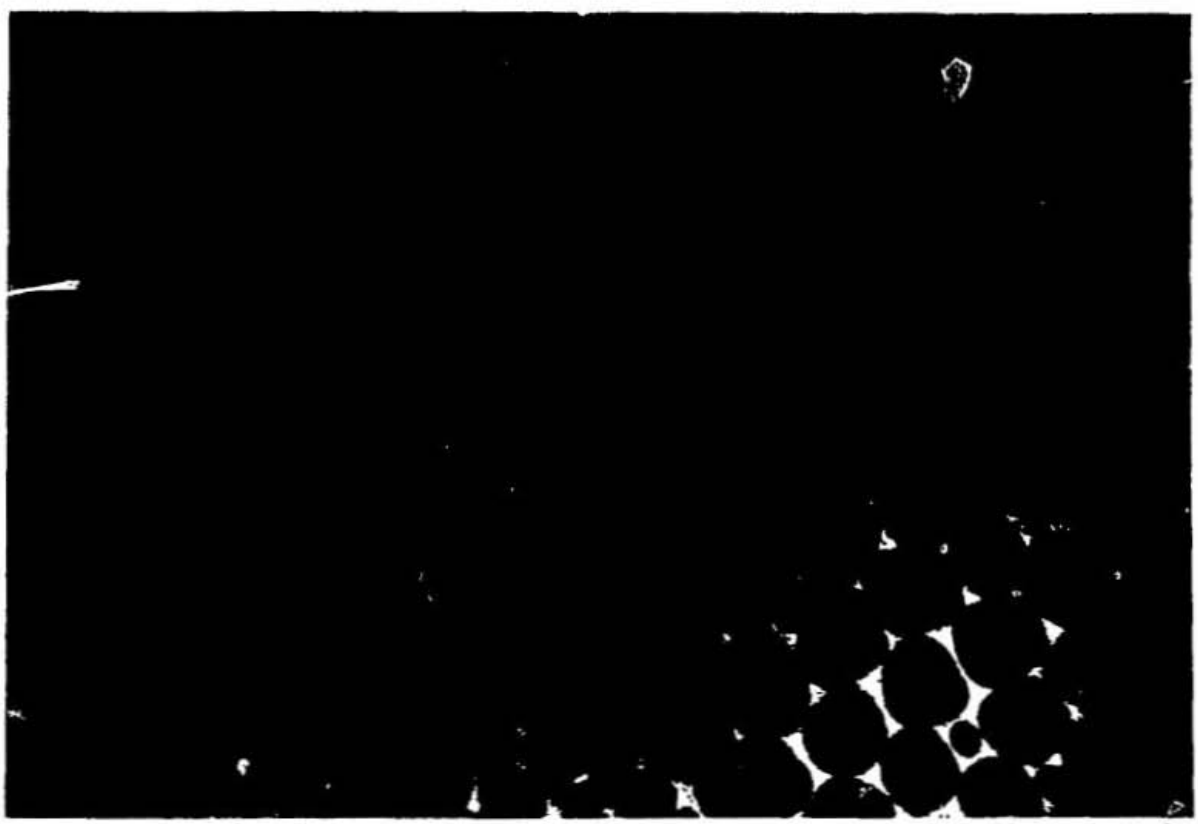

b

larger size and somewhat more regular order as shown in Figure.14b, whereas with DOPC no domain formation was observed up to the point of monolayer collapse. These results suggest that the phenomenon of domain formation may be limited to phospholipids which are below their thermotropic transition temperature. The domain structures showed some sort of orientational order with respect to each other and could not be fused or merged together by compressing them to high surface pressures.

The following observations are subjective evaluations on monolayer architecture and formed the basic groundwork for the quantitative study.

III. LE to LC Phase Transition of DPPC in Monolayers

A typical isotherm of DPPC + 1mol% of NBD-PC at 26°C is shown in Figure.15a. The isotherm was constructed by compressing the monolayer at a velocity of 4Å^2/molecule/sec in 20 steps. At each step the barrier movement was stopped for one minute and visual observation recorded on a VCR. The points on the isotherm where compression was stopped are marked by solid triangles.

The isotherm shows a "lift off" or detectable change of surface pressure above 0 mN/m, at 98 Å^2/molecule (equivalent to a slight decrease of surface tension from 72 mN/m). The surface tension vs % pool area plot of the same monolayer is shown in

Figure 15. a) Surface pressure vs area/molecule isotherm of a DPPC monolayer at 26 °C. b) surface tension vs % of monolayer area plot of the same monolayer. Note the reduction of surface tension to about 3 mN/m at 20 % of monolayer area.

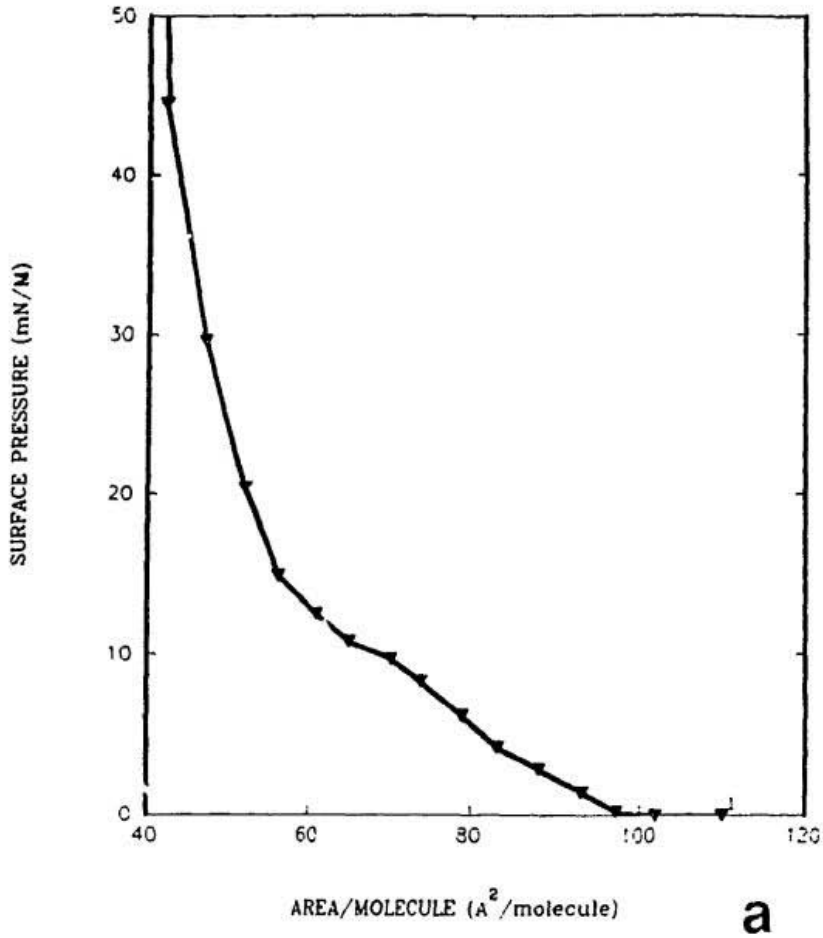
SURFACE PRESSURE (mN/M)
50
40
30
20
10
0
40
60
80
100
120
AREA/MOLECULE (A^2/molecule)

a

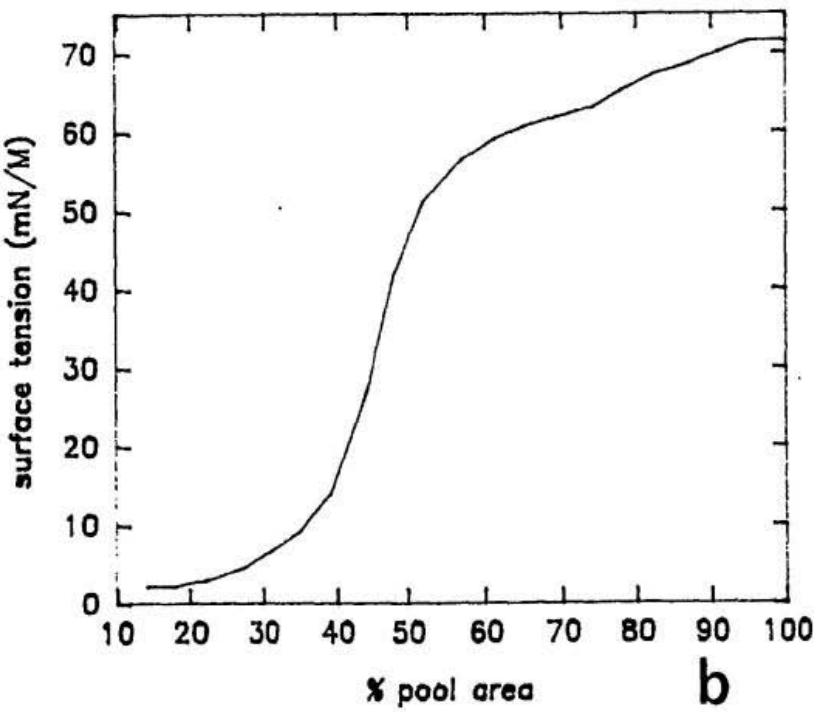
surface tension (mN/M)
70
60
50
40
30
20
10
0
10
20
30
40
50
60
70
80
90
100
% pool area

b

Figure 15b. The LE to LC phase transition was observed to start around 73 $Å^2$/molecule, and is shown in the isotherm as a change in slope of the curve of isotherm. The surface pressure increased from 8.3 mN/m to 12.5 mN/m during a decrease of molecular area from 73 to 53 $Å^2$/molecule. This portion of the curve with a low slope indicates the liquid - expanded to liquid - condensed phase transition of the lipid. Compressing the molecules below a molecular area of 50 $Å^2$ resulted in a sharp increase of surface pressure from 12.5mN/m to 50 mN/m. This was considered as another phase transition occurring in the monolayer. The characteristic of this phase transition was assumed to be of a diffuse nature as observed by the less sharp (between b and d of Fig.16 a) break in the isotherm. At molecular areas smaller than 40 $Å^2$/molecule and surface pressure above 50 mN/m we observed some evidence suggestive of leakage of the monolayer. DPPC monolayers were shown to have similar isothermal phase behaviour by others (Chapman 1968). The monolayers were also shown to collapse at molecular areas of 40 $Å^2$/mol and surface pressures of 72 mN/m at 25°C by other workers (Notter 1980). The final collapse phenomena was observed by us at a lower molecular area of 20 $Å^2$/molecule likely due to leakage of the monolayer around the barrier at high surface pressures above 50 mN/m. The area in question where leakage may be occurring is shown in the isotherm in Figure 16. The dashed line in the isotherm indicates the collapse of the monolayer around

Figure 16. Isotherm of a DPPC monolayer at 24°C compressed without barrier stoppage at a rate of 4 $Å^2$/molecule/sec. The collapse is shown by point P on the isotherm at area/molecule of 20 $Å^2$/molecule. The dashed line represents the collapse of the monolayer at ~ 40 $Å^2$/molecule observed by some workers in a leak free balance (Notter 1980). The LE to LC phase transition occurs approximately between points b and d.

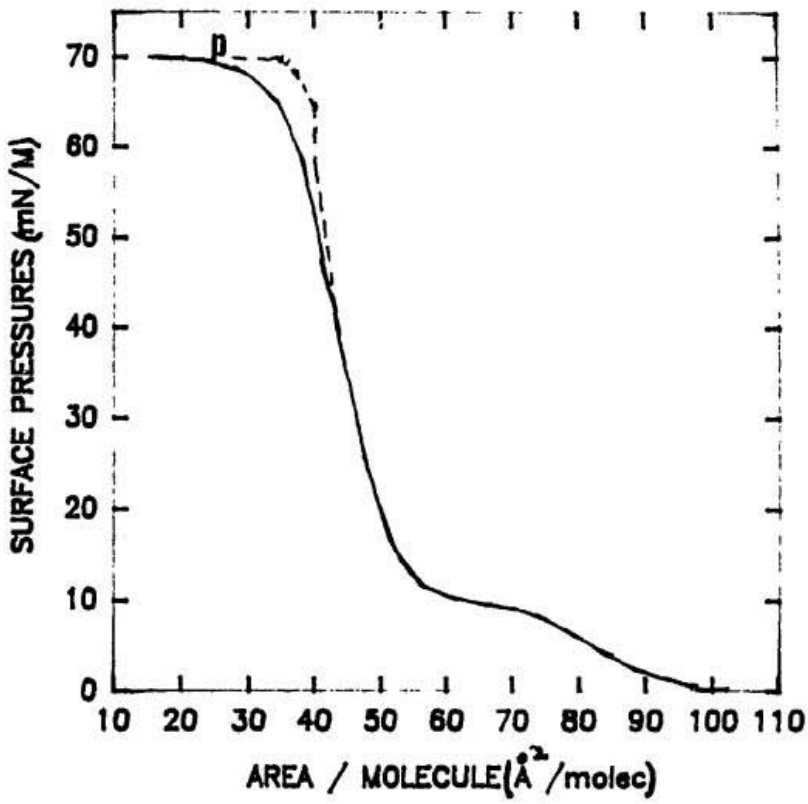
SURFACE PRESSURES (mN/M)
70
60
50
40
30
20
10
0
D
10 20 30 40 50 60 70 80 90 100 110
AREA / MOLECULE(Å²/molec)

40 A^2/molecule as observed by other workers (Notter 1980). The collapse of DPPC monolayer is also recorded as maintenance of the constant low surface tension of $\lesssim$ 2 mN/m below 80% pool area, as shown in Figure 15b.

The typical images during the phase transition of the DPPC monolayer compressed at 4 A^2/molecule/sec are shown in Figure 17b. The points a1, a2, b, c, d, e, f and g are marked in the isotherm in figure 17a, indicating the surface pressures where the barrier movement was stopped and visual observation performed. The frequency distribution of number of domains vs their size were obtained for two independent experiments, for a number of molecular areas. Two frequency distributions of domain size obtained at the same molecular area from two independent experiments performed at 21 °C ± 1°C are shown in Figure 18. The size distribution of the domains for the same molecular areas between the two experiments were found to be somewhat different. The difference was observed in the range the and peak of the distributions. This observed difference between the data could have been introduced due to the slight temperature difference between experiments.

From point b in the isotherm in figure 17a the domains were found to grow with surface pressure up to a pressure of 30 mN/m. At higher surface pressures they appeared to touch each other and no fusion of domains was observed. The domains were observed to decrease in size when the surface pressure was decreased, and they disappeared at lower pressures. The process of domain

Figure 17. a) Isotherm of DPPC + 1 mol% NBD-PC compressed at a rate of 4 $Å^2$/molecule/sec obtained at a temperature of 26°C. The squares represent the areas where the barrier was stopped. The points marked a_1 - g represents the surface pressures at which images were recorded on a video tape.

b) Sequential images from the monolayer at different surface pressures. a1 and a2 are from the gas phase where foam like structures with fluorescent outlines are observed, b to d at the LE/LC region and e to g at the solid phase. The black areas at a1 and a2 are larger in area than the domains observed in the LE-LC coexistance region,and they may represent regions of the surface devoid of probe. The surface pressures(P) of the monolayers at which the images were obtained are given below the images.

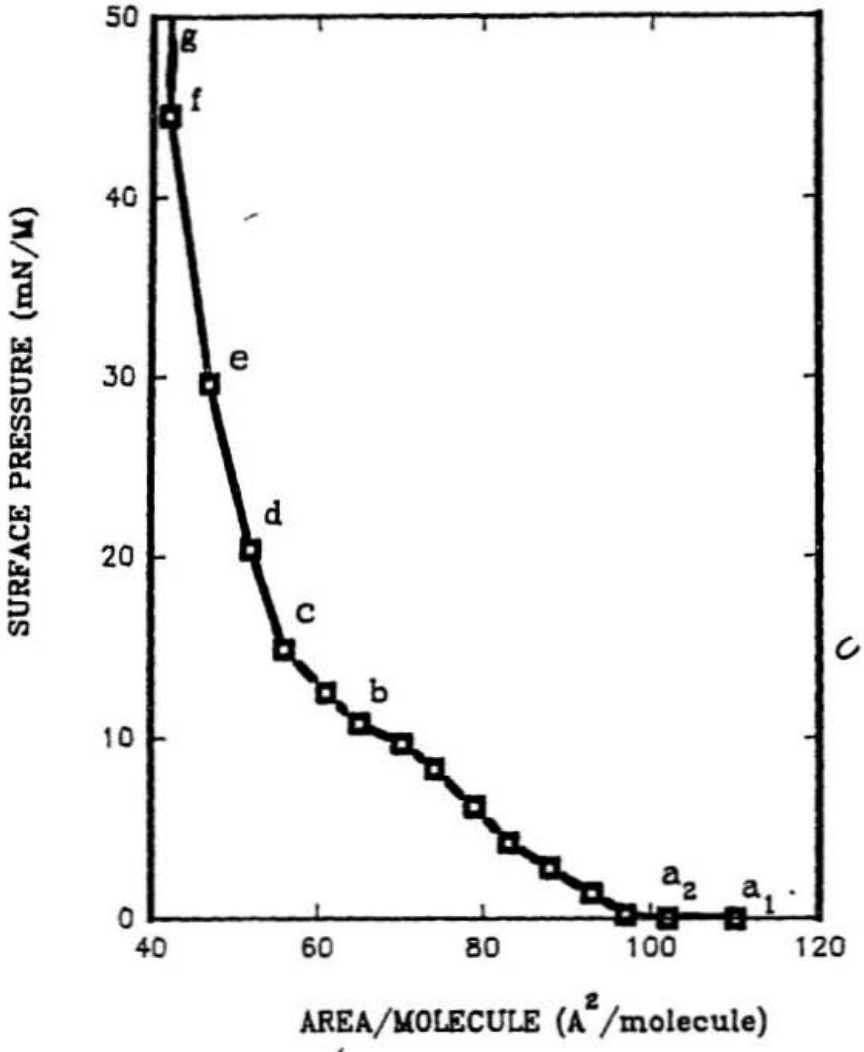
SURFACE PRESSURE (mN/M)
AREA/MOLECULE (A²/molecule)
50
40
30
20
10
0
40
60
80
100
120
g
f
e
d
c
b
a2
a1

a

a_1

P-0

a_2

P-0

b

P-10

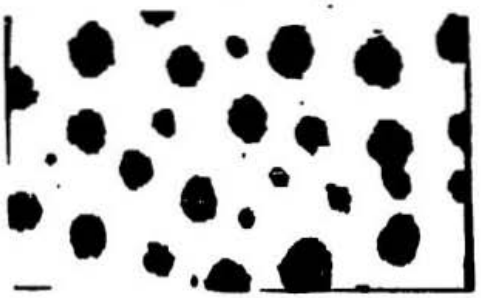

c

P-14

d

P-20

e

P-30

f

P-45

g

25 μ

P-450

Figure 18. Frequency distribution of domain size obtained from analyzing the images recorded from two monolayers at a molecular area of 52 $Å^2$/molecule. The monolayers were compressed at a fast speed of 4 $Å^2$/molecule/sec.

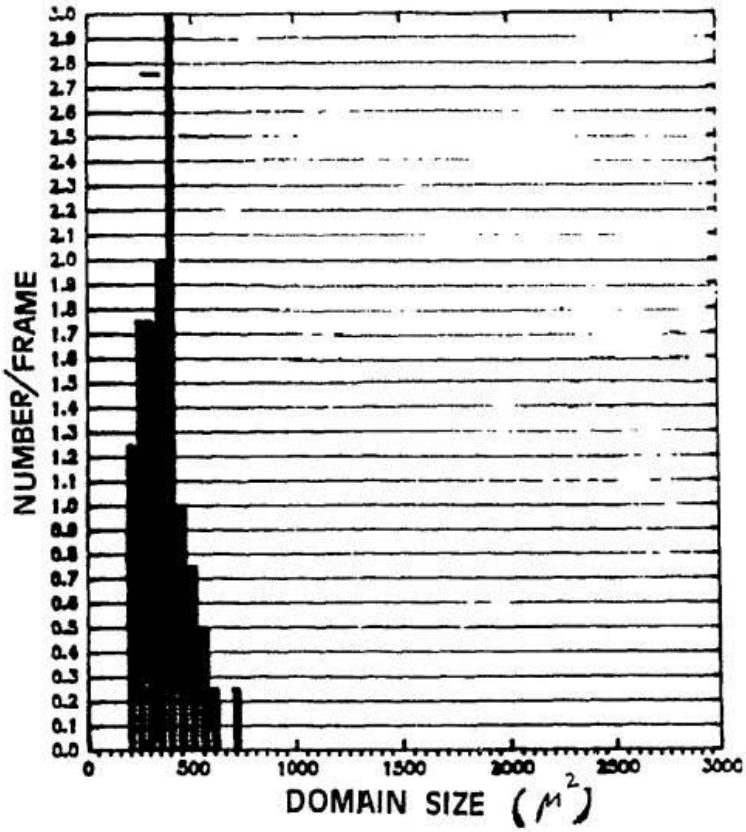
NUMBER/FRAME
0.0
0.1
0.2
0.3
0.4
0.5
0.6
0.7
0.8
0.9
1.0
1.1
1.2
1.3
1.4
1.5
1.6
1.7
1.8
1.9
2.0
2.1
2.2
2.3
2.4
2.5
2.6
2.7
2.8
2.9
3.0
0
500
1000
1500
2000
2500
3000
DOMAIN SIZE (μ^2)

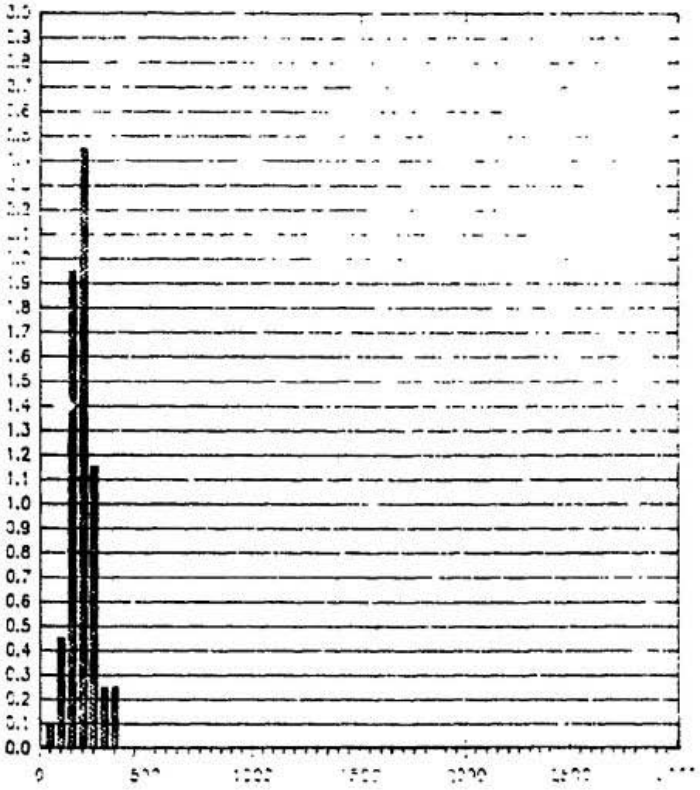

domain formation and difference could be observed for a number of compression expansion cycles of the same monolayer.

To investigate the dynamics of domain growth we performed some experiments in which monolayers were compressed to the end of LE/LC phase coexistence region (to a surface pressure of 9.4 mN/m) and visually observed over time. The isotherm and the plot of domain size as a function of time obtained from this experiment are shown in Figure 19. The visual recording was performed for 1 hour at a surface pressure of 9.4 mN/m, shown by the arrow mark in the isotherm of figure 19a. No surface pressure change was noticed over the 1 hour period of visual recording. The images analyzed were recorded at 10 sec, 10 min, 20 min, 30 min and 45 min after barrier stoppage and the average size of domains for 20 frames estimated. The plot of average domain size as a function of time from barrier stoppage is shown in Figure 19b. As shown in Figure 19b the average domain size did not increase with time. The average size of domains observed at all the points of the plot was 150 μ^2. Earlier reported domain sizes for DPPC monolayers by another group were 5 times larger at these surface pressures (Florsheimer 1989) under a different set of experimental condition. These workers compressed the monolayer at a much lower velocity to determine whether the domains were an equilibrium feature or not (Florsheimer 1989).

To observe the DPPC monolayer under slow compression rates isotherms were constructed and visually observed at a 30

Figuree 19. a) Isotherm of DPPC + 1mol % NBD-PC compressed at a rate of 4Å^2/molecule/sec. The barrier was stopped at a surface pressure of 9.4mN/m shown by the point and arrow mark on the isotherm. Images were recorded after 10 sec, 10 mins, 20 mins, 30 mins and 45 mins after barrier stoppage.

b) The average area of the domains plotted as a function of time after barrier stoppage.

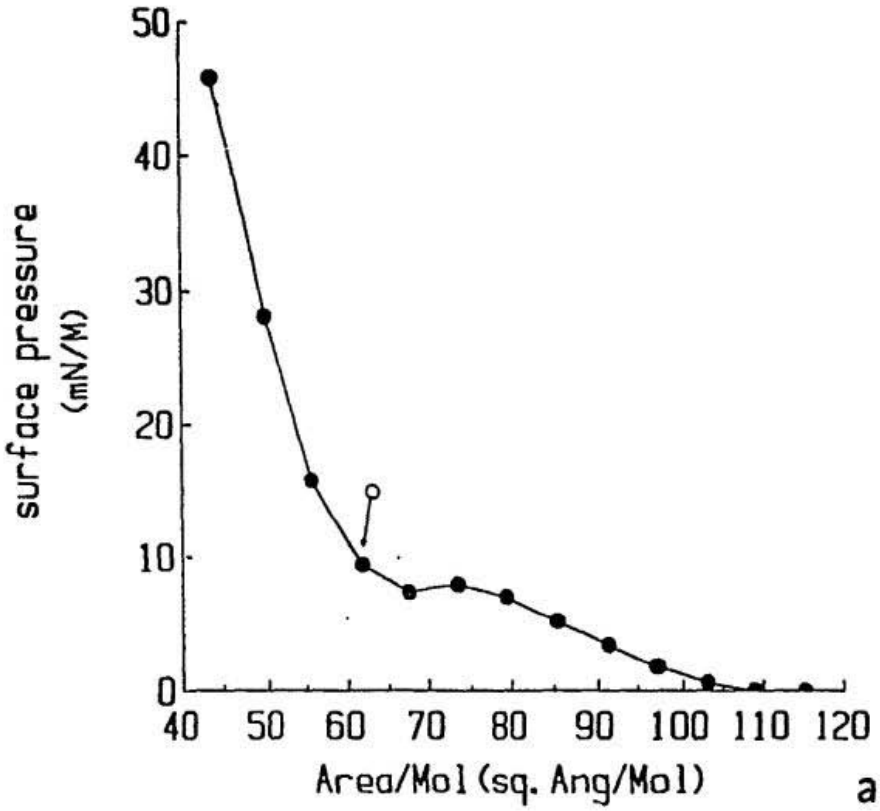
surface pressure
(mN/M)
50
40
30
20
10
0
40 50 60 70 80 90 100 110 120
Area/Mol (sq. Ang/Mol)
a

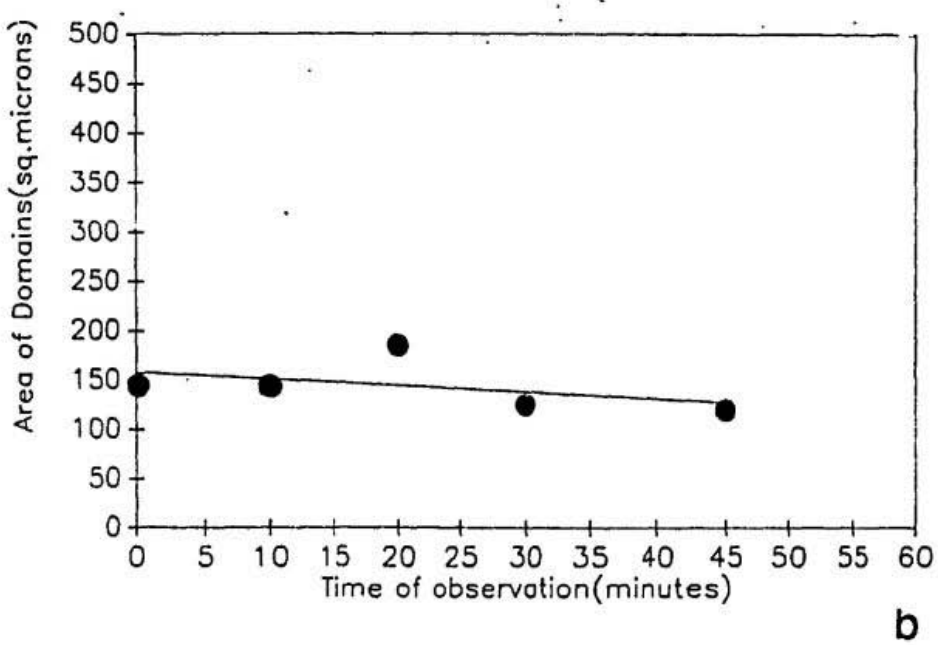
Area of Domains(sq.microns)
500
450
400
350
300
250
200
150
100
50
0
0 5 10 15 20 25 30 35 40 45 50 55 60
Time of observation(minutes)
b

fold slower compression velocitiey. At a number of molecular areas visual observations were performed 9 minutes after barrier stoppage, visual recording performed for the 10th minute and an average of 10 frames analyzed. The isotherm for a typical experiment performed at 19°C +- 1°C is shown in Figure 20a. The monolayer was compressed at a velocity of 0.13 $Å^2$/mol sec. The typical images observed at molecular areas of 76, 71, 61, 56 and 51 $Å^2$/molecule (+-2 $Å^2$/molecule) [shown by the points A, B, C, D and E on the isotherm] are shown in Figure 20b. The growth of the domains was observed to persist beyond the horizontal portion of the isotherm up to a surface pressure of 13 mN/m. The visual field at surface pressures beyond point E of the isotherm could not be recorded. This happened due to low fluorescence observed from the monolayer which may have been caused by self quenching of the probes at high surface pressures. The domains were visually observed to come into contact with one another at surface pressure of 15 mN/m but no fusion was seen. The shapes and peaks of the frequency distribution of the domains observed at this slow velocity of compression showed some what similar features between two experiments. The domain size distribution at identical area per molecule of two such experiments are shown in Figure 21.

IV. Quantative Analysis Of The Surface Architecture

The maximum size of domains observed for experiments conducted at slow compression rate was between 500 μ^2 and 1200μ^2

Figure 20. a) Isotherm of DPPC + 1mol% NBD-PC compressed in steps at a rate of 0.13$Å^2$/molecule/sec and a temperature of 19°C. The points A-E were visualized and recorded after 9 minutes of barrier stoppage on a video tape. b) Typical frame grabbed images from various regions of the isotherm. The fields were obtained at the following surface pressures(mN/M) A - 4.2, B - 4.5, C - 6.7, D - 9.6 and E - 15.1.
The white background represents the fluorescent areas and the dark areas the LC domains. Scale bar is 25 microns.
c) Frequency distribution of domain size analyzed from 20 images obtained at surface pressures A to E.

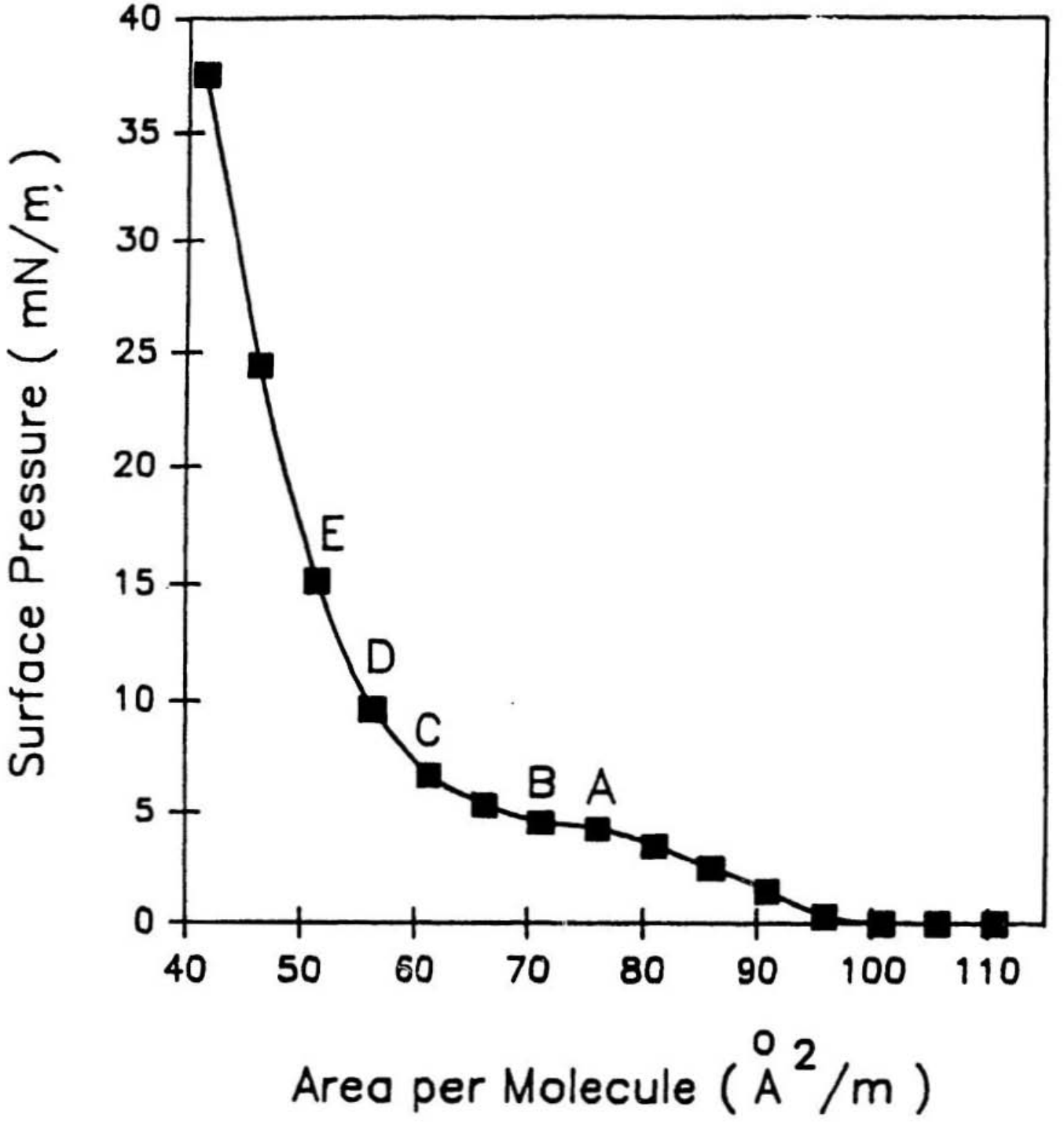
Surface Pressure (mN/m)
40
35
30
25
20
15
10
5
0
E
D
C
B
A
40
50
60
70
80
90
100
110
Area per Molecule (Å 2 /m)

a

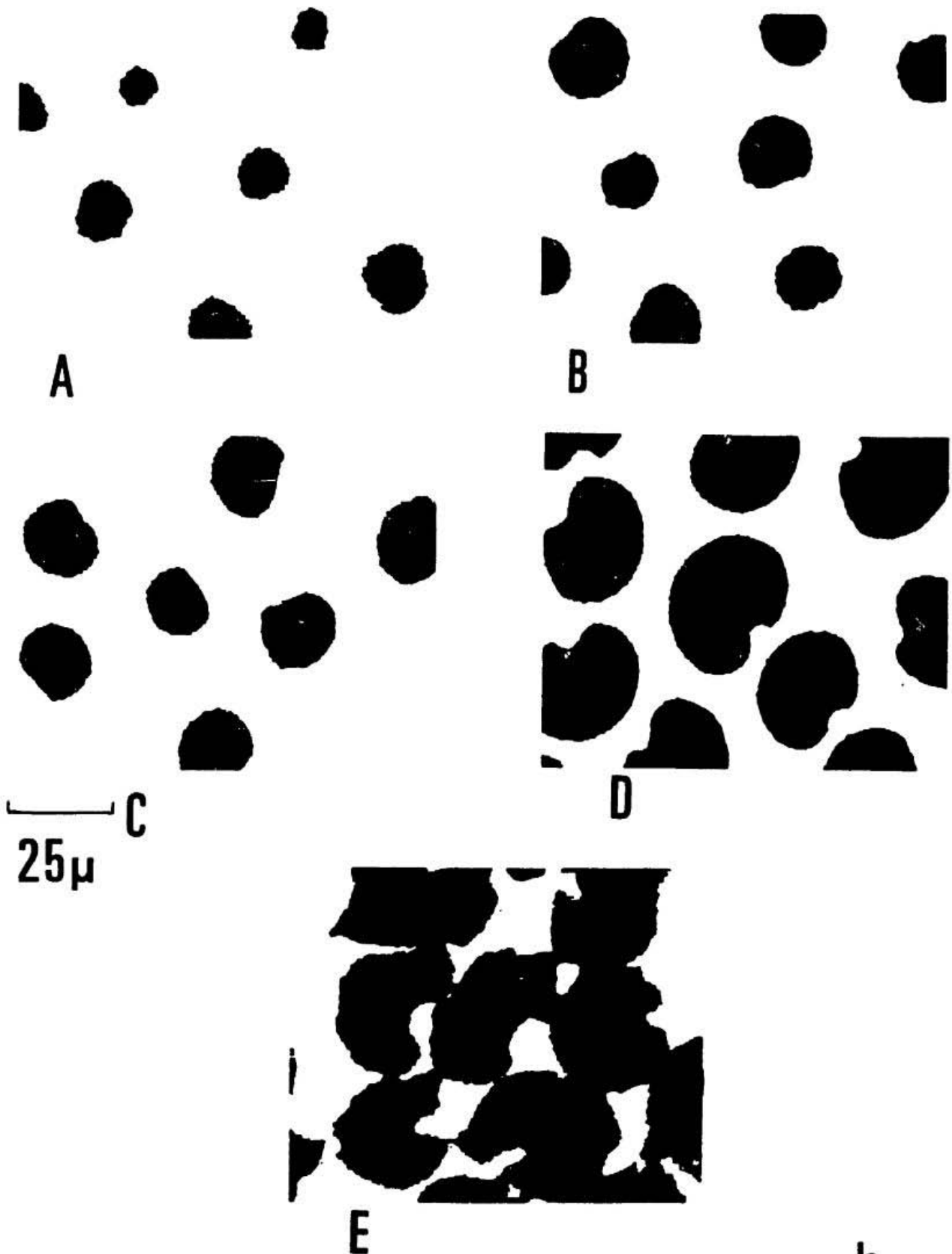
A
B
C
25μ
D
E
b

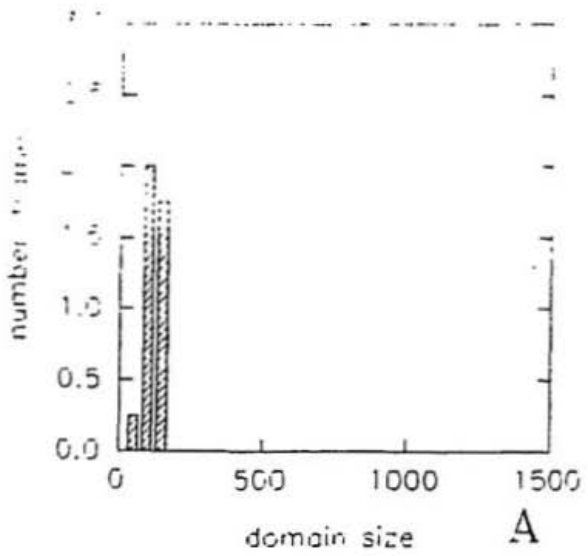
0.5
0.0
0
500
1000
1500
domain size
A

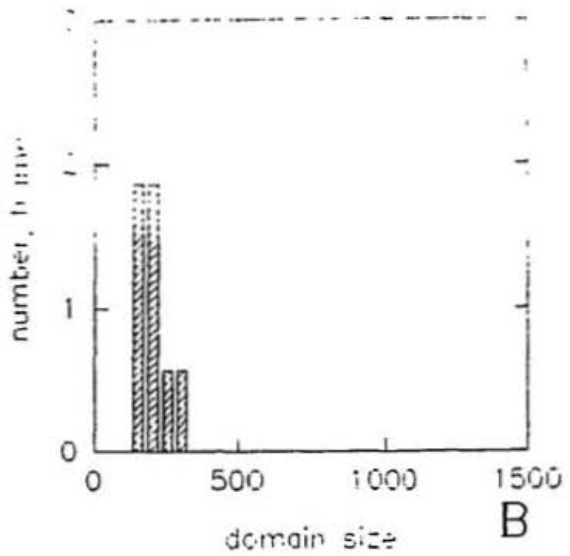
1
0
0
500
1000
1500
domain size
B

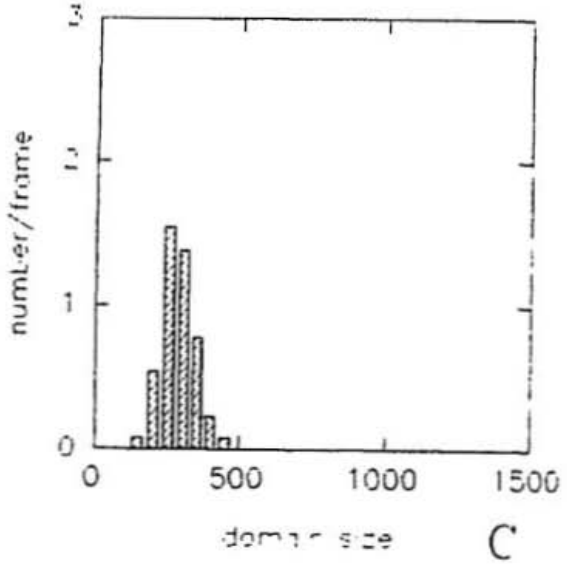
number/frame
1
0
0
500
1000
1500
C

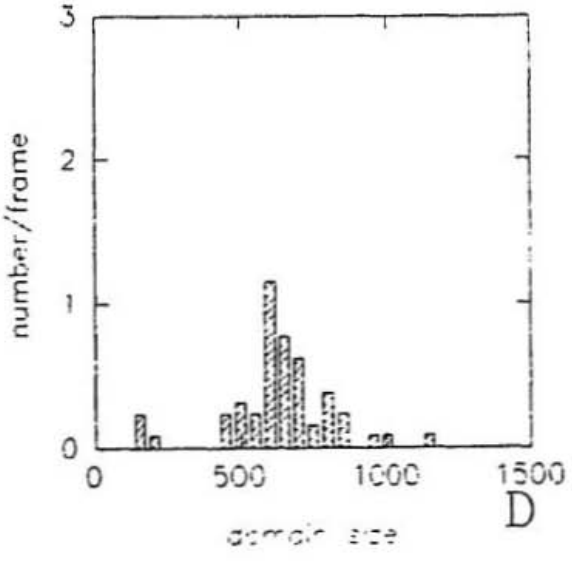
number/frame
3
2
1
0
0
500
1000
1500
D

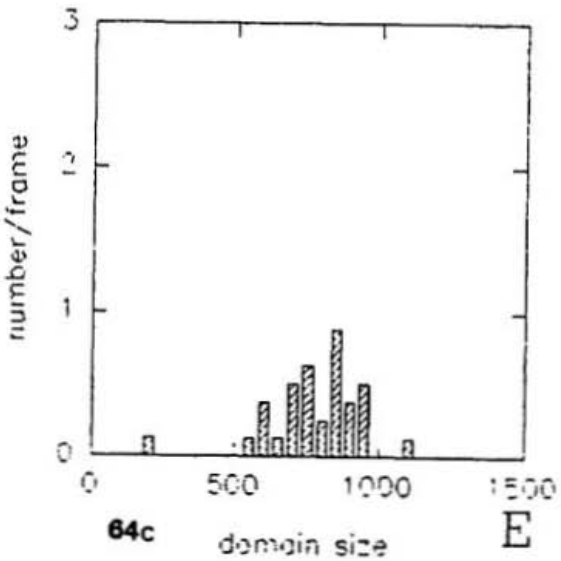
number/frame
3
1
0
0
500
1000
1500
E

64c

C

Figure 21. Frequency distributions of domain size obtained from two independent experiments. The images analyzed were obtained at a molecular area of 57 $Å^2$/molecule from individual experiments. The monolayers were compressed at a slow velocity of 0.13 $Å^2$/molecule/sec and the images obatained 9 minutes after barrier stoppage.

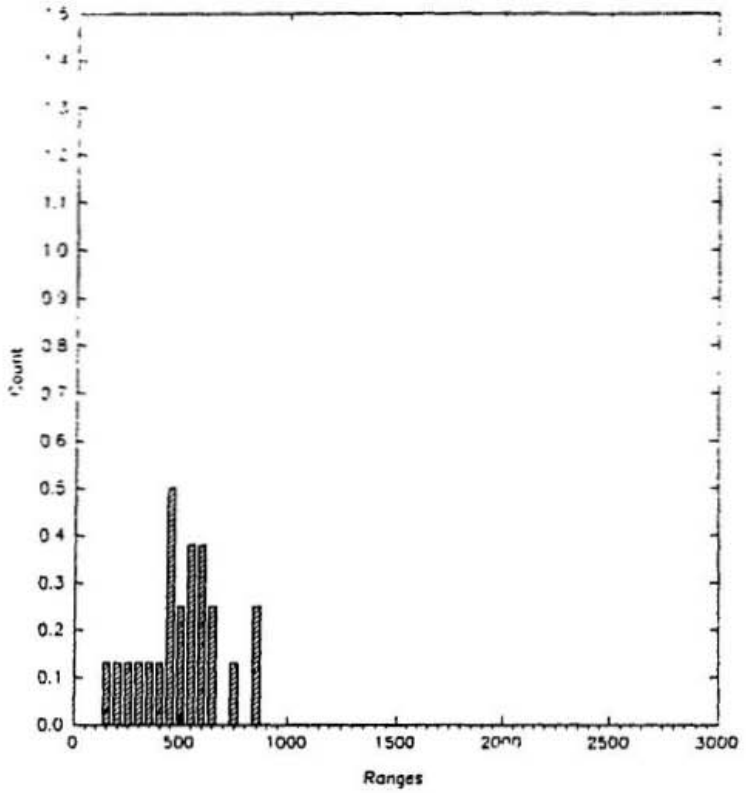
Count
0.0
0.1
0.2
0.3
0.4
0.5
0.6
0.7
0.8
0.9
1.0
1.1
1.2
1.3
1.4
1.5
0
500
1000
1500
2000
2500
3000
Ranges

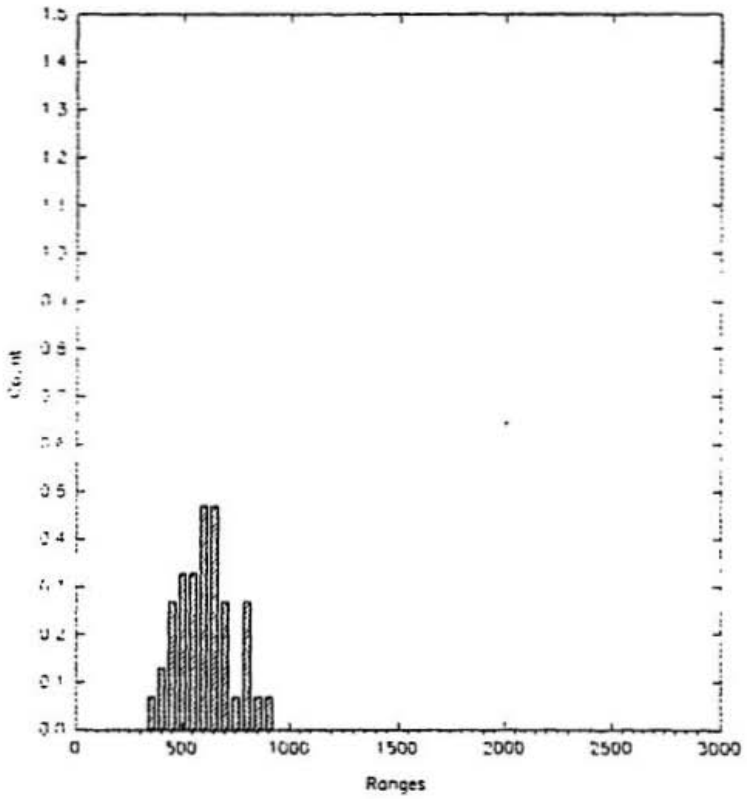
0
500
1000
1500
2000
2500
3000
Ranges

at molecular areas of ~ 50 A^2/molecule. These domains were mainly circular in shape at low surface pressures and did not change in shape with time, whereas at higher surface pressures the domains changed to a kidney bean shape with time. The frequency distributions of domain sizes are shown in Figure 20c. The frequency distributions of domain size were obtained by analyzing an average of 20 images obtained at specific molecular areas indicated by letters A to E in the isotherm shown in Figure 20a. The distributions of the domains at all the molecular areas analyzed were unimodal. At low surface pressures of 4.2 and 4.5mN/m the sizes of the objects were more regular as shown by the sharp peaks of the distributions A and B. At higher surface pressures the domains showed a more scattered distribution (D and E in Figure 20c) though they were very regular in shape. The size and shapes of the domains agree with the previously published data to a certain extent (Florsheimer 1989). We visually compared the domain shapes with the published images of these authors and performed some measurement on their images to determine domain width.

To compare the dimensions of the domains during fast and slow rates of compressions experiments were performed at a room temperature of 21°C (+- 1°C). The isotherms were printed on transparencies and the plots matched visually by overlaying the axis of one on the other. The surface pressure vs area/molecule numerical data of each of these isotherms were also

compared. The molecular areas between two sets of isotherms obtained at different velocities of compression had a deviation of 2 $Å^2$/molecule at any particular surface pressure. An average domain size comparison at molecular areas of 73, 62, 57 and 52 $Å^2$/molecule between two independent experiments at slow compression speeds are shown in Figure 22. The solid and the dashed lines represent the two individual experiments and the error bars indicate the standard deviation of domain size at any given area. At low surface pressures we observed a small scatter in domain size (as seen by the error bars) of about +-150μ^2. The standard deviation at higher surface pressures (or lower molecular areas of 57 and 52 $Å^2$/molecule) showed a greater scatter of size ranging to about +- 350μ^2. The results also indicate that when slow compression rates were applied there was a non linear dependency of domain size on area per molecule of the monolayer.

V. Domain growth dependency on compression rates

The frequency distributions of domain sizes for monolayers compressed at slow and fast compression rates at 21.5 +-1°C are shown in Figure.23a and 23b. As shown in the Figure 22a the average size of the domains at an area per molecule of 73 $Å^2$/molecule during slow compression was about 300 μ^2 whereas for the fast rates the average size at the same area per molecule was about 150 μ^2.

Figure 22. Average domain size plotted as a function of molecular area of two monolayers compressed at slow speed of 0.13 $Å^2$/molecule/sec. The solid and the dashed lines represent the data from two independent experiments performed at 21°C. The error bars represent the standard deviation of the domain size from the average. Note the growth of the domains are non linear as a function of molecular area.

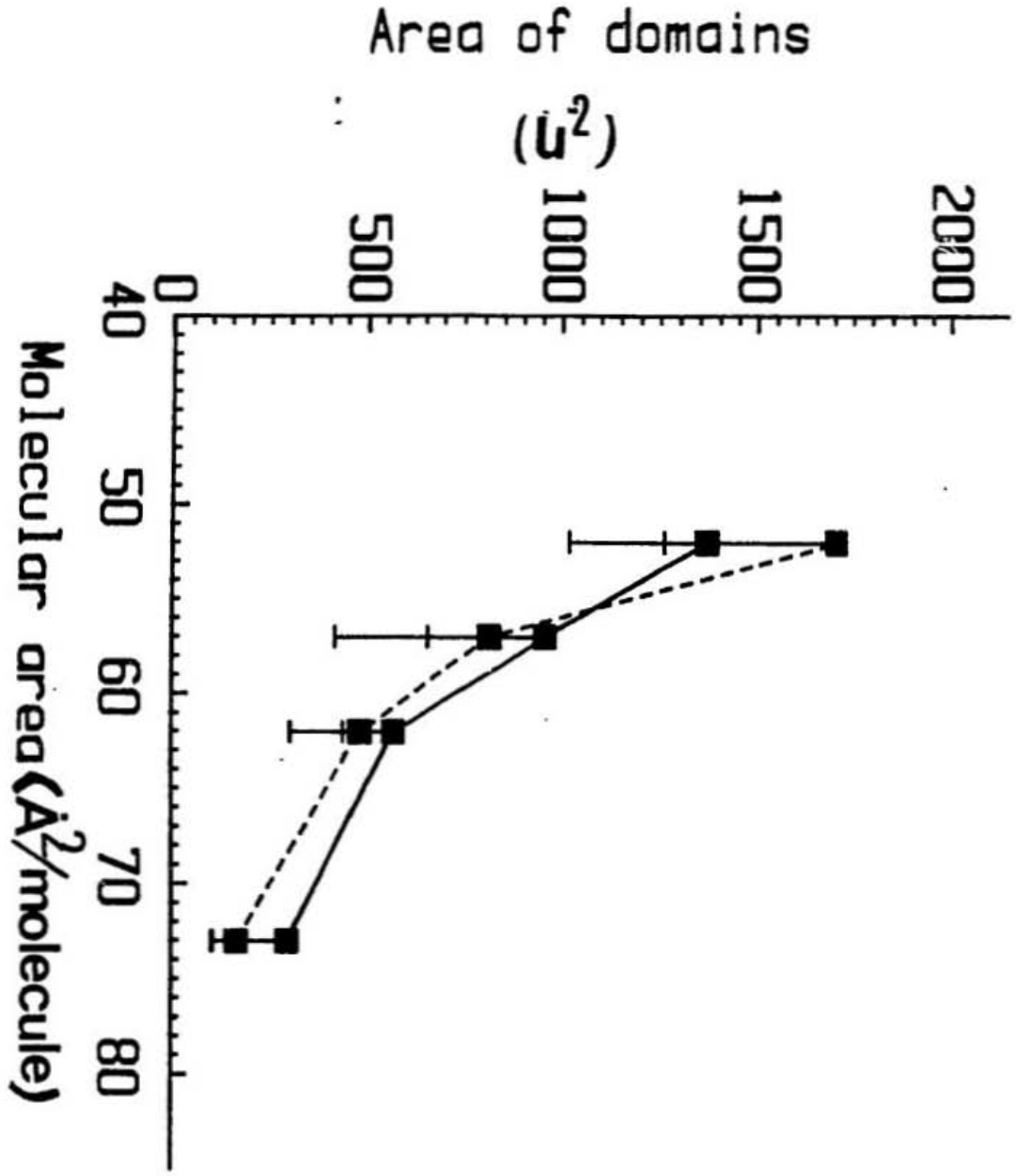
Area of domains
(μ^2)
0
500
1000
1500
2000
40
50
60
70
80
Molecular area ($Å^2$/molecule)

Figure 23.(a) Frequency distribution of domain size obtained from analyzing 20 randomly selected images of a monolayer compressed at 4 $Å^2$/molecule/sec (fast). The images were acquired from the monolayer at molecular area ($Å^2$/molecule) : A. 73, B. 62, C.57, D. 52 immidiately after barrier stoppage.
(b) Frequency distribution of domain size obtained from analyzing images from the same molecular areas of a monolayer compressed at 0.13 $Å^2$/molecule/sec (slow). Note the greater scatter of size observed in the distribution at low molecular areas (C and D).

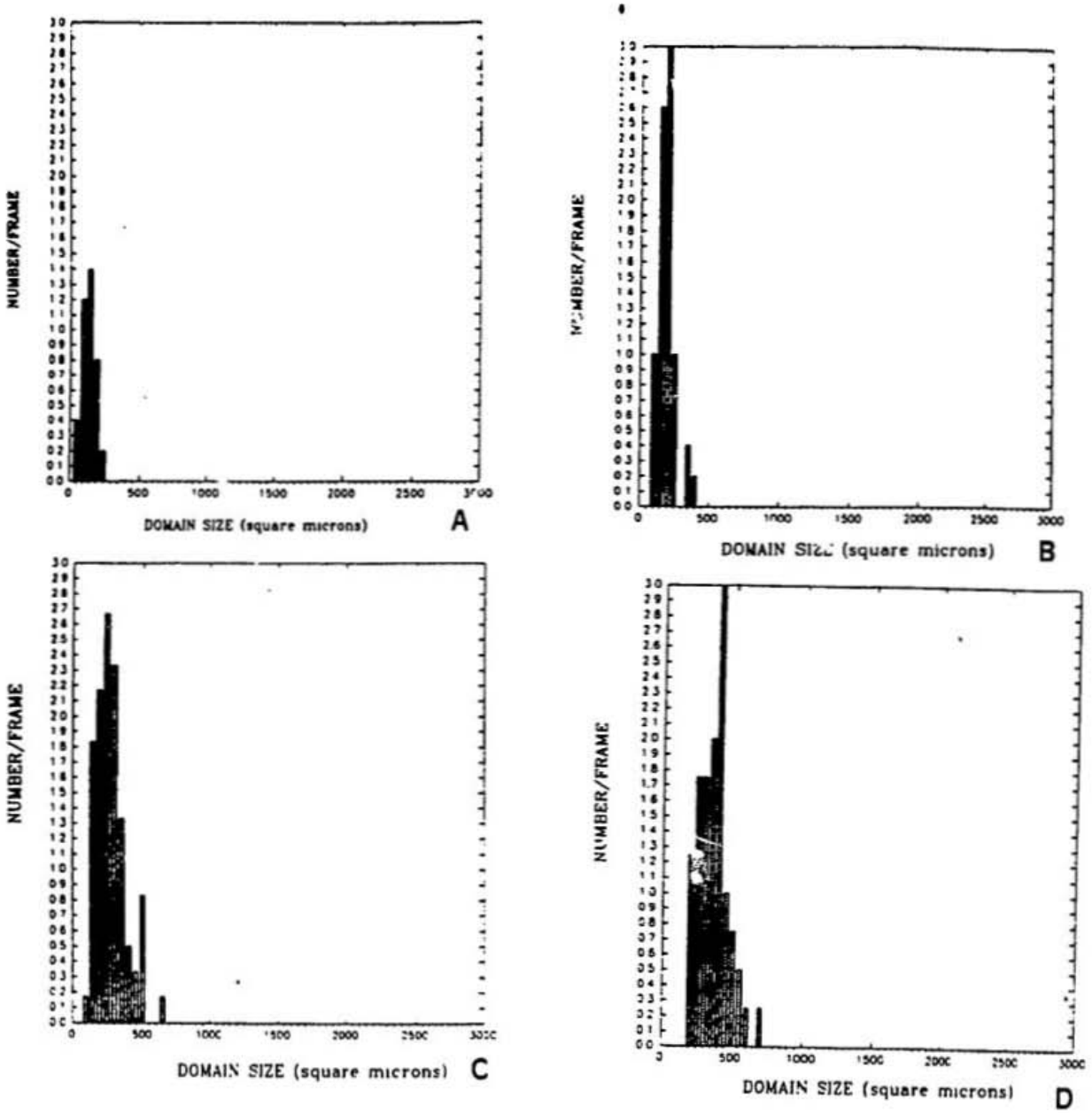
NUMBER/FRAME
DOMAIN SIZE (square microns)
A
B
C
D
a

The frequency distributions shown in Figure 23 show a greater scatter of size at low molecular areas (C and D in Fig.23b) at slow rates than at fast rates (C and D in Fig.23a) of compression. This pattern seemed to reverse itself when we considered the shapes of the domains. At high surface pressures the domains for the slow rates were homogenously kidney shaped over a large number of fields analyzed. These structures were visually observed to distribute themselves more regularly with nearly equal inter domain distances. This observation was also documented by other authors who compressed the monolayer at very slow speeds 10 - 30 $Å^2$/molecule hour (Rice 1984, Florsheimer 1989). The shapes of domains at the faster rate were complex and non homogenous as shown earlier in figure 16b.

Two comparative frequency distributions of domain size for fast and slow rates of compression are displayed in Figure 24A and 24B respectively. The frequency distributions were obtained from analyzing images from approximately the same surface pressure of 9 mN/m and identical molecular areas. Typical images analyzed for constructing the frequency distributions are shown in the inset of Figure 24A and 23B.

To examine the difference in the pattern of domain growth during the two different rates of compression the average size of the domains were plotted against their molecular areas as shown in Fig.25. The open squares in the plot represent the average size of the domains during slow compression and the solid

Figure 24. Frequency distribution of domain sizes calculated from two independent experiments compressed at different speeds, but at the same surface pressure. The images were recorded at a surface pressure ~ 9 mN/m (immidiately after barrier stoppage) during fast compression[4 $Å^2$/molecule/sec] (A), and at slow compression [0.13 $Å^2$/molecule/sec] (B)(9 mins after barrier stoppage). The typical images analyzed are shown inset of the distributions.

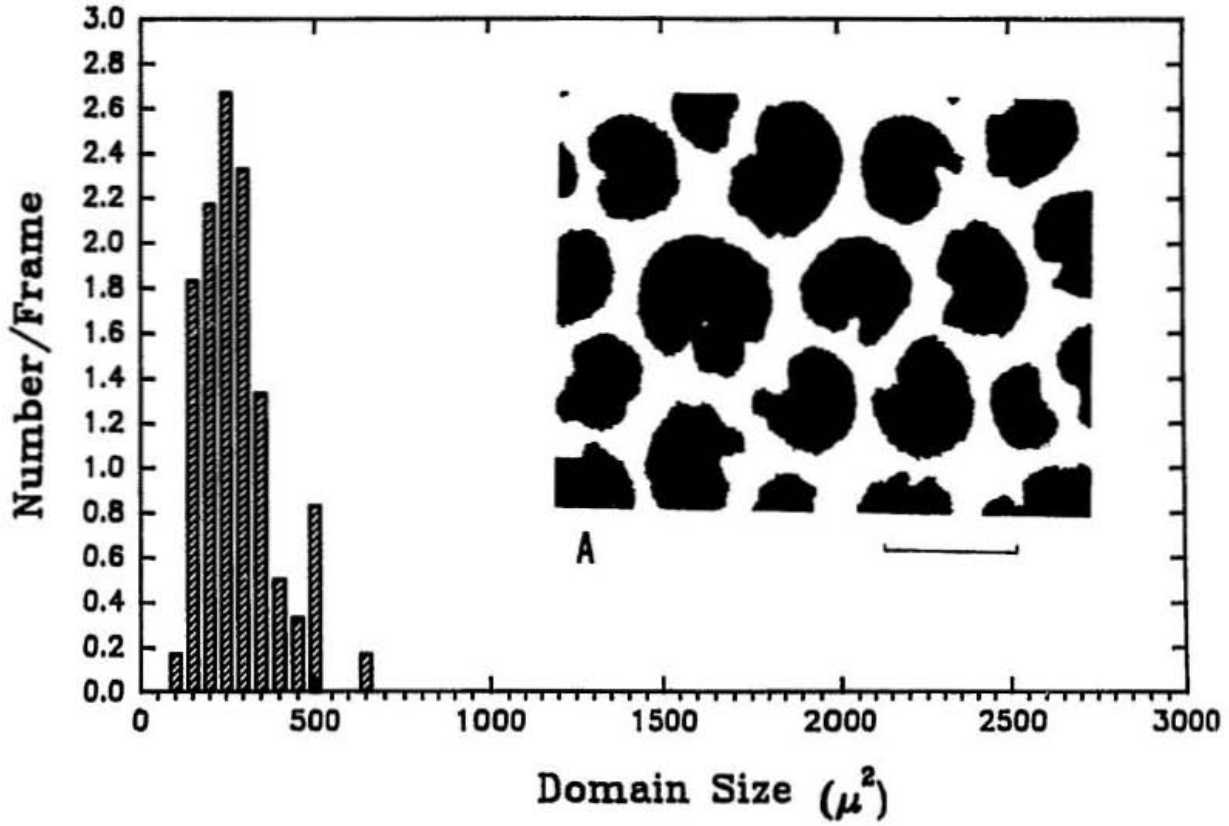
Number/Frame
Domain Size (μ^2)
A

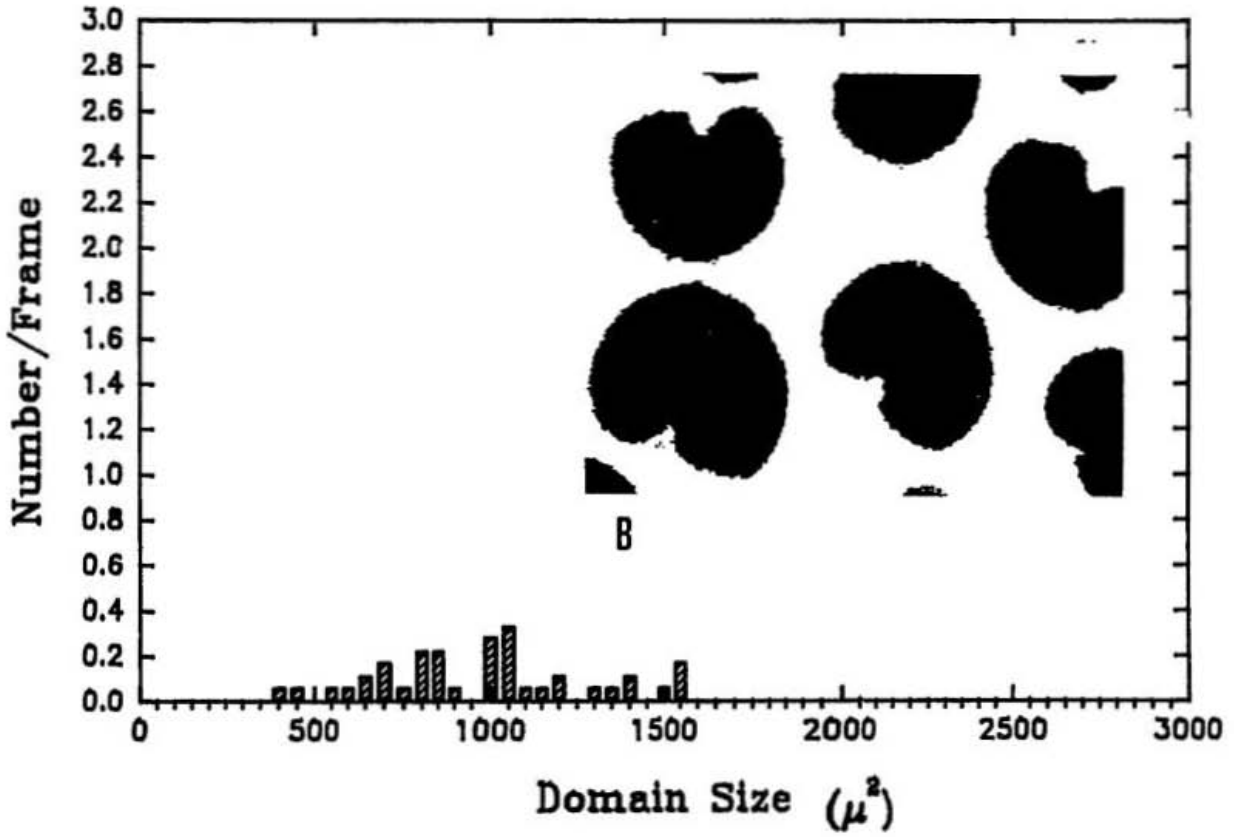
Number/Frame
Domain Size (μ^2)
B

Figure 25. Linear regression of domain size as a function of molecular area obtained from four independent experiments. The squares represent the average domain size during slow rates and the triangles the average domain size from fast rates. A straight regression line for the slow rate is drawn for comparitive purpose but regression may be non linear. (As indicated in Figure 22)

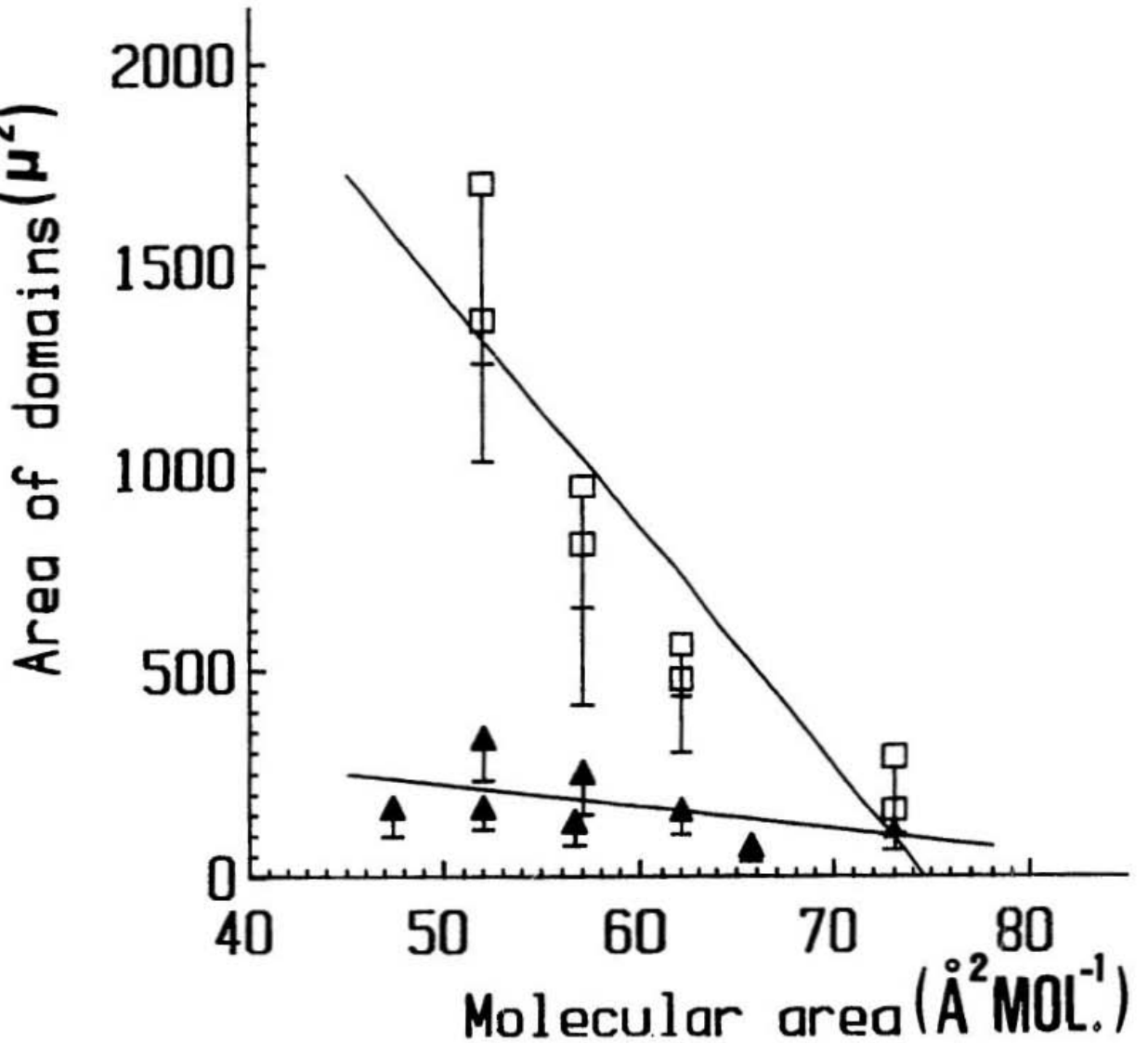
Area of domains (μ^2)
2000
1500
1000
500
0
40
50
60
70
80
Molecular area ($Å^2 MOL^{-1}$)

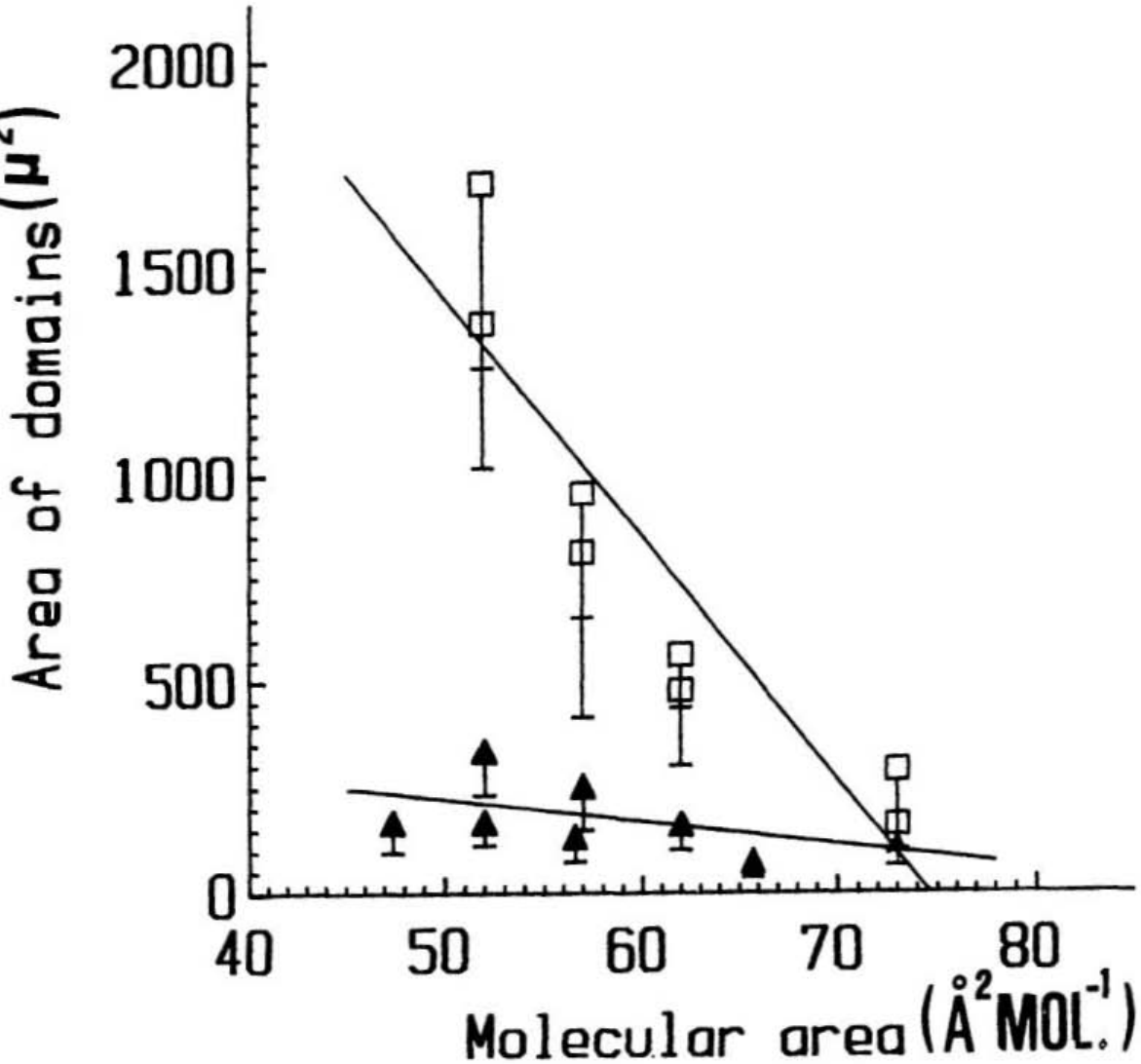
2000
1500
1000
500
0
Area of domains (μ²)
40
50
60
70
80
Molecular area (Å² MOL.⁻¹)

Figure 26. Histogram of average value of percent coverage by dark domains plotted against molecular area. The error bars in the histogram indicate standard deviation of the percentage data between two experiments. The percent coverage was obtained from analyzing 10 frames at each area per molecule from two independent experiments performed at 0.13 $Å^2$/molecule/sec.

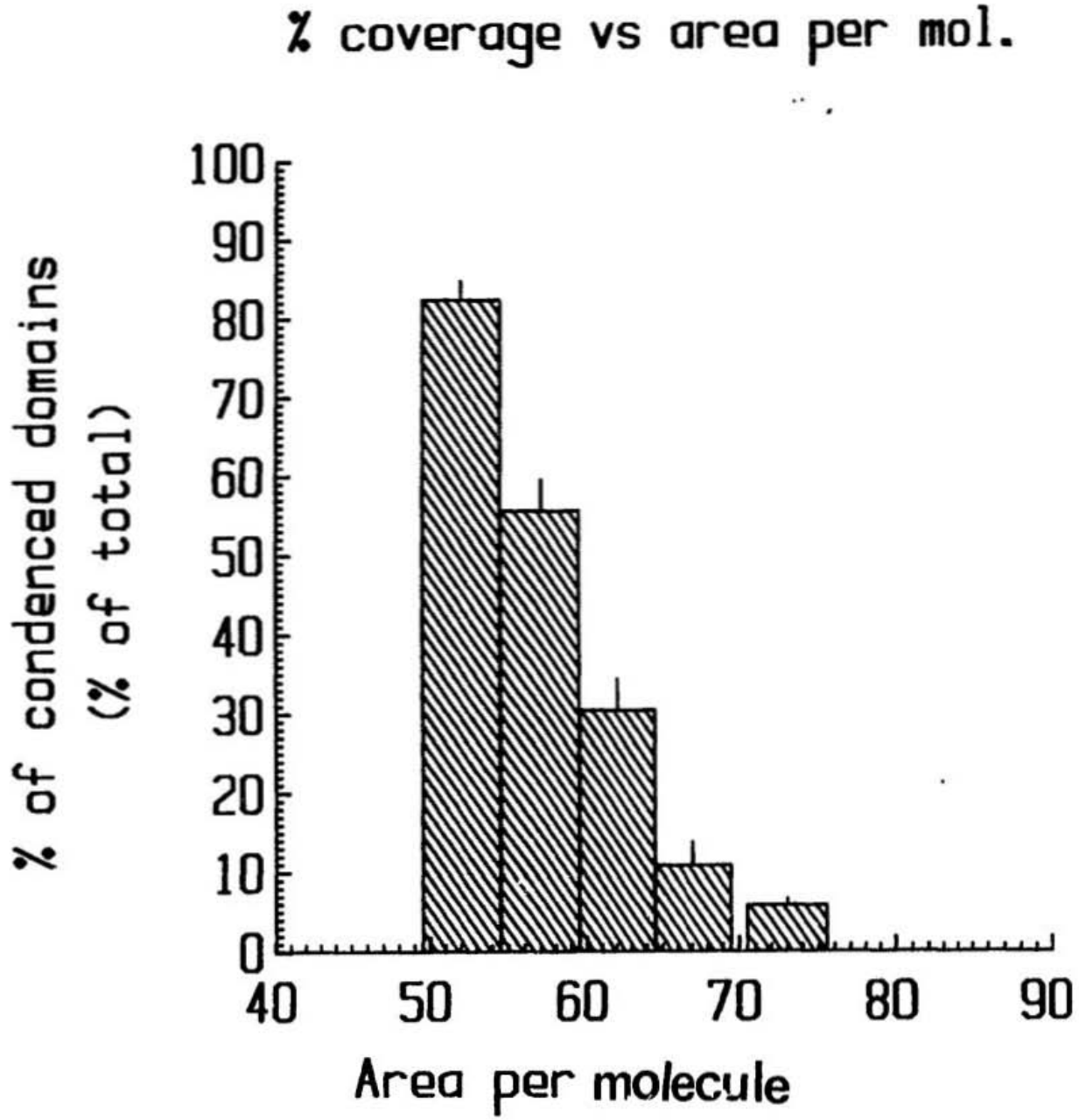
% coverage vs area per mol.
% of condenced domains
(% of total)
100
90
80
70
60
50
40
30
20
10
0
40
50
60
70
80
90
Area per molecule

VI. Other Monolayers

To observe whether domain formation occurred in the monolayer for lipid above its thermotropic phase transition temperature (T_c) 1-stearoyl,2-oleoyl phosphatidylcholine was compressed in a monolayer with 1 mol% of the probe NBD-PC. This phospholipid has one of its acyl chains unsaturated and is known to be in a chain - melted form at room temperature (Davis 1980). No break was noticed in the isotherm up to the point of monolayer collapse indicating that a LE to LC transition did not occur in this phospholipid. The isotherm of the monolayer is shown in Figure 27. Visually a continuous fluorescent field was observed to persist throughout the compression process from 0 mN/m up to 55 mN/m. This suggested a continuous liquid expanded phase persisted during compression. This result also suggests that the chain rigidity and tight packing of amphiphiles in the monolayer are major factors in domain formation and occurrence of a lateral phase seperation.

Another experiment with a binary mixture of lipids, DPPC + 2mol% cholesterol, showed distinctly different architecture of the monolayer in the phase transition region as shown in Figure 28. The dark domains seemed to form from distinct nucleation sites but grow to spiral shapes with increase of surface pressure. This observation indicates the susceptibility

Figure 27. Isotherm of SOPC + 1 mol% NBD-PC compressed at slow speed at a room temperature of 24°C. The collapse of the monolayer is indicated in the plot at 55 mN/m by the point c.

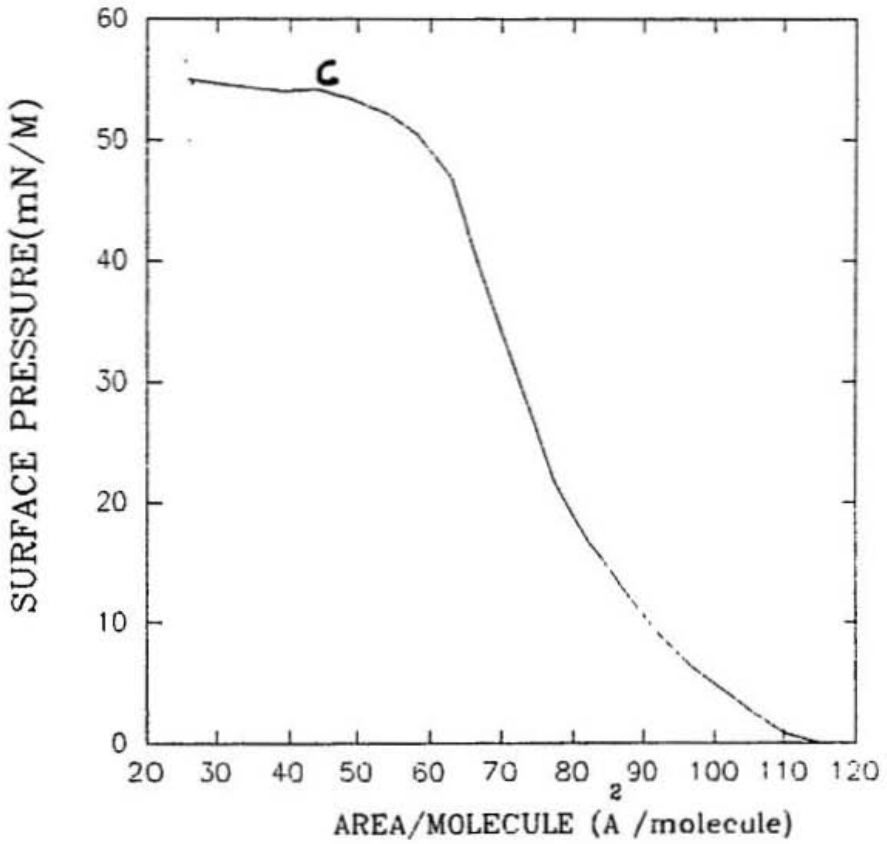
SURFACE PRESSURE(mN/M)
AREA/MOLECULE (A /molecule)
C
0
10
20
30
40
50
60
20
30
40
50
60
70
80
90
100
110
120

Figure 28. Typical image of DPPC + 2 mol% cholesterol obtained at a surface pressure of 5 mN/m, from the LE/LC phase transition region. Scale bar is 25 microns.

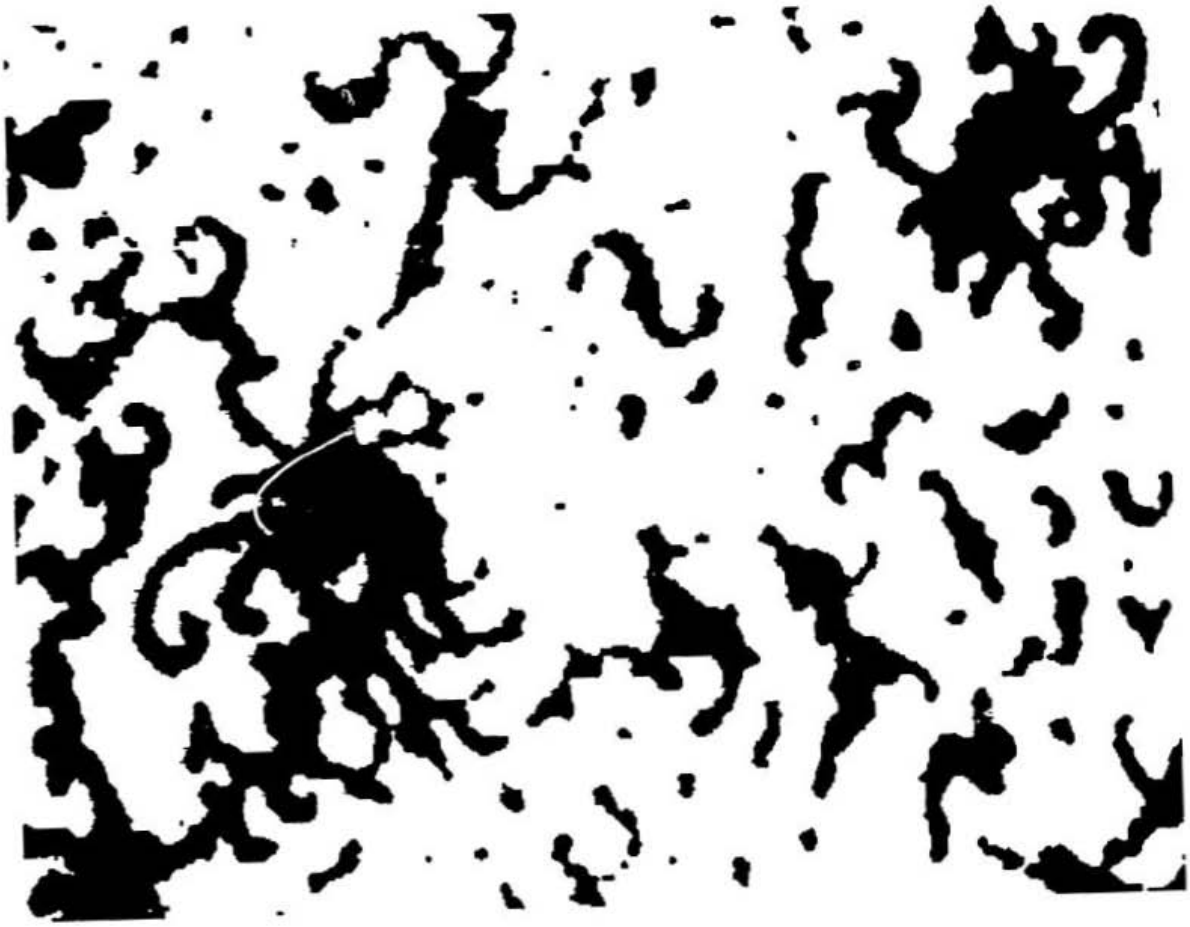
25 μ

that the lateral packing of the molecules of DPPC can be distinctly disrupted by small amounts of other substance. Others have also observed spiral and complex domain structures in DMPA/cholesterol (Heckle 1988) monolayers.

DISCUSSION

I. The Epifluorescence Microscopic Surface Balance (EMSB):Performance

In the last decade conventional surface balances have been modified for specific purposes, some for observation of monolayer architecture (McConnell 1984, Meller 1988, Mojtabai 1989), for diffusional rate measurement (Peters 1983), and for vibrational spectroscopy through FT-IR (Dluhy 1988). Our main objective in constructing this balance was ultimately to study the interaction of various lipids at the air - water surface in relation to the role of various components of the pulmonary surfactant in lowering the surface tension in the lungs. The balance could also be applied to study a number of physical phenomenon at the air - water interface and to study monolayers as models for membranes. Our instrument has a number of major advantages and some disadvantages when compared with other designs.

The balance was constructed to obtain fast rates of compression, as often used for pulmonary surfactant studies (Hawco 1981, Notter 1884). Through the stepper control motor and

programme, speeds of compression from 20 mm^2/sec (219 % of maximum area/min) to about 600 mm^2/sec can be achieved while visually observing the monolayer. The speeds of compression and expansion can be altered beyond these limits using the control programme (TEMP 6). Another worthwhile feature of this balance is that a number of cycles of monolayer compression and expansion can be performed without appreciable photobleaching of the probe, even with observation times over hours. In addition, surface pressure or surface tension as well as visual characteristics of the monolayer can be monitored as a function of time or area.

A large trough was used so as to obtain high compression ratios and facilitate the observation of any collapse phenomena at higher pressures. This could also aid the study of the transition phenomena from gas through to solid condensed phase of lipid monolayers. Our results with DPPC indicate that the monolayers could be compressed without leakage up to a surface pressure of 50 mN/m. DPPC monolayers at room temperature were shown by some workers to collapse at 72 mN/m surface pressure and at a molecular area of 40 A^2/ molecule (Notter 1984). A certain amount of leakage appeared to occur in our balance at high surface pressures, as we could observe the collapse occurring at 20 A^2/molecule (Shown in Fig. 17). This leakage may occur due to the molecules squeezing to an open interface around the barrier, or creeping up the walls of the trough at high surface pressures. Leakage has also been noticed

by others (Hildebran 1979, Notter 1981) and is a general problem faced in designs of Wilhelmy balances. A suggestion by one group (Goerke 1981) to alleviate this leakage and creep by applying a mixture of lanthanum/DSPC coating on the inner walls of the trough was attempted. Though our isotherms indicated a decrease of monolayer leakage when we applied the method in studying pure DPPC monolayers under rapid compression, we observed a definite contamination of the monolayer with DSPC during long observation times. Long observation times and a initial 30 minutes spreading time for the monolayer is necessary during any visual observation experiments. When a DPPC monolayer was compressed in the trough with the coating after 30 minutes of spreading, an isotherm having the characteristics of DSPC was observed. This observation indicated that DSPC leached out from the coating mixture and formed a monolayer over time. Thus we did not apply the method to our studies. These observations suggest that a different trough design needs to be considered in the future to monitor such high surface pressure regions of monolayers.

In an earlier design of EMSB high convective velocities of the monolayer at subphase depths above 1.6 mm was reported (Losche 1984). These workers observed a convective velocity of 10 micrometer/sec at a subphase depth of 1.6 mm. No appreciable changes of the convective velocities of the film were observed for subphase depths of 2 - 6 mm in our balance.

Convective velocities in the monolayer of about 10 micrometer/sec and about 4 micrometer/sec were estimated for the liquid expanded region and the liquid condensed region, respectively, for a typical isotherm of DPPC at room temperature. The velocities were determined from the time taken for a spot or domain to move a distance of 100 microns in the microscopic field of view. This slight movement of the monolayer has an advantage of allowing for sampling of a large number of images, since it leads to a large number of fields passing under the microscope objective.

Using the balance a problem was encountered in observing the monolayers at temperatures higher than that of the surrounding environment. The problem was caused due to vapour condensation in the objective lens limiting the visibility of the fluorescence from the interface. This problem was not encountered in an earlier design of EMSB by using an inverted fluorescence microscope to observe the monolayer from the subphase (Losche 1984). This method of using an inverted microscope has an apparent disadvantage. As the microscopic objective was fixed to the base of the trough in this design, fine adjustment of subphase depth was required to bring the monolayer into focus. Thus we did not incorporate this particular design in our construction of the EMSB. Further modifications of the balance are necessary to perform visual observation of the monolayer under conditions of variable temperature.

II. The EMSB : Application Perspective

The (EMSB) designed by us can be applied to study a number of physical and biological processes. Not only is the balance a valuable tool for studying physical properties of pulmonary surfactant but can be used to study monolayers as models of membranes and biochemical interactions at the interface.

As we have demonstrated the EMSB has the capability of performing fast compression and expansion of monolayers and allows visualization of this process. This capability can be utilized to investigate processes such as surface readsorption, respreading and mixing of lipids in monolayers over a short and long times. At present it is not very clear how a number of component lipids in pulmonary surfactant interact and enhance the adsorption and respreading of material in vivo during respiratory recycling of the monolayer (Keough 1984). During the cyclic compression of the monolayer the unsaturated lipid components may be squeezed out of the monolayer as suggested by some workers (Hawco 1981, Egberts 1989). It has been also been observed that DPPC respreads slowly in to monolayers (Galdstone 1967). *In vitro* studies show a reduction in the amount of the material from the monolayer with increasing number of compression - expansion cycles performed as long as the monolayer is compressed beyond

the point of collapse before expansion. This surface loss is observed as a gradual decrease in the total area of the hysteresis of surface tension - % pool area plots with increasing number of cycles performed on the DPPC monolayer. Understanding this process may be possible using the EMSB by observing the characteristics and number of the DPPC domains after performing a number of cycles on the monolayer. This information could be evaluated and correlated to pulmonary surfactant dynamics in vivo. The velocity of barrier movement of the EMSB can be adjusted to reflect respiratory rates.

Processes such as the effect of various ions on the domain structures of DMPA and DMPE have been studied using EMSB by a number of workers (Helm 1986, Eklund 1988). The effect of monovalent and divalent cations on DPPA domain shapes has been characterised by one group (Helm 1986). Another group has shown the effect of a range of Ca^{2+} ion concentration on phase separation of DPPA in monolayers (Eklund 1988). These data indicate that the domain shapes are susceptible to ionic changes of the subphase and the observation of these shape changes can be used as a criteria for studying ionic interaction of the polar molecules in monolayers. The instrument used by these workers and the one constructed by us allowed for easy manipulation of the subphase ionic condition. It has been shown by some workers that the alveolar lining fluid contains about 1.6 mM Ca^{2+} ions (Nielson 1984). Others have proposed that pulmonary surfactant

proteins have a role in forming the surface active monolayer and that they may interact with calcium ions from the fluid subphase (Scarpelli 1988). The subphase ions especially Ca^{2+} have been suggested to adjust orientation or alignment of surfactants at the air interface so that near zero surface tension could be achieved during compression (Bangham 1979). The EMSB may be used to perform a number of studies to evaluate the interaction of ions with charged phospholipids and protein components of the pulmonary surfactant.

Other applications of the EMSB could be in comprehending lipid-lipid and lipid-protein interactions as shown by some workers (Mohwald 1988,1990). Our balance has the capability of allowing a number of experimental parameters such as subphase pH, temperature and compression rates to be varied. These parameters have a crucial role in normal pulmonary surfactant activity <u>in vivo</u> as shown by some workers (Hildebran 1979). Studying the monolayer under variable conditions in the balance can yield important information on surfactant action in the alveolus.

A number of authors have used the EMSB to study monolayers as models for membranes using mixtures of lipids and proteins (Heckle 1988, Mohwald 1990). Molecular diffusion rates of DLPC and DPPC in monolayers has been calculated using one of the earliest designs of the balance (Peters 1982). Others have shown various patterns of interfacial arrangements of DPPC/

cholesterol (McConnell 1984), DMPA/cholesterol (Heckle 1988) and DPPC/glycolipid (Heckle 1985) mixtures in monolayers using the EMSB. Lipid interactions with a number of cytochrome proteins and bacterial antenna protein B-800 in monolayers has also been studied using the EMSB (Heckle 1985, Mohwald 1990). Though these monolayer lipid-protein studies are simplistic models for biomembrane lipid-protein association, a lot of valuable information was gained about protein arrangement in lipid environments from these studies.

Biochemical processes such as enzyme hydrolysis of DMPC in monolayers (Grainger 1990), binding of biotin to avidin (Blankenburg 1989) and acetylcholine interaction with its receptors (Krull 1990) were visualized using different designs of EMSB. Immunochemical binding of antigen to antibodies in monolayers of lipids has also been studied by another group using a modified version of the EMSB (Thompson 1988, Subramanium 1986) Some of the above mentioned results on DPPC and DMPA monolayer visual architecture have been substantiated by charge decoration electron microscopy (Fischer 1985), synchrotron X ray diffraction (Mohwald 1990) and fluorescence dichroism (Thompson 1984) techniques. These studies revealed the orientations of the phospholipid molecules on the interface, domain structural change due to the biochemical processes occurring, and a number of important dynamics of biomembranes, such as diffusional and lateral motion of the lipid molecules.

EMSB study on various fatty acids and phospholipid monolayers also have direct relevance in the field of applied physics, polymer science and the emerging fields of biosensor technology.(Meller 1989, Mohwald 1990). A number of workers have used the EMSB to study liquid crystals of organic molecules polymer films (Meller 1989) and fractal pattern formation (Miller 1986). The instrument can also be used in studies directly pertaining to designing biosensor electrodes (Kuhn 1989) and molecular electronic devices (Mohwald 1988). Attempts to characterize physical processes such as foam formation (Moore 1983, Knobler 1990), dipole orientation at the interface for amphiphiles (Florsheimer 1989) and surface photoreactions (Seul 1990) using the EMSB were undertaken recently by some workers.

These varied applications demonstrate that the EMSB can be used as a versatile tool for emerging fields of research in biological and physical sciences. From our preliminary work on DPPC monolayers it is clear that the instrument has certain capabilities and limitations in studying pulmonary surfactant in vitro.

III. Lateral Compression of Amphiphiles: Domain Structures

Amphiphilic molecules organized at the air-water interface affect the surface tension property of a water surface. The molecules, when compressed together in a monolayer have a

reduction of their area per molecule and inter - molecular distances and thus decrease the area of the open water interface. This decrease of open interface can be monitored as a decrease in the surface tension of the water or an increase in the surface pressure. The increase in surface pressure for most amphiphiles having double acyl chain and large headgroups, such as DPPC, is nonlinear. The non - linearity can be recorded as isothermal phase transitions as indicated by certain horizontal breaks in the isotherm (Shown in section II of Results). By analogy to a three dimensional compression of a gas, the phase transition process in monolayers occur from gas to liquid, and finally from liquid to solid, with increasing surface pressure. By using the EMSB some of these phase transitions for DPPC could be observed. The liquid - expanded to liquid - condensed transition for DPPC was visually observed to occur with some interesting characteristics and could be examined with ease using the EMSB.

The LE/LC phase transition process can be modelled as organizing of the molecules in various regions of a DPPC monolayer as shown in Figure 29. These ordered areas can be visualized as dark domains (as shown in figure 21b) which were observed by us and other workers (Florsheimer 1989). Depending on the size of the headgroup of the lipid molecule the acyl chains are suggested to be oriented normal to the monolayer plane (as for DMPE and DMPA) or tilted (as for DPPC) giving rise to different domain shapes (Sackmann 1987, Vanderlick 1990). The

Figure 29. Diagrammatic representation of a model showing the possible arrangement of DPPC in the LC (dark areas) and the LE regions (light areas) of a monolayer. The fluorescent probe (F) molecule preferentially remains in the liquid regions, due to chain disorder of that phase. (Drawn by Jesus Perez Gil)

DV
HYPOPHASE
LC
LE
AIR

shapes of domains observed by these workers range from circular and elliptical to more complex flower like structures. The liquid - expanded areas are suggested to have disorganization of chains (Fischer 1984), and the probe molecule being a lipid analogue with a bulky fluorescent group associates itself with these disorganized lipid regions. The probe 3,3,-dioctadecycloxacarbocyanine perchlorate, which associates with liquid - condensed areas due to their appropriate molecular orientation, was shown to produce fluorescent domains in DPPC monolayers at the phase coexistence region (Meller 1988). The DPPC domain structures observed by us are similar to the structures of DMPA monolayers observed by charge decoration electron microscopy (Sackmann 1987). FT-IR studies of the LE/LC region of the DPPC monolayers showed a high degree of acyl chain order (Dluhy 1989). We can thus infer from these studies and our results that the structures observed are not a probe artefact but real organization of the molecular species occurring at the LE/LC phase transition of the DPPC monolayer.

As observed by us (section III of results) and others the DPPC domains exhibit various shapes. For DPPC monolayers compressed at speeds of 10 A^2/molecule/hour the domains were mainly elliptical or "kidney bean" shaped (Florsheimer 1989). Others have shown different domain shapes depending on the chirality of the DPPC molecules (Weis 1984). Using the R-isomeric form of the lipid as found in nature we observed

two different shapes of domains depending on the rate at which the monolayer was compressed. Our results indicate that the domains are circular in shape at low surface pressures for both fast and slow rates of compressions. Above the surface pressure of ~ 10mN/m the shapes of the domains become irregular for fast speeds of compression. For slow speeds of compression the domain shapes are elliptical and with time become kidney - shaped as shown in section III of the results. We have also observed that the growth process occurs by finger like projection occurring at the edge of the domains. Figure 30 shows the domains growing from image A with these finger-like projections and shape changes to the structures shown in image C. Figure 30C was taken 10 minutes after barrier stoppage whereas 30B was obtained during the compression process. It seems probable from our results that at high surface pressures the domains may undergo a change or deformation of shapes from circular to kidney bean. This evidence allows us to believe that the domains are metastable structures, the shape depending on local microscopic instabilities of the surface pressure.

Recently it has also been shown that the domain shapes are actually the result of a structural transition, from string to hexagonal phases (McConnel 1990, Vanderlick 1990). These phases arise due different molecular arrangement of the headgroup and chain of the phospholipids at the interface during compression (McConnel 1990). The calculations of this group (McConnel 1989) and others (Vanderlick 1990) suggest that under.

Figure 30. Sequential images showing the growth of individual domains from a surface pressure of 11 mN/m (A) to 18 mN/m (C). The image B in the middle was obtained at a intermediate pressure between A and C without barrier stoppage. Scale bar is 25 microns.

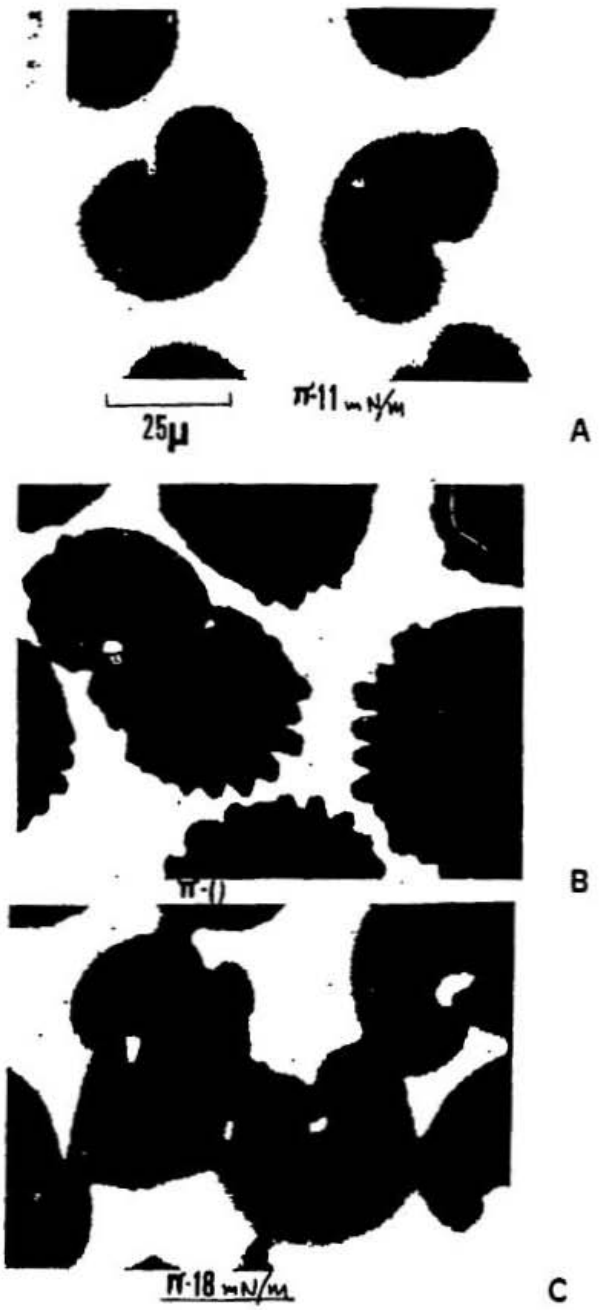
25μ
π-11 mN/m
A
π-1
B
π-18 mN/m
C

specific conditions, isolated finite lipid domains can undergo a shape transition (Keller 1987). This transition is assumed to occur due to change from a hexagonal arrangement of the molecules inside a domain at lower surface pressure to a string - like arrangement at higher surface pressures. The string like arrangement can be enhanced and visualized by incorporating cholesterol in trace amounts in the monolayer. Our suggestion is that the shape transition may also be dependent on compression rates of the monolayer, and that the change of molecular arrangements are dependent on time.

To comprehend whether the domains are equilibrium or non - equilibrium structures one has to consider the forces acting on them. Some workers have shown that DPPC domains have a net electrostatic charge on them due to the headgroup alignment in the condensed phase, the headgroups acting as individual dipoles, and the domains as collection of dipoles (Florsheimer 1989). The dipoles inside a domains are oriented in a regular manner and thus the domains possess a net dipole moment. Due to this total dipole moment in the condensed phase of the monolayer the domains repel each other. The domains can thus be attracted or repelled by an electrical field applied parallel to the interface (Florsheimer 1989, Mohwald 1990). The domains are suggested to also have a line tension at their boundaries, involving the topologically one -dimensional interface between regions of condensed and expanded phase (Moy 1988). These workers suggest that the equilibrium shapes of domains are

determined by a competition between this line tension and the long range electrostatic repulsions between molecular dipoles of the lipid (Moy 1989). We suggest that the different rates of compression might affect the line tension and the dipole alignment of the molecules in different ways, thus resulting in the difference of shapes and size of the domains. During slow rates the molecules have more time for stabilization of these forces acting on them. Due to this non random alignment of the headgroups are possible and more regular shaped domains were observed during slow rate of compression.

The heterogeneity of domain shapes observed during fast rates could be explained as some process critically changing the effects just described, and not allowing the molecules in the domains to organize in a regular manner. Our results with observing domain shapes and size with time (shown in section III of Result) showed no change of domain size and shape with time during fast rates of compression. This suggests that once altered the line tension and electrostatic forces are not changed any further with time, or at least over the time period that we used for observation. And thus the domains were observed to grow to a specific shape and size and did not show structural changes with time. Thus we may speculate that the domains are meta stable structures at the fast rate of compression.

IV. Quantitative Analysis of the Surface Texture

Quantitative estimation of the domain size and distribution for DPPC monolayers has been limited to work by two groups until now (Florsheimer 1989, McConnell 1984). Most of these workers were investigating either the properties of biological membranes or the phase transition process in two dimensions. The information available from their work is complex and comparison of our data with theirs could only be performed subjectively. The methods of image analysis performed by these workers (Florsheimer 1989, McConnell 1984) are different than ours. Their quantative estimates of domain perimeter and width were based on assumptions of the domain shapes being circular. Their measurements were performed mainly on circular domains of DPPA monolayers (Losche 19[illegible]) and some averaged data for domain width for DPPC monolayer were published (Florsheimer 1989). The dimensions of the non - circular domains were calculated by complex formulas based on their method of image analysis. Due to this difference in methods of analysis between us and the above mentioned workers, only some of our estimates of domain size and percentage of LC/LE areas for DPPC monolayers could be compared but they agreed to a certain extent with their data as discussed below. There is also no information available on the statistical estimates these workers used to analyze images, such as number of frames counted, time of image acquisitions, the surface pressure at which the images were recorded. .

Our quantitative estimates are based on randomly-selecting recorded frames which had been obtained in real time, and averaging the data of domain size, total area of LC regions per frame and domain perimeter. Our analysis of the images showed a distribution of domain size at all surface pressures as shown in the section IV of the results. For fast speeds of compression the distribution of domain size ranged from 100 to 400 μ^2 from the beginning to the end of LC phase respectively, and from 100 to 1500 μ^2 for slow speeds. For both rates of compression the frequency distribution always showed a modal distribution at higher molecular areas, as discussed in the section IV of the results. A decrease in molecular area below ~70 $Å^2$/molecule caused the domains to fall in two different paths of growth depending on compression speeds shown by the two different slopes of the regression lines in the domain size vs area/molecule plot in Figure 25. Large domains with greater scatter in size were observed during slower speeds at low area/molecule. Small domains (100 - 400 μ^2) with less scatter in size were observed during fast speeds of compression (Section IV of Results) at low and high area per molecule. These results indicate a larger scatter of size of domains at low molecular areas for the slow compression experiments. The average width of domains at the onset of the LC phase transition calculated by one group (Florsheimer 1989) for DPPC monolayers at 30 °C was about 12 μ.

We calculated the diameter of domains at nearly the same molecular area, from an isotherm at 21°C to be about 10 μ. The calculation is performed from our data of average size of the domains on the assumption that the domains are mainly circular in shape at this molecular area. Considering the domains observed by this group were circular the average size of domains can be estimated (from their data on domain diameter) to range between 150 - 250 μ^2 at the onset of the LC region. This can be compared with our estimated average size of domains shown in figure 25 of about 200 μ^2 at a area per molecule of 73 A^2/molecule. Another group of workers have shown the distribution of domain width for DMPA monolayers at the onset of the LE/LC phase transition to show a modal frequency distribution (Losche 1988). The domain sizes at all surface pressures in our results usually showed a modal distribution. Though the data from these workers allow some comparison with our results, a greater amount of quantitative information on the LC/LE phase is required for direct comparison. Due to the different experimental conditions used between the other groups and ours, we can only form a rough comparison of the LC/LE phase transition of DPPC monolayers.

During slow compression rates the average size of domains with decreasing molecular area showed a non-linear increase of domain size as shown in the figure 22. These preliminary quantitative estimates allow us to speculate that the

domain growth is dependent on compression rates, as well as other factors shown by earlier workers (Florsheimer 1989, McConnell 1984). The slow rates of compression allow the domains to grow to a large size and more regular shape, though their size distribution at low molecular areas are scattered over a large range. This scatter was not observed in the frequency distribution of domains at low molecular areas in the monolayers compressed at fast speeds.

The % of total area of dark domains (condensed phase) in the monolayer as observed by us and others (Florsheimer 1989) showed a coverage of 85% - 90% of the total area at surface pressures where the LC to solid phase transition occurs. The fact that the % dark area does not reach 99 % at that region may be due to the probe not allowing the molecules to be packed at higher densities. It is also possible that a single solid phase may not exist at those pressures. A suggestion put forward by some workers (Florsheimer 1989) states that a condensed to solid phase transition may occur at high surface pressure in DPPC monolayers, and thus the features observed do not describe a single homogenous phase. They also suggest that the nature of this transition may be diffuse and of a higher order than unity. Thus it is possible that we could not observe any change of architecture of the monolayer other than a reduction of convective velocity to 0 cm^2/sec, or a rigidity of the monolayer occurring at high surface pressures. The quantitative

characterization of high surface pressure regions by EMSB have been limited in experiments to date. We observed a decrease in fluorescence to occur at these surface pressures due to possible fluorescence quenching. The quenching may occur due to squeezing of the probe molecules together, thus limiting visual observation. Some other method such as decreasing probe concentration in the monolayer needs to be applied for observing high pressure regions. We did not observe any architectural changes and dynamics of the monolayer indicative of a collapse, at pressures of ~ 72 mN/m. This region of the isotherm is thought to indicate a collapse of the monolayer. The collapse may occur due to the monolayer folding on itself and forming multilayers in the air or the subphase. None of the other workers has mentioned or produced evidence of visualizing this area of the isotherm using the EMSB.

V. Applicability to the Study of Lung Surfactant

DPPC was investigated by us mainly because of it's presence in pulmonary surfactant in major amounts and it's surface tension lowering properties in monolayers. This lipid was suggested to be responsible for lowering the surface tension of the alveolar fluid interface at 37°C (King 1972). Above the thermotropic transition temperature (T_c) of 41°C the molecule could only reduce surface tension to 20mN/m. This phenomenon suggests that some sort of molecular ordering of the acyl chains

does occur at the interface during reduction of surface tension . This phenomenon was also observed with short chain fatty acid lecithins such as DMPC below it's T_c suggesting that the behaviour of surface tension reduction was dependent on chain rigidity rather than the nature of the fatty acyl chains (Hawco 1982). Most biological systems have PC with one or more of its chains melted at 37°C. DPPC thus seems to be a unique molecular species present in the lungs of warm blooded animals and possessing rigid acyl chains at physiological temperature. Suggestions have been made that animals living at low temperature may not require a significant amount of DPPC in their surfactant (Lau 1981).

The domain structures observed are directly related to this acyl chain rigidity. Our preliminary results on SOPC and DOPC monolayer seems to indicate this. Monolayers of these molecules, due to one or both of the chains being unsaturated are above their T_c at room temperature and show no such structural arrangement as in DPPC, but also show a melted or liquid expanded phase. As our preliminary results show that 2 mol% of cholesterol can cause dramatic change in domain shapes it can be speculated that the line tension mentioned earlier is altered by trace amount of other lipid in lecithin monolayers as suggested by some workers (Mohwald 1990). Thus we suggest that EMSB studies can be fruitful in evaluating complex lipid mixtures and, possibly pulmonary surfactant in monolayers.

As visual observation is possible for a number of cycles in the EMSB it would be interesting to investigate the role of various components of the surfactant, especially the charged amphiphiles such as PG, PI and PS. Phenomena such as squeeze out and surface resorption may be amenable to investigation by our method.

Recently another group of workers using FT-IR have shown that a large degree of conformational order exists in monolayers of DPPC at the phase transition region (Mitchell 1988). This conformational order as measured by the CH stretching modes of acyl chains was also observed in monolayers of pulmonary surfactant (Dluhy 1989). These workers suggest that the additional components of the surfactant do affect the acyl chain ordering of DPPC in monolayers (Dluhy 1989). The EMSB may be used to study these complex monolayers, and new insights as to the configuration of surfactant phospholipids and protein at the air - alveolar interface can be derived from the studies.

CONCLUSIONS

Some general conclusions can be made about the instrument and the preliminary results obtained from the studies of DPPC monolayers:

1. The EMSB can be used to study a number of pulmonary surfactant components and their mixtures in monolayers, under slow and fast compression rates.

2. The fluorescent lipid analogue NBD-PC did not substantially perturb the DPPC monolayer. Fluorescence from the monolayers can be observed for long periods of time. The technique may be used for observing the monolayer under a number of cycles of compression and expansion. These studies can shed light on poorly understood processes such as surface loss of material, squeeze - out, readsorption and respreading of molecules, as thought to occur in vivo to maintain a surface active monolayer in the lungs.

3. Beside its use in studying lipid distribution the instrument can be useful in studying lipid-protein interactions in monolayers, models for biological membranes and biochemical interactions at the air fluid interface.

4. DPPC domain formation is an indication of liquid - expanded to liquid - condensed phase transition in monolayers. The size, shape and distribution of liquid condensed domains are dependent on compression rates of the monolayer.

5. The DPPC domains grow from distinct nucleation sites during compression of the monolayer, and this growth in size is directly dependent on surface pressure. Individual domains do not fuse or coalesce with each other even at high surface pressures. No discrete liquid condensed to solid phase transition was observed visually at high surface pressures.

6. At a molecular area of 52 $Å^2$/molecule when 1 mol% of probe NBD-PC was in the monolayer the domains occupied about 85% of the monolayer area.

7. The process of packing DPPC into domains can be distinctly changed by cholesterol. Spiral and complex non - circular domains were observed at high surface pressures in a DPPC/cholesterol monolayer, compressed at 0.13 $Å^2$/molecule/sec.

8. The unsaturated lipid SOPC did not show any domain formation and phase transition when compressed in monolayers.

REFERENCES

Adam N.K. The physics and chemistry of surfaces. Ch.2, 3rd ed. Oxford University Press, N.Y. **1968.**

Albrecht O. The construction of a microprocessor-controlled film balance for precision measurement of isotherms and isobars. Thin Solid Films, 99:227 **1983.**

Albrecht O., Gruler H. and Sackmann E. Polymorphism of phospholipid monolayer. J. Physiq. (Paris), 39:301 **1978.**

Ashbaugh D.G., Bigelow D., Petty T.L. and Levine B.E. Acute respiratory distress in adults. Lancet, 2:319 **1967**

Avery M.E. and Mead J. Surface properties in relation to atelectasis and hyaline membrane disease. A.M.A.J. Dis. Childr.97:517 **1959.**

Bachofen H., Schürch S, Urbindli M and Weiber E.R. Relation among alveolar surface tension, surface area, volume and recoil pressure. J. Appl. Physio., 62:1878 **1987.**

Bangham A.D. Lung surfactant: How It Does and Does not Work. Lung, 165:17 **1987.**

Bangham A.D., Morley C.J and Phillips M.C. The physical properties of an effective lung surfactant. Biochim. Biophys. Acta, 573:552 **1979.**

Berge B., Simon A.J. and Libchaber A. Dynamics of gas bubbles in monolayer. Phys. Rev.A, 41 (12):6884 **1990.**

Birdi K.S. Lipid And Biopolymer Monolayer At Liquid Interfaces. Ch.4, Plenum Press, N.Y. **1988.**

Blankenburg R., Meller P., Ringsdorf H. and Salesse C. Interaction between Biotin lipids and Streptavidin in monolayers : Formation of oriented two dimensional protein domains induced by surface recognition. Biochem., 28:8214 **1989.**

Buckingham S. and Avery M.E. Time of appearance of lung surfactant in foetal mouse. Nature, 193:688 **1962.**

Burghardt T.P. and Thompson N.L. Effect of planar dielectric interfaces on fluorescence emission and detection. Evanescent excitation and high aperture collection. Biophys. J., 36:420 **1984.**

Cadenhead D.A. Monomolecular films as biomembrane models.in Structure and Properties of Biomembranes Vol.III, CRC Press Inc. Florida **1985.**

Cadenhead D.A. and Müller-Landau F. Molecular packing in steroid lecithin monolayers IV.Mixed films of epicoprostenol with dipalmitoylphosphatidylcholine. Can. J. Bioch. Cel. Biol. 62:732 **1984.**

Cadenhead D.A., Müller-Landau F. and Kellner B.M.J. Phase transitions in insoluble one and two-component films at the air/water interface,in Ordering in Two Dimensions, Elseiver/North Holland, Amsterdam, **1980.**

Chapman D., Williams R.M. and Ladbrooke B.D. Physical studies of phospholipids IV. Thermotropic and lyotropic mesomorphism of some 1,2,-diacyl phosphatidylcholines (lecithins). Chem. Phys. Lip., 1:445 **1967.**

Clements J.A. and King R.J. Composition of the surface active material in The Biochemical basis of pulmonary function. Vol.2 Mercer Dekker N.Y. **1976.**

Daneilli J.F and Davson H.A. A contribution to the permeability of thin films. J. Cel. Com. Physiol., 5:495 **1934.**

Davis P.J., Coolbear K.P. and Keough K.M.W. Differential scanning calorimeter studies of the thermotropic behaviour composition of Dipalmitoyl lecithin and mixed acid unsaturated lecithins. Can. J. Bioch. 58:851 **1980.**

Dluhy R.A., Reilly K.E, Hunt R.D., Mitchell M.L., Mautone A.J. and Mendelssohn R. Infrared spectroscopic investigation of pulmonary surfactant:Surface film transitions at the air-water interface and bulk phase thermotropism. Biophys. J., 56:1173 **1989.**

Egberts J., Sloot H., and Mazure A. Minimal surface tension, squeeze out and transition temperature of binary mixtures of dipalmitoyl phosphatidylcholine and unsaturated phospholipids. Biochim. Biophys. Acta, 1002:109 **1989.**

Eklund K.K., Vurinen J., Mikkola J., Virtanen J.A., and Kinnuen P.K.J. Ca^{++}-Induced lateral phase separation in phosphatidic acid/phosphatidylcholine monolayers as revealed by fluorescence microscopy. Biochem., 27:3433 **1988.**

El Mashak E.M., Lakhdhar-Ghazal F. and Tocanne J.F. Effect of pH, mono and divalent cations on mixing of phosphatidylglycerol and phosphatidylcholine. A monolayer and fluorescence study. Biochim. Biophys. Acta, 688:465 **1982.**

Enhorning G. Pulsating bubble techniques for evaluating pulmonary surfactant. J. App. Physiol., 43:198 **1977.**

Enhorning G. Surfactant research of interest to the clinicians. Prog. Resp. Res. 25:209 **1990.**

Fischer A. and Sackmann E. Electron microscopy and electron diffraction study of coexisting phases of pure and mixed monolayers transferred onto solid substrate. J. Col. Int. Sci., 112:1 **1986.**

Fischer A. and Sackmann E. a charge-decoration technique for studying the heterogeneity of coexistent monolayer phases by electron microscopy. Nature, 313:299 **1985.**

Florsheimer M. and Mohwald H. Development of equilibrium domain shapes in phospholipid monolayer phase transition. Chem. Phys. Lip., 49:231 **1989.**

Forward K. A theoretical and experimental study of phospholipid phase behaviour. NSERC Summer Report, Memorial University of Newfoundland. **1987.**

Fujiwara T. Surfactant replacement in neonatal RDS. Pulmonary Surfactant. ed. Van Golde and Battenberg, Elseiver, Amsterdam.

Gaines G.L. Insoluble monolayers at the Liquid-Gas Interface. Wiley Interscience, N.Y., **1966.**

Gladstone M. and Shah D.O. Surface properties and hysteresis of Dipalmitoyl lecithin in relation to alveolar lining layer. Biochim. Biophys. Acta, 137:255 **1967.**

Gaub H.E., Moy V.T. and McConnell H.M. Reversible formation of plastic two-dimensional liquid crystals. J. Phys. Chem., 90:1721 **1986.**

Grainger D.W., Reichert A., Ringsdorf H. and Salesse C. An enzyme caught in action:direct imaging of hydrolytic function and domain formation of phospolipase A_2 in phospatidylcholine monolayers. FEBS Lett., 252 (1,2) 73 **1989.**

Grainger D.W., Reichert A., Ringsdorf H. and Salesse C. Hydrolytic action of phospolipase A_2 in monolayers in the phase transition region : direct observation of enzyme domain formation using fluorescence microscopy. Bichim. Biophys. Acta, 1023:365 **1990.**

Gershfeld N.L. Physical chemistry of lipid films at fluid interface. Ann. Rev. Phys. Chem., 27:349 **1976.**

Gershfeld N.L. The liquid condensed/liquid expanded transition in lipid films : a critical analysis of film balance experiment. J. Coll. Int. Sci., 85:28 **1982.**

Georgallas A. and Pink D.A. Phase transition in monolayers of saturated lipids : Exact results and Monte Carlo simulations. J. Coll. Int. Sci., 89:107 **1982.**

Goerke R.J. Lung surfactant. Biochim. Biophys. Acta, 344:241 **1975.**

Goerke R.J. and Gonzales J. Temperature dependence of dipalmitoyl phosphatidylcholine monolayer stability. J. Appl. Physiol. 51:1108 **1981.**

Gorter E. and Grendel F. On biomolecular layer of lipids on the chromocytes of blood. J. Exp. Med. 41:439 **1935.**

Hallman M., Merrit T.A., Cochrane C.G. and Gluck L. Human surfactant substitution in severe respiratory distress. Prog. Resp. Res., 18:193 **1984.**

Hawco M.W., Coolbear K.P., Davies P.J. and Keough K.M.W. Exclusion of fluid lipid during compression of monolayers of mixtures of dipalmitoylphosphatidylcholine with some other phosphatidylcholines. Biochim. Biophys. Acta, 646:185 **1981.**

Hawgood S.B. Pulmonary surfactant apoproteins: A review of proteins and genomic structure. Am. J. Physiol., 257:L-13 **1989.**

Hawgood S.B., Benson J. and Hamilton R.L(Jr) Effects of surfactant associated protein and calcium ions on the structure and surface activity of lung surfactant lipids. Biochem., 24:184 **1985.**

Heckle W.M. Personal communication.

Heckl W.M., Cadenhead D.A. and Mohwald H. Cholesterol concentration dependence of quasi-crystalline domains in mixed monolayers of the cholesterol-DMPA system. Langmuir, 4:1352 **1988.**

Heckl W.M., Losche M., Scheer H. and Mohwald H. Protein/Lipid interactions in phospholipid monolayers containing the bacterial antennae protein B800-850. Biochim. Biophys. Acta, 810:73 **1985.**

Helm C.A. Laxhauber L., Losche M. and Mohwald H. Electrostatic interactions in phospholipid membranes.I.Influence of monovalent ions. Coll. Polym. Sci.,264:46 **1986.**

Helm C.A. and Mohwald H. Equilibrium and nonequilibrium features determining superlattices in phospholipid monolayers. J. Phys. Chem., 92:1262 **1988.**

Hildebran J.N., Goerke J. and Clements J.A. Pulmonary surface film stability and composition. J. Appl. Physiol., 47:604 **1979.**

Keller D.J., Korb J.P. and McConnell H.M. Theory of shape transition in two dimensional phospholipid domains. J. Phys. Chem. 91:6417 **1987.**

Keough K.M.W. Physical Chemical properties of some mixtures of lipids and their potential for use as Exogenous pulmonary surfactant. Prog. Resp. Res., 18:257 **1984.**

Keough K.M.W. and Kariel N. Differential scanning calorimetric studies of aqueous dispersions of phosphatidylcholines containing two polyenoic chains. Biochim. Biophys. Acta, 902:11 **1987.**

King R.J. and Clements J.A. Surface active material from dog lung. Amer. J. Physiol., 223:727 **1972.**

King R.J., Klass D.J., Gikas E.J. and Clements J.A. Isolation of apoproteins from canine surface active material. Amer. J. Physiol., 224:788 **1973.**

Knobler C.A. Seeing phenomena in flatland: Studies of monolayers by fluorescence microscopy. Science, 249:870 **1990.**

Korenbrot J.J. and Huang S.B. Proton transport by bacteriorhodopsin in planar membranes assembled from air water interface films. J. Gen. Physiol., 76:649 **1980.**

Krull U.J., Brennan J.D., Brown R.S., Hosein D., and Vandenberg E.T. Chemical transduction with fluorescent lipid membranes using selective Acetylcholine receptors with agonist/antagonist and Acetylcholine esterase with substrate. Analyst 115:147 **1990.**

Kuenzig M.C., Hamilton R.W. and Peltier L.F. Dipalmitoyl lecithin: Studies on surface properties. J. Appl. Physiol., 20:779 **1965.**

Kuhn H. Present status and future prospects of Langmuir-Blodgett film research. Thin Solid Films, 178:1 **1989.**

Lau M.J. and Keough K.M.W. Lipid composition of lung and lung lavage fluid from map turtles (Malclevys geographica) maintained at different environmental temperatures. Can. J. Bioch., 59:208 **1981.**

Losche M. Duwe H.P. and Mohwald H. Quantative analysis of surface textures in phospholipid monolayer phase transition. J. Coll. Int. Sci., 126:132 **1988.**

Losche M. and Mohwald H. A fluorescence microscope to observe dynamical process in monomolecular layers at the air water interface. Rev. Sci. Instr., 55:1968 **1984.**

Magoon M.W., Wright J.R., Bartussio A., Williams M.C., Goerke J., Benson B.J., Hamilton R.L. and Clements J.A. Subfractionation of lung surfactant : implication for metabolism and surface activity. Biochim. Biophys. Acta, 750:18 **1983.**

McConnell H.M. Harmonic shape transition in lipid monolayer domains. J. Phys. Chem., 94:4728 **1990.**

McConnell H.M. Theory of Hexagonal and stripe phases in monolayers. Proc. Nat. Acad. Sci.(USA), 86:3452 **1989.**

McConnell H.M., Tamm L.K. and Weiss R.M. Periodic structures in lipid monolayer phase transition. Proc. Nat. Acad. Sci.(USA), 81:3249 **1984.**

Meller P. Computer - assisted video microscopy for the investigation of monolayers on liquid and solid substrate. Rev. Sci. Instr., 59:2225 **1988.**

Meller P., Peters R. and Ringsdorf H. Microstructure and lateral diffusion in monolayers of polymerizable amphiphiles. Coll. Polym. Sci., 267:97 **1989.**

Miller A., Knoll W. and Mohwald H. Fractal growth of crystalline phospholipid domains in monomolecular layers. Phys. Rev. Lett. 56:2633, **1986.**

Mitchell M.L. and Dluhy R. In situ FT-IR investigation of phospholipid monolayer phase transition at the air - water interface. J. Am. Chem. Soc., 110:712 **1988.**

Mojtabai F. A convection free monolayer trough for fluorescence microscopic monitoring of ultrathin organic films. Thin Solid Films 178:115 **1989.**

Moore B., Knobler M.C., Broseta D. and Rondelez F. studies of phase transition in Langmuir monolayers by fluorescence microscopy. J. Chem. Soc.(Far.Trans.), 82:1753 **1983.**

Moy V.T., Keller D.J. and McConnell H.M. Molecular order in finite two dimensional crystals of lipid at the air - water interface. J. Phys. Chem., 92:5233 **1988.**

Mulıer B., Hasche H., Hohorst G., Skurk C., Puchnar A., Berhard W., and von Wichert D. Alteration of surfactant homeostasis in diseased lung. Prog. Resp. Res. 25:209 **1990.**

Mohwald H. Phospholipid and phospholipid protein monolayers at the air/water interface. Ann. Rev. Phys. Chem., 41:441 **1990.**

Nakagaki M. and Okamura E. The penetration of lysine into monolayers of lecithin from underlying aqueous solution. Bull. Chem. Soc. Jpn., 55:1352 **1982.**

Neuman R.D., Fereshtekhou S. and Ovalle R. Electron microscopic observations of LE/LC phase transition in dipalmitoyl phosphatidylcholine. J. Coll. Interf. Sci. 101:309 **1984.**

Nielson D.W. Electrolyte composition of the alveolar subphase in anesthesized rabbits. Ped. Res., 18:400 Abs.No. 1862 **1984.**

Notter R.H. Surface chemistry of Pulmonary Surfactant: the role of individual component. in Pulmonary Surfactant Ed. Van Golde. Elseiver, Amsterdam, Ch.2 **1984.**

Notter R.H., Tabak S.A. and Mavis R.D. Surface properties of binary mixtures of some pulmonary surfactant components. J. Lip. Res., 21:10 **1980.**

Obaldem M., Scwarz H., Kattner E. and Stephen P. Results with artificial surfactant: Aspects of morphological appearance , surface activity and in vivo activity of artificial surfactant. Prog. Resp. Res., 25:209 **1990.**

Pagano R.E., Martin O.C., Schroit A.T. and Struck D.K. Formation of asymmetric phospholipid membrane via spontaneous transfer of fluorescent lipid analogues. Biochem., 20:4920 **1981.**

Pattle E.R. The cause of stability of bubbles derived from the lung. Physiol. Med. Biol., 5:11 **1960.**

Peters R. and Beck K. Translational diffusion in phospholipid monolayers measured by fluorescence microphotolysis. Proc. Nat. Acad. Sci (USA), 80:7183 **1983.**

Phillips M.C. and Chapman D. Monolayer characteristics of saturated 1,2,diacyl phosphatidylcholines (lecithins) and phosphatidylethanolamines at the air water interface. Biochim. Biophys. Acta, 163:301 **1968.**

Rice P.A. and McConnel H.M. Critical shape transition of monolayer lipid domains. Proc. Nat. Acad. Sci., 86:6445 **1989.**

Sackmann E., Fischer A. and Frey W. Polymorphism of monolayers of monomeric and macromolecular lipids: On the defect structure of crystalline phases and the possibility of hexatic order formation. in Physics of Amphiphilic Layers. Springer Proceedings in Physics 21 **1987.**

Scurch S., Goerke J. and Clements J.A. Direct determination of volume and time dependence of alveolar surface tension in excised lungs. Proc. Nat. Acad. Sci., (USA) 75:3417 **1978.**

Scurch S. New insights into principles of function and physiology of surfactants including its role in small airways. Prog. Resp. Res., 18:1 **1984.**

Scarpelli E.M. Surfactants and the lining of the lung. John Hopkins University Press, Baltimore **1988.**

Seul M. and Sammon M.J. Competing interactions and domain shape instabilities in monomolecular film at the air water interface. Phys. Rev. Lett., 64:1903 **1990.**

Suzuki Y. Effect of protein, cholesterol and phosphatidylglycerol on the surface activity of lipid-protein complex reconstituted from pig surfactant. J. Lip. Res., 23:62 **1982.**

Sklar L.A., Hudson B.S. and Simon R.D. Conjugated fatty acids as fluorescent probes: synthetic phospholipid membrane studies. Biochem., 16:819 **1977.**

Struck K.D. and Pagano R.E. Insertion of fluorescent phospholipids into the plasma membrane of a mammalian cell. J. Biol. Chem., 255:5404 **1980.**

Subramanium S., Seul M. and McConnell H.M. Lateral diffusion of specific antibodies bound to lipid monolayers on alkylated substrate. Proc. Nat. Acad. Sci. (USA), 83:1169 **1986.**

Thompson N.L., Palmer A.G., Wright L.L. and Scarborough A. Fluorescence techniques for supported planar model membranes. Comm. Mol. Cel. Biophy., 5:109 **1988.**

Thompson N.L., McConnel H.M. and Burghardt T.P. Order in supported phospholipid monolayers detected by the dichroism of fluorescence excited with polarized evanescent illumination. Biophys.J., 46:739 **1984.**

Van Golde L.M.G. The lipid components of the pulmonary surfactant system. in Report of 96thRoss Conference on Pediatric Research **1988.**

Vanderlick T.K. and Mohwald H. Mode selection and shape transitions of phospholipid monolayer domains. J. Phys. Chem., 94:886 **1990.**

Von Tscharner V. and McConnell H.M. An alternative view of the phospholipid phase behaviour at the air water interface:Microscope and film balance studies. Biophys. J., 36:409 **1981.**

Weis R.M. and McConnell H.M. Two dimensional chiral crystals of phospholipid. Nature 310:47 **1984.**

Wright J.R. and Stevens P.A. Surfactant metabolism in vivo. in Report of 96thRoss Conference of Pediatric Research. **1988.**

Zuckermann M.J., Pink D.A., Costas M. and Sanctuary B.C. A theoretical model for phase transition in lipid monolayers. J. Chem. Phys. 76:4206 **1982.**

APPENDIX A

NAMES AND STRUCTURES OF LIPIDS:

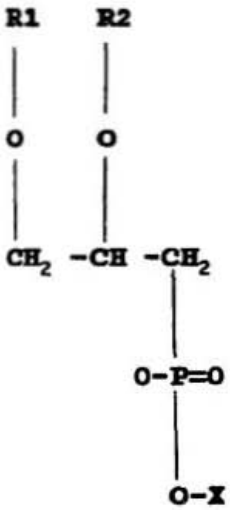

X- $(CH_2)_2 N^+(CH_3)_3$

X^1- $(CH_2)_2 N^+ H_3$

X^2- H

NBD- 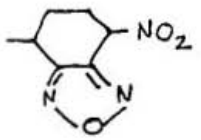

		R1 Acyl	R2 Acyl	X
DPPC	Dipalmitoyl phosphatidylcholine	$CH_3(CH_2)_{14}C=O$	$CH_3(CH_2)_{14}C=O$	X
DOPC	Dioleylphosphatidyl choline.	$CH_3(CH_2)_7CH=CH(CH_2)_7C=O$	$CH_3(CH_2)_7CH=CH(CH_2)_7C=O$	X
SOPC	1-stearoyl-2-oleoyl phosphatidylcholine	$CH_3(CH_2)_{16}C=O$	$CH_3(CH_2)_7CH=CH(CH_2)_7C=O$	X
NBD-PC	1-palmitoyl-2-NBD dodecanoyl phosphatidylcholine.	$CH_3(CH_2)_{14}C=O$	NBD-$NH(CH_2)_{11}C=O$	X

Pa-PC	**1-palmitoyl 2-paraniroyl phosphatidylcholine.**	$CH_3(CH_2)_{14}C=O$	$C_2H_5(CH=CH)_4(CH_2)_7(C=O)_2$	X
DMPC	**Dimyristoyl phosphatidylcholine**	$CH_3(CH_2)_{12}C=O$	$CH_3(CH_2)_{12}C=O$	X
DLPC	**Dilauryl phosphatidylcholine**	$CH_3(CH_2)_5C=O$	$CH_3(CH_2)_5C=O$	X
DMPE	**Dimyristoyl phosphatidylethanolamine**	$CH_3(CH_2)_{12}C=O$	$CH_3(CH_2)_{12}C=O$	X^1
NBD-PE	**Dipalmitoyl -NBD phosphatidylethanolamine.**	$CH_3(CH_2)_{14}C=O$	$CH_3(CH_2)_{14}C=O$	$(CH_2)_2NH$-NBD
DMPA	**Dimyristoyl phosphatidic acid.**	$CH_3(CH_2)_{12}C=O$	$CH_3(CH_2)_{12}C=O$	X^2

APPENDIX B

Programme TEMP6/ C language
Written and compiled by Carl Boland.

```
/*#####################################################################
############*/
#include <dir.h>
#include <errno.h>
#include <stdio.h>
#include <dos.h>
#include <conio.h>
#include <graphics.h>
#include <stdlib.h>
#include <ctype.h>
#include <string.h>
#include <math.h>

/*#####################################################################
############*/

#define BACKGROUND1     GREEN
#define BACKGROUND2 LIGHTGRAY
#define PLOTTING    BLUE
#define GRID        WHITE
#define BG  setbkcolor(BACKGROUND1)
#define FG1 setcolor(BACKGROUND2)
#define FG2 setcolor(PLOTTING)
#define FG3 setcolor (GRID)

#define MOUSE 0x33
#define SM inregs.x.ax=1; int86(MOUSE,&inregs,&outregs)
#define HM inregs.x.ax=2; int86(MOUSE,&inregs,&outregs)

#define WIDTH       7.8
#define LENGTH          19.1
#define STEPSIZE    0.00254
#define COLLAR          17.2
#define MOLAREACONST    16.6113
#define POOL        148.9
#define WORKING         166.1

#define CLOCKFREQ   100000
#define DEFAULTRATE     70

#define UPPER1          75
#define LOWER1          0
```

```
#define UPPER2              70
#define LOWER2              0
#define MBASE          0x310
#define DBASE          0x300
#define CHANNEL        0x000

#define AORSEL0     control=(control    &    0x0fe);
outportb(MBASE+0,control)
#define AORSEL1     control=(control    |    0x001);
outportb(MBASE+0,control)
#define CONSTFOR    92
#define CONSTBAK    84
#define MAXSTEPS    7200
#define HOME        85
#define PHASE               2
#define EXCITATION          0
#define LOGIC               0
#define CLOCK               16
#define STANDSTILL          32
#define START               255
#define HIGH                100
#define ADLOW               200
#define ADHIGH              0

/*##################################################################
############*/

void display_screen(unsigned short int motorate, unsigned short int
volume, float molarity,
                unsigned int samplerate, unsigned short int r1,
unsigned short int r2, float x1, float x2,
                float y1, float y2, unsigned maxscale, unsigned int
minscale);

void clear_plots(unsigned short int r1, unsigned short int r2,
float x1, float x2,
                 float y1, float y2, unsigned int maxscale, unsigned int
minscale);

void initialize(unsigned short int phase, unsigned short int
excitation,
          unsigned short int logic, unsigned short int clock,
          unsigned short int standstill, unsigned short int start,

          unsigned short int high, unsigned short int adlow,
          unsigned short int adhigh);

void go_home(void);

float ad_conversion(unsigned int readingspersec);

void move_constant_speed(unsigned short int command, unsigned short
```

```
int rate,
                unsigned int increments);

struct filedata *f_recall(void);

void print_plot(int x1, int y1, int x2, int y2);

int round(double value);

union REGS inregs, outregs;

struct filedata {
     char fname[13];
     struct filedata *next;
     struct filedata *prev;
     } ;

/*****************************************************************
************/
/*****************************************************************
************/
/*****************************************************************
************/

main()
{

unsigned short int control=0x004, status;
unsigned int samplerate;
char sampleratestr[6];
unsigned short int volume;
char volumestr[3];
float molarity;
char molarstr[10];
u    n    s    i    g    n    e    d              i    n    t
x1s=0,y1s=0,x2s=0,y2s=0,prevx1s=0,prevy1s=0,prevx2s=0,prevy2s=0;

float temparray[1000];
int x;

unsigned char  dam_action=0, dam_mode=0, notcomplete=1,
          to_disk=0, abort=0, distilled_read=0,
          file_select=0, file_save=0, file_recall=0;

float smoothpress, smootharea, smoothsurftens, smoothpool;
unsigned int stot_count, scom_count, sexp_count;
struct filedata *ptr;
struct date rundate;
unsigned char recallaction, recallmode;
unsigned short int increment, recallsteps, recallvolume;
FILE *recall;
char datestr[15];
```

```
float
recallmotorspeed,recalldistilled,recallmg,recallpress,recallareap
ermol,
     recallsurftens,recallperct,recallmolarity;
u    n    s    i    g    n    e    d              i    n    t
recallplotpress,recallplotperct,recallplotarea,recallplotsurftens;

unsigned   int   oldrecallplotpress,   oldrecallplotperct,
oldrecallplotarea, oldrecallplotsurftens;

double maxarea, minarea;
unsigned int maxscale, minscale, x2range;

unsigned int sigdig=4;


unsigned short int rate;
unsigned int total, motorspeed;
long int j;
int gdevice=EGA, gmode=EGAHI;
unsigned int range1, range2;
float xint1, xint2, yint1, yint2;
unsigned int command;
int  plotst=0,  plotp=0,  plotarea=0,  plotperct=0,  oldplotp=0,
oldplotarea=0, oldplotst=0, oldplotperct=0;
float mg, surftens, pooleft, percentage, pressure, areapermol,
adjusted, distilled=0.0, pressdrop;
int position, i;
FILE *output=NULL, *printer=NULL;

unsigned int size, oldx, oldy, newx;
void * buffer;
unsigned short int steps;
char    stepstr[4],    diststr[4],    mgstr[4],    presstr[3],
motorspeedstr[4];

char c;
char filename[13];
int pa_vpl=265, pa_vpt=75, pa_vpr=638, pa_vpb=348;
int sp_vpl=1, sp_vpt=135, sp_vpr=258, sp_vpb=348;




getdate(&rundate);
initgraph(&gdevice,&gmode,"");

rate=82;
```

```
steps=20;
volume=25;
molarity=1.0;
samplerate=50;

total=MAXSTEPS/steps;
range1=UPPER1-LOWER1;
range2=UPPER2-LOWER2;
xint1=200.0/100.0;
maxarea=ceil(WORKING*MOLAREACONST)/((double)  volume  *  (double)
molarity);
maxscale=(int) ((ceil(maxarea/10.0))*10.0);
minarea=floor(COLLAR*MOLAREACONST)/((double)  volume  *  (double)
molarity);
minscale=(int) ((floor(minarea/10.0))*10.0);
x2range=maxscale-minscale;
xint2=300.0/(float)x2range;
yint1=150.0/(float) range1;
yint2=210.0/(float) range2;

BG;
FG2;

display_screen(rate,volume,molarity,samplerate,range1,range2,xint
1,xint2,yint1,yint2,maxscale,minscale);
HM;

oldx=63; oldy=102;
size=imagesize(63,102,83,112);
buffer=malloc(size);
getimage(63,102,83,112,buffer);


inregs.x.ax=0;
int86(MOUSE,&inregs,&outregs);
if(outregs.x.ax && 0) exit(1);


SM;

initialize(PHASE,EXCITATION,LOGIC,CLOCK,STANDSTILL,START,HIGH,ADL
OW,ADHIGH);

while(notcomplete)
{
     abort=0;
     inregs.x.ax=3;
     int86(MOUSE,&inregs,&outregs);
     if(outregs.x.bx & 1)
     {

          if(outregs.x.dx>89    &&    outregs.x.dx<105    &&
```

```
outregs.x.cx>166 &&
                outregs.x.cx<258 && dam_action==0)
                {
                dam_action=1;
                HM;
                setviewport(168,92,256,128,1); clearviewport();
                setviewport(0,0,639,349,1);
                line(166,110,258,110);
                FG3;
                outtextxy(195,95,"Smooth");
                outtextxy(185,115,"Increments");
                SM;
                delay(250);
                FG2;
                continue;
                }
           if(outregs.x.dx>105    &&    outregs.x.dx<130    &&
outregs.x.cx>166 &&
                outregs.x.cx<258 && dam_action==0)
                {
                dam_action=2;
                HM;
                setviewport(168,92,256,128,1); clearviewport();
                setviewport(0,0,639,349,1);
                line(166,110,258,110);
                FG3;
                outtextxy(195,95,"Smooth");
                outtextxy(185,115,"Increments");
                SM;
                delay(250);
                FG2;
                continue;
                }

                 if(outregs.x.dx>89    &&    outregs.x.dx<110    &&
outregs.x.cx>166 &&
                outregs.x.cx<258 && dam_action>0 && dam_mode==0)
                {
                dam_mode=1;
                FG2;
                HM;
                outtextxy(195,95,"Smooth");
                SM;
                continue;
                }

           if(outregs.x.dx>110    &&    outregs.x.dx<130    &&
outregs.x.cx>166 &&
                outregs.x.cx<258 && dam_action>0 && dam_mode==0)
                {
                dam_mode=2;
                HM;
```

```
                setviewport(168,112,256,128,1); clearviewport();
                setviewport(0,0,639,349,1);
                line(200,110,200,130);
                line(220,110,220,130);
                for(x=0;x<=10;x++)
                     {
                     line(185-x,115+x,185+x,115+x);
                     line(240-x,125-x,240+x,125-x);
                     }
                itoa(steps,stepstr,10);
                outtextxy(205,115,stepstr);
                SM;
                continue;
                }


          if(outregs.x.cx>=3    &&    outregs.x.cx<=143    &&
outregs.x.dx>102
                && outregs.x.dx<112)
                {
                setviewport(0,0,250,170,1);
                FG2;
                newx=outregs.x.cx;
                      HM;
                putimage(oldx,oldy,buffer,XOR_PUT);
                putimage(newx,oldy,buffer,COPY_PUT);
                rate=145-newx;

motorspeed=round((CLOCKFREQ/(rate*DEFAULTRATE))*STEPSIZE*WIDTH*10
0);
                itoa(motorspeed,motorspeedstr,10);
                setviewport(3,114,75,128,1); clearviewport();
                setviewport(0,0,250,170,1);
                outtextxy(50,115,motorspeedstr);
                oldx=newx;
                SM;
                continue;
                }

                 if(   outregs.x.dx>110   &&   outregs.x.dx<130   &&
dam_mode==2)
                {
                if(outregs.x.cx>168 && outregs.x.cx<196 && steps<50)

                     {
                     FG2;
                     steps++;
                          total=MAXSTEPS/steps;
                     itoa(steps,stepstr,10);
                     HM;
                     setviewport(201,111,219,128,1);
                     clearviewport();
```

```
                    setviewport(0,0,639,349,1);
                    outtextxy(205,115,stepstr);
                    SM;
                    delay(150);
                    continue;
                    }
               if(outregs.x.cx>220 && outregs.x.cx<256 && steps>1)

                    {
                    FG2;
                    steps--;
                              total=MAXSTEPS/steps;
                    itoa(steps,stepstr,10);
                    HM;
                    setviewport(201,111,219,128,1);
                    clearviewport();
                    setviewport(0,0,639,349,1);
                    outtextxy(205,115,stepstr);
                    SM;
                    delay(150);
                    continue;
                    }
               }

          if(outregs.x.dx>46 && outregs.x.dx<68)
          {
               if(outregs.x.cx>89 && outregs.x.cx<115)
                    {
                    if(volume<50)
                              {
                    volume++;
                    maxarea=ceil(WORKING*MOLAREACONST)/((double)
volume * (double) molarity);
                    maxscale=(int) ((ceil(maxarea/10.0))*10.0);
                    minarea=floor(COLLAR*MOLAREACONST)/((double)
volume * (double) molarity);
                    minscale=(int)  ((floor(minarea/10.0))*10.0);

                    x2range=maxscale-minscale;
                    xint2=(300.0/(float)x2range);
                    itoa(volume,volumestr,10);
                    HM;
                    setviewport(116,48,142,68,1);clearviewport();

                    setviewport(0,0,639,349,1);
                    outtextxy(125,55,volumestr);
                    SM; delay(150);
                    continue;
                    }
                    }
               if(outregs.x.cx>143 && outregs.x.cx<169)
                    {
```

```
                    if(volume>15)
                                {
                    volume--;
                    maxarea=ceil(WORKING*MOLAREACONST)/((double)
volume * (double) molarity);
                    maxscale=(int) ((ceil(maxarea/10.0))*10.0);
                    minarea=floor(COLLAR*MOLAREACONST)/((double)
volume * (double) molarity);
                    minscale=(int)  ((floor(minarea/10.0))*10.0);

                    x2range=maxscale-minscale;
                    xint2=(300.0/(float)x2range);
                    itoa(volume,volumestr,10);
                    HM;
                                setviewport(116,48,142,68,1);
clearviewport();
                    setviewport(0,0,639,349,1);
                    outtextxy(125,55,volumestr);
                    SM; delay(150);
                    continue;
                    }
                    }

          }


          if(outregs.x.dx>46 && outregs.x.dx<70)
          {
               if(outregs.x.cx>3    &&    outregs.x.cx<29    &&
samplerate<250)
                    {
                    samplerate+=10;
                    itoa(samplerate,sampleratestr,10);
                    HM;
                    setviewport(30,48,56,68,1);  clearviewport();

                    setviewport(0,0,639,349,1);
                    outtextxy(35,55,sampleratestr);
                    SM; delay(150);
                    continue;
                    }
               if(outregs.x.cx>57    &&    outregs.x.cx<83    &&
samplerate>10)
                    {
                    samplerate-=10;
                    itoa(samplerate,sampleratestr,10);
                    HM;
                                setviewport(30,48,56,68,1);
clearviewport();
                    setviewport(0,0,639,349,1);
                    outtextxy(35,55,sampleratestr);
                    SM; delay(150);
```

```
                    continue;
                    }
          }

          if(outregs.x.dx>46 && outregs.x.dx<70)
          {
               if(outregs.x.c: 175    &&    outregs.x.cx<201    &&
molarity<2.4)
                    {
                    molarity+=0.1;
                    maxarea=ceil(WORKING*MOLAREACONST)/((double)
volume * (double) molarity);
                    maxscale=(int) ((ceil(maxarea/10.0))*10.0);
                    minarea=floor(COLLAR*MOLAREACONST)/((double)
volume * (double) molarity);
                    minscale=(int)  ((floor(minarea/10.0))*10.0);

                    x2range=maxscale-minscale;
                    xint2=(300.0/(float)x2range);
                    gcvt(molarity,sigdig,molarstr);
                    HM;
                    setviewport(202,48,229,68,1);clearviewport();

                    setviewport(0,0,639,349,1);
                    outtextxy(210,55,molarstr);
                    SM; delay(250);
                    continue;
                    }
               if(outregs.x.cx>230    &&    outregs.x.cx<256    &&
molarity>0.5)
                    {
                    molarity-=0.1;
                    maxarea=ceil(WORKING*MOLAREACONST)/((double)
volume * (double) molarity);
                    maxscale=(int) ((ceil(maxarea/10.0))*10.0);
                    minarea=floor(COLLAR*MOLARLACONST)/((double)
volume * (double) molarity);
                    minscale=(int)  ((floor(minarea/10.0))*10.0);

                    x2range=maxscale-minscale;
                    xint2=(300.0/(float)x2range);
                    gcvt(molarity,sigdig,molarstr);
                    HM;
                              setviewport(202,48,229,68,1);
clearviewport();
                    setviewport(0,0,639,349,1);
                    outtextxy(210,55,molarstr);
                    SM; delay(250);
                    continue;
                    }
          }
```

```
                    if(outregs.x.cx>=15 && outregs.x.cx<=75 &&
                    outregs.x.dx >=1 && outregs.x.dx <= 25)
                    {
                    go_home();
                    HM;

clear_plots(range1,range2,xint1,xint2,yint1,yint2,maxscale,minsca
le);
                    setviewport(168,92,25c,128,1); clearviewport();

                    setviewport(0,0,639,349,1);
                         line(166,105,258,105);
                    FG3;
                    outtextxy(180,92,"Compression");
                    outtextxy(180,105,"Compression");
                    outtextxy(185,115,"Expansion");
                    FG2;
                    SM;
                    dam_action=0; dam_mode=0;
                    file_select=0; file_save=0; file_recall=0;
                    setviewport(407,7,523,18,1); clearviewport();

                    setviewport(0,0,639,349,1);
                    HM; outtextxy(450,8,"FILE"); SM;
                    continue;
                    }
     if(outregs.x.cx>=95 && outregs.x.cx<=155 && outregs.x.dx >=1
&&
          outregs.x.dx <= 25 && distilled_read && dam_action>0 &&

          dam_mode>0)
          {

          if(dam_mode==1)
               {
               HM;
               stot_count=0;
               scom_count=0;
               sexp_count=0;
               for(x=1;x<=dam_action;x++)
                    {
                    if(x==1) command=CONSTFOR;
                    else command=CONSTBAK;

move_constant_speed(command,rate,MAXSTEPS);
                    delay(200);
                    AORSEL1;
                    status=inportb(MBASE+1);
                    while((status & 4)==4)
```

```
                              {
temparray[stot_count]=ad_conversion(samplerate);
                              status=inportb(MBASE+1);
                              stot_count++;
                              if(x==1) scom_count++;
                              if(x==2) sexp_count++;
                              }
                         }


                              if(to_disk)
                         {
fprintf(output,"%d/%d/%d\n",rundate.da_mon,rundate.da_day,rundate
.da_year);
                              fprintf(output,"%d\n",dam_action);
                         fprintf(output,"%d\n",dam_mode);
                         fprintf(output,"%d\n",stot_count);
                         fprintf(output,"%d\n",motorspeed);
                         fprintf(output,"%4.1f\n",distilled);
                         fprintf(output,"%d\n",volume);
                         fprintf(output,"%4.1f\n",molarity);
                         }
                    for(x=0; x<stot_count; x++)
                         {
                         if(dam_action==2 && x>=scom_count)
                              {
                              i=sexp_count;
                              position=stot_count-x-1;
                              }
                         else {
                              i=scom_count;
                              position=x;
                              }

smoothpool=100.0-((float)position*(100.0/(float)(i-1)));

smootharea=(maxarea-((float)position*(maxarea-minarea)/(float)(i-
1)));
                         smoothpress=(distilled-temparray[x])*0.196;
                         smoothsurftens=temparray[x]*0.196;
                         x1s=30+(int)((100.0-smoothpool)*xint1);

x2s=40+(int)((smootharea-(float)minscale)*xint2);
                         y2s=230-(int)(smoothpress*yint2);
                         y1s=165-(int)(smoothsurftens*yint1);
                         if(x==0)
                              {
                              setviewport(3,157,256,346,1);
                              putpixel(x1s,y1s,1);
```

```
                              setviewport(267,92,626,346,1);
                              putpixel(x2s,y2s,1);
                              }
                         else
                              {

setviewport(3,157,256,346,1);
                              line(prevx1s,prevy1s,x1s,y1s);
                              setviewport(267,92,626,346,1);
                              line(prevx2s,prevy2s,x2s,y2s);
                              }
                         prevx1s=x1s; prevy1s=y1s;
                         prevx2s=x2s; prevy2s=y2s;
                         if(to_disk)
                              fprintf(output,"%d %4.1f %4.1f %4.1f %4.1f
%4.1f\n",

x,temparray[x],smoothpress,smootharea,smoothsurftens,smoothpool);

                              }
                    SM;
                    continue;
                    }

               if(dam_mode==2)
                    {
                                        if (to_disk)
                                             {

fprintf(output,"%d/%d/%d\n",rundate.da_mon,rundate.da_day,rundate
.da_year);
                              fprintf(output,"%d\n",dam_action);

fprintf(output,"%d\n",dam_mode);
                              fprintf(output,"%d\n",steps);
                              fprintf(output,"%d\n",motorspeed);
                              fprintf(output,"%4.1f\n",distilled);
                              fprintf(output,"%d\n",volume);
                              fprintf(output,"%3.1f\n",molarity);
                              }


for(j=0;j<=((dam_action>1)?(steps*2):(steps));j++)
                              {
                              if(j>steps)
                                   {
                                   position=(steps*2)-j;
                                   command=CONSTBAK;
                                   }
                              else
                                        {
                                   position=j;
```

```
                    command=CONSTFOR;
                    }

                if (j>0)

move_constant_speed(command,rate,total);
                mg=ad_conversion(samplerate);
                adjusted=distilled-mg;
                pressure=adjusted*0.196;
                        surftens=mg*0.196;


setviewport(3,157,256,346,1);
                plotst=(int) (surftens*yint1);

pooleft=WORKING-(STEPSIZE*(float) total*(float) position*WIDTH);

                percentage=(pooleft/WORKING)*100.0;
                plotperct=((100.0-percentage)*xint1);
                        if(j<1)
                    putpixel(plotperct+30,165-plotst,1);

                e   l   s   e
line(oldplotperct+30,165-oldplotst,plotperct+30,165-plotst);

                oldplotperct=plotperct;
                oldplotst=plotst;

                setviewport(267,92,626,346,1);
                plotp=(int) (pressure*yint2);
                areapermol=(((MAXSTEPS-((float)
p   o   s   i   t   i   o   n   *   (   f   l   o   a   t   )
total))*STEPSIZE*WIDTH)+COLLAR)*MOLAREACONST)/((double) volume *
(double) molarity);
                plotarea=(int)    ((areapermol-(float)
minscale)*xint2)+40;
                FG2;

                if(j<1)
                    putpixel(plotarea,230-plotp,1);
                else
line(oldplotarea,230-oldplotp,plotarea,230-plotp);
                        SM;

                if (to_disk)   fprintf(output,"%d  %4.1f
%   4   .   1   f       %   4   .   1   f       %   4   .   1   f
%4.1f\n",position,mg,pressure,areapermol,surftens,percentage);
                        if(j<steps*2)
                {
                do
                            {
                            inregs.x.ax=3;
```

```
int86(MOUSE,&inregs,&outregs);

if((outregs.x.bx&3)==3)
                              {
                              abort=1;
                              break;
                              }
                              }
                                        while   ((outregs.x.bx   &
2)!=2);
                         }
                         if(abort)
                                                  {
                                                  go_home();
                              HM;

clear_plots(range1,range2,xint1,xint2,yint1,yint2,maxscale,minsca
le);
                              SM;
                              break;
                              }

                         if(j<=steps)
                         {
                         mg=ad_conversion(samplerate);
                         pressdrop=(distilled-mg)*0.196;
                         if((pressure-pressdrop)>0)
                              {
                              setviewport(267,92,626,346,1);

setlinestyle(DOTTED_LINE,0,NORM_WIDTH);

line(plotarea,230-plotp,plotarea,230-plotp+(plotp-(int)
(pressdrop*yint2)));

setlinestyle(SOLID_LINE,0,NORM_WIDTH);
                              }
                         }
                                        oldplotp=plotp;
                         oldplotarea=plotarea;
                                        }
               continue;
               }
               file_select=0;    file_save=0;    file_recall=0;
to_disk=0;
               fclose(output);
               setviewport(407,7,523,18,1); clearviewport();
               setviewport(0,0,639,349,1);
               HM; outtextxy(450,8,"FILE"); SM;
          }
```

```
                if(outregs.x.cx>=265 && outregs.x.cx<=385 &&
                     outregs.x.dx >=1 && outregs.x.dx <= 25)
                     {
                                 delay(250);
                     setviewport(0,0,639,349,1);
                     FG2; HM; outtextxy(275,8,"DISTILLED:");

if((distilled=ad_conversion(samplerate))<-50.0) exit(5);
                                  itoa((int)distilled,diststr,10);

                     setviewport(340,8,384,19,1); clearviewport();

                     setviewport(0,0,639,349,1);
                     outtextxy(350,8,diststr); SM;
                     distilled_read=1;
                     continue;
                                 }

                         if(outregs.x.cx>=405 && outregs.x.cx<=525
&&
                     outregs.x.dx  >=1  &&  outregs.x.dx  <=  25  &&
!file_select)
                     {
                     if(to_disk) fclose(output);
                     to_disk=1;
                     HM;
                     setviewport(406,7,524,19,1); clearviewport();

                     setviewport(0,0,639,349,1);
                     line(450,7,450,19);
                     line(451,7,451,19);
                     FG2; outtextxy(415,8,"SAVE");
                     outtextxy(470,8,"RECALL"); SM;
                     delay(350);
                     file_select=1;
                     continue;
                     }


                if(outregs.x.cx>=406 && outregs.x.cx<450 &&
                     outregs.x.dx>=7 && outregs.x.dx<=19 &&
                     file_select && !file_save && !file_recall)
                          {
                          HM;

setviewpc   ;406,7,524,19,1); clearviewport();
                          setviewport(0,0,639,349,1);
                          SM;
                          for(i=0;i<13;i++) filename[i]=NULL;
                          HM; outtextxy(445,12,"--------"); SM;
                          i=0;
```

```
                        while(i<8)
                              {
                              if(i==0)    (if(isalpha(c=getch()))
filename[i++]=c;}
                              else    (if(isalnum(c=getch()))
filename[i++]=c;}
                              HM; outtextxy(445,5,filename); SM;

                              }
                        strncat(filename,".trh",4),
                        if((output=fopen(filename,"w"))==NULL)
                                    exit(2);
                        file_save=1;
                        continue;
                        }


                  if(outregs.x.cx>450 && outregs.x.cx<=524 &&
                        outregs.x.dx>=7 && outregs.x.dx<=19 &&
                        file_select && !file_recall && !file_save)
                              {
                              HM;

setviewport(406,7,524,19,1); clearviewport();
                              setviewport(0,0,639,349,1);
                              for(i=0;i<9;i++)
                                    {
                                    line(416-i,8+i,416+i,8+i);
                                    line(514-(8-i),8+i,514+(8-i),8+i);

                                    }
                              line(426,7,426,19);
                              line(504,7,504,19);

                              if ((ptr=f_recall())==NULL)
                                                  {
                                    outtextxy(430,8,"NO FILES");
                                    delay(250);
                                    SM;
                                    continue;
                                    }
                              else  outtextxy(430,8,ptr->fname); SM;
                              SM; delay(250);
                              file_recall=1;
                              continue;
                              }


                        if(outregs.x.cx>406 && outregs.x.cx<426 &&
                              outregs.x.dx>=7 && outregs.x.dx<=19 &&
                              file_recall && !file_save)
                              {
```

```
                                        if(ptr->prev!=NULL)
                                        {
                              ptr=ptr->prev;
                              HM;
                              setviewport(427,7,503,19,1);
clearviewport();
                              setviewport(0,0,639,349,1);
                              outtextxy(430,8,ptr->fname);
                              delay(250); SM;
                              }
                              continue;
                              }
                         if(outregs.x.cx>504 && outregs.x.cx<524 &&
                              outregs.x.dx>=7 && outregs.x.dx<=19 &&
                              file_recall && !file_save)
                              {
                                        if(ptr->next!=NULL)
                              {
                              ptr=ptr->next;
                              HM;
                              setviewport(427,7,503,19,1);
clearviewport();
                              setviewport(0,0,639,349,1);
                              outtextxy(430,8,ptr->fname);
                              delay(250); SM;
                              }
                              continue;
                              }
                         if(outregs.x.cx>426 && outregs.x.cx<514 &&
                              outregs.x.dx>=7 && outregs.x.dx<=19 &&
                              file_recall && !file_save)
                              {
                              HM;
                              if((recall=fopen(ptr->fname,"r"))==NULL)
exit(5);
                              fscanf(recall,"%*s",datestr[0]);
                              fscanf(recall,"%d",&recallaction);
                              fscanf(recall,"%d",&recallmode);
                              fscanf(recall,"%d",&recallsteps);
                              fscanf(recall,"%*d",&recallmotorspeed);

                              fscanf(recall,"%*f",&recalldistilled);
                              fscanf(recall,"%d",&recallvolume);
                              fscanf(recall,"%f",&recallmolarity);
                              if(recallvolume!=volume    ||
recallmolarity!=molarity)
                                   {
                                   volume=recallvolume;
                                   molarity=recallmolarity;

maxarea=ceil(WORKING*MOLAREACONST)/((double)  volume  *  (double)
molarity);
```

```
                                maxscale=(int)
((ceil(maxarea/10.0))*10.0);

minarea=floor(COLLAR*MOLAREACONST)/((double) volume * (double)
molarity);
                                minscale=(int)
((floor(minarea/10.0))*10.0);
                                x2range=maxscale-minscale;
                                xint2=300.0/(float)x2range;
                                itoa(volume,volumestr,10);

gcvt(molarity,sigdig,molarstr);
                                setviewport(116,48,142,68,1);
clearviewport();
                                setviewport(0,0,639,349,1);
                                outtextxy(125,55,volumestr);

setviewport(202,48,229,68,1); clearviewport();
                                setviewport(0,0,639,349,1);
                                outtextxy(210,55,molarstr);

clear_plots(range1,range2,xint1,xint2,yint1,yint2,maxscale,minsca
le);
                                }

                                if(recallmode==2)
                                     {

for(i=0;i<=((recallaction>1)?(recallsteps*2):(recallsteps));i++)

                                          {
                                          fscanf(recall,"%d %f %f %f
%f %f",

&increment,&recallmg,&recallpress,&recallareapermol,

&recallsurftens,&recallperct);

recallplotsurftens=(recallsurftens*yint1);

recallplotperct=((100-recallperct)*xint1);

recallplotpress=(recallpress*yint2);

recallplotarea=((recallareapermol-10)*xint2);

setviewport(3,157,256,346,1);
                                          if (i==0)
putpixel(recallplotperct+30,165-recallplotsurftens,1);
                                          else
line(oldrecallplotperct+30,165-oldrecallplotsurftens,recallplotpe
rct+30,165-recallplotsurftens);
```

```
setviewport(267,92,626,346,1);
                                        if (i==0)
putpixel(recallplotarea+40,230-recallplotpress,1);
                                        else
line(oldrecallplotarea+40,230-oldrecallplotpress,recallplotarea+4
0,230-recallplotpress);

oldrecallplotperct=recallplotperct;

oldrecallplotsurftens=recallplotsurftens;

oldrecallplotarea=recallplotarea;

oldrecallplotpress recallplotpress;
                                        }
                                    }

                                                if(recallmode==1)

                                    {
                                    for(i=0;i<recallsteps;i++)
                                                        {
                                        fscanf(recall,"%d %f %f %f
%f %f",

&increment,&recallmg,&recallpress,&recallareapermol,

&recallsurftens,&recallperct);

recallplotperct=30+(int)((100.0-recallperct)*xint1);

recallplotarea=40+(int)((recallareapermol-(float)minscale)*xint2);


recallplotpress=230-(int)(recallpress*yint2);

recallplotsurftens=165-(int)(recallsurftens*yint1);
                                        if(x==0)
                                            {

setviewport(3,157,256,346,1);

putpixel(recallplotperct,recallsurftens,1);

setviewport(267,92,626,346,1);

putpixel(recallplotarea,recallplotpress,1);
                                            }
                                        else
                                            {
```

```
setviewport(3,157,256,346,1);

line(oldrecallplotperct,oldrecallplotsurftens,recallplotperct,rec
allplotsurftens);

setviewport(267,92,626,346,1);

line(oldrecallplotarea,oldrecallplotpress,recallplotarea,recallpl
otpress);
                                                    }

oldrecallplotperct=recallplotperct;

oldrecallplotsurftens=recallplotsurftens;

oldrecallplotarea=recallplotarea;

oldrecallplotpress=recallplotpress;

                                              }
                                            }
                                  SM;
                                  fclose(recall);
                                  continue;
                             }


                                 if(outregs.x.cx>=545 && outregs.x.cx<=625
&&
                           outregs.x.dx >=1 && outregs.x.dx <= 25)
                           {
                           HM;
                           print_plot(pa_vpl,pa_vpt,pa_vpr,pa_vpb);
                           print_plot(sp_vpl,sp_vpt,sp_vpr,sp_vpb);
                           SM;
                           continue;
                           }


                      if(outregs.x.cx>=175 && outregs.x.cx<=235 &&
                           outregs.x.dx >=1 && outregs.x.dx <= 25)
                           notcomplete=0;
          }

}
fclose(output);
fclose(printer);
cleardevice();
closegraph();
exit(0);
}
```

```
/*****************************************************************
************/
/* * * * * * * * * * * * * * * * * * * * * * * *      FUNCTIONS
*********************************/
/*****************************************************************
************/

void display_screen(unsigned short int motorate, unsigned short int
volume, float molarity,
              unsigned int samplerate, unsigned short int r1,
unsigned short int r2, float x1, float x2,
              float y1, float y2, unsigned maxscale, unsigned int
minscale)
{
unsigned int x;
unsigned int motorspeed;
unsigned short int tick1=2, tick2=4;
char motorspeedstr[6], volstr[3], samplestr[6], molarstr[10];
unsigned int i, sigdig=3;
char axislabel[4];

settextstyle(SMALL_FONT,0,4);


line(29,47,29,68);
line(57,47,57,68);
line(115,47,115,68);
line(143,47,143,68);
line(201,47,201,68);
line(230,47,230,68);

for(x=0;x<=10;x++)
     {
     line(16-x,53+x,16+x,53+x);
     line(70-x,63-x,70+x,63-x);
     line(102-x,53+x,102+x,53+x);
     line(156-x,63-x,156+x,63-x);
     line(188-x,53+x,188+x,53+x);
     line(243-x,63-x,243+x,63-x);
     }

line(13,100,153,100);
line(1,113,164,113);
for(x=0;x<=140;x+=2)
     line(13+x,100-tick1,13+x,100);
for(x=0;x<=140;x+=10)
     line(13+x,100-tick2,13+x,100);
for(x=0;x<=10;x++)
     line(73-x,102+x,73+x,102+x);
```

```
motorspeed=(CLOCKFREQ/(motorate*DEFAULTRATE))*STEPSIZE*WIDTH*100;

itoa(motorspeed,motorspeedstr,10);
outtextxy(30,115,motorspeedstr);
outtextxy(80,115,"mm");outtextxy(100,113,"2");outtextxy(110,115,"
/sec");


for(x=0;x<=5;x++)
     {
     FG1;
     if((x<2)||(x>4)) FG2;
     rectangle(10+x,1+x,80-x,25-x);
        rectangle(90+x,1+x,160-x,25-x);
        rectangle(170+x,1+x,240-x,25-x);
     rectangle(260+x,1+x,390-x,25-x);
     rectangle(400+x,1+x,530-x,25-x);
     rectangle(540+x,1+x,630-x,25-x);
     }
FG2;
for(x=0;x<=1;x++)
        {
        rectangle(1+x,135+x,258-x,348-x);
     rectangle(265+x,75+x,638-x,348-x);

     rectangle(1+x,30+x,85-x,70-x);
     rectangle(87+x,30+x,171-x,70-x);
     rectangle(173+x,30+x,258-x,70-x);

     rectangle(1+x,75+x,164-x,130-x);
     rectangle(166+x,75+x,258-x,130-x);
     }

FG1;
for(x=0;x<15;x++)
     {
     line(267,x+77,636,x+77);
     line(3,x+137,256,x+137);

     line(3,x+77,162,x+77);
     line(168,x+77,256,x+77);

     line(3,x+32,83,x+32);
     line(89,x+32,169,x+32);
     line(175,x+32,256,x+32);
     }
FG2;
line(265,91,638,91);
line(1,151,258,151);
line(1,91,164,91);
line(166,91,258,91);
line(1,46,85,46);
```

```
line(87,46,171,46);
line(173,46,258,46);
line(166,105,258,105);

itoa(volume,volstr,10);
outtextxy(125,55,volstr);
itoa(samplerate,samplestr,10);
outtextxy(35,55,samplestr);
gcvt(molarity,sigdig,molarstr);
outtextxy(210,55,molarstr);
FG3;
outtextxy(180,92,"Compression");
outtextxy(180,105,"Compression");
outtextxy(185,115,"Expansion");
outtextxy(275,8,"DISTILLED:");
outtextxy(450,8,"FILE");
outtextxy(555,8,"PRINT PLOTS");

FG2;
outtextxy(30,8,"RESET");
outtextxy(110,8,"START");
outtextxy(195,8,"EXIT");

outtextxy(350,78,"Surface Pressure vs. Area per Molecule");
outtextxy(30,138,"Surface Tension vs. % Pool Area");

outtextxy(50,78,"Motor Speed");
outtextxy(175,78,"Motor Movement");

outtextxy(20,33,"Readings");
outtextxy(110,33,"Volume");
outtextxy(190,33,"Molarity");

setviewport(3,157,256,346,1);
clearviewport();
FG2;
line(20,15,20,165);
line(30,175,230,175);
for (i=0;i<=100;i+=2)
     line((i*x1)+30,175,(i*x1)+30,175-tick1);

for (i=0;i<=100;i+=10)
     {
     itoa(100-i,axislabel,10);
     outtextxy((i*x1)+30-5,177,axislabel);
     line((i*x1)+30,175,(i*x1)+30,175-tick2);
     setcolor(15);
     line((i*x1)+30,165,(i*x1)+30,15);
     FG2;
     }

for (i=0;i<=r1;i+=15)
```

```
      {
      setcolor(15);
      line(30,165-(i*y1),230,165-(i*y1));
      FG2;
      line(20,165-(i*y1),20+tick2,165-(i*y1));
      itoa(i,axislabel,10);
      outtextxy(5,165-(i*y1)-5,axislabel);
      }

for (i=0;i<=r1;i+=1)
      line(20,165-(i*y1),20+tick1,165-(i*y1));


setviewport(267,92,626,346,1);
clearviewport();

line(32,20,32,230);
line(40,240,(int)((float)(maxscale-minscale)*x2)+40,240);
for (i=0;i<=(maxscale-minscale);i++)

line((int)((float)i*x2)+40,240,(int)((float)i*x2)+40,240-tick1);

for (i=0;i<=maxscale-minscale;i+=10)
      {
         setcolor(15);
      line((int)((float)i*x2)+40,230,(int)((float)i*x2)+40,20);
      FG2;

line((int)((float)i*x2)+40,240,(int)((float)i*x2)+40,240-tick2);

      itoa(i+minscale,axislabel,10);
      outtextxy((int)((float)i*x2)+40-5,242,axislabel);

      }

for (i=0;i<=r2;i++)
      line(32,230-(i*y2),32+tick1,230-(i*y2));

for (i=0;i<=r2;i+=10)
      {
      line(32,230-(i*y2),32+tick2,230-(i*y2));
      itoa(i,axislabel,10);
      outtextxy(17,230-(i*y2)-5,axislabel);
         setcolor(15);

line(40,230-((int)((float)i*y2)),40+(int)((float)(maxscale-minsca
le)*x2),230-(int)((float)i*y2));
      FG2;
      }
setviewport(0,0,639,349,1);
}
```

```
/*****************************************************************
************/
void initialize(unsigned short int phase, unsigned short int
excitation,
          unsigned short int logic, unsigned short int clock,
          unsigned short int standstill, unsigned short int start,

          unsigned short int high, unsigned short int adlow,
          unsigned short int adhigh)
{
unsigned short command, control=0x004, status;

outportb(MBASE+3,0);
delay(200);
control=0x004;
command=phase+excitation+logic+clock+standstill;
AORSEL1;
do
     status=inportb(MBASE+1);
while((status & 4)==4 || (status & 2)==2);
outportb(MBASE+1,command);
do
     status=inportb(MBASE+1);
while((status & 2)==2);
AORSEL0; outportb(MBASE+1,start);
AORSEL1;
do
     status=inportb(MBASE+1);
while((status & 2)==2);
AORSEL0; outportb(MBASE+1,high);
AORSEL1;
do
     status=inportb(MBASE+1);
while((status & 4)==4 || (status & 2)==2);
AORSEL0; outportb(MBASE+1,adlow);
AORSEL1;
do
     status=inportb(MBASE+1);
while((status & 2)==2);
AORSEL0; outportb(MBASE+1,adhigh);
}
/*****************************************************************
************/

void go_home(void)
{
unsigned short int rate=4, status, control=0x004;

AORSEL1;
do
     status=inportb(MBASE+1);
while((status & 4)==4 || (status & 2)==2);
```

```
outportb(MBASE+1,HOME);
do
     status=inportb(MBASE+1);
while((status & 2)==2);
AORSEL0;
outportb(MBASE+1,DEFAULTRATE); delay(100);
outportb(MBASE+6,rate); delay(100);
AORSEL1;
do
     status=inportb(MBASE+1);
while((status & 4)==4);

}

/*****************************************************************
************/

float ad_conversion(unsigned int readingspersec)
{
int dword, out_freq, i;
unsigned short int hibyte, lobyte, status, rate=1000;
unsigned long int intel_8254=2386400;
float min, max, range, average, sum=0.0, mgram[250], yint, xint;

int newx, newy, oldx, oldy, plot_average, plot_max, plot_min;
char astr[6], hstr[6],lstr[6];

out_freq=intel_8254/rate;
hibyte=(int) (out_freq/256);
lobyte=out_freq-(hibyte*256);

outportb(DBASE+2,CHANNEL);
outportb(DBASE+7,0xb4);
outportb(DBASE+6,lobyte);
outportb(DBASE+6,hibyte);

do
     status=inportb(DBASE+2);
while((status & 16)!=16) ;

for(i=0;i<readingspersec;i++)
     {
     do
          status=inportb(DBASE+2);
     while((status & 8)!=8) ;

     outportb(DBASE+1,0);
     outportb(DBASE+2,0);
     while(inportb(DBASE+2)>=128) ;
     dword=((inportb(DBASE+1)*16)+(inportb(DBASE+0)/16))-2048;
        mgram[i]=((((float) dword)*5.0)/2048.0)*100.0;
        if(i==0)
```

```
            {
          min=mgram[i];
          max=mgram[i];
          }
     if(mgram[i] < min) min=mgram[i];
     if(mgram[i] > max) max=mgram[i];
     sum+=mgram[i];
     }


setviewport(290,30,600,70,1);
HM; clearviewport();
range=max-min;
yint=40.0/range;
xint=250.0/(float)readingspersec;
for(i=0;i<readingspersec;i++)
     {
     newx=(int)(xint*(float)i)+30;
     newy=(int)(40.0-((mgram[i]-min)*yint));
        if(i==0) putpixel(newx,newy,0);
     else     line(oldx,oldy,newx,newy);
     oldx=newx;
     oldy=newy;
     }

average=sum/(float)readingspersec;
plot_average=(int)((average-min)*yint);
plot_min=(int)((min-min)*yint);
plot_max=(int)((max-min)*yint);
itoa((int)average,astr,10);
itoa((int)max,hstr,10);
itoa((int)min,lstr,10);
FG3;
line(30,40-plot_average,280,40-plot_average);
outtextxy(5,40-plot_average-5,astr);
FG2;
line(30,40-plot_min,280,40-plot_min);
outtextxy(285,40-plot_min-10,lstr);
line(30,40-plot_max,280,40-plot_max);
outtextxy(285,40-plot_max,hstr);
SM;
setviewport(0,0,639,349,1);
return(average);
}

/*****************************************************************
************/

void move_constant_speed(unsigned short int command, unsigned short
int rate,
                unsigned int increments)
{
```

```
unsigned short int status, control=0x004;
unsigned short int pulse1, pulse2, pulse3=0;


AORSEL1;
do
     status=inportb(MBASE+1);
while((status & 4)==4 || (status & 2)==2);
outportb(MBASE+1,command);
do
     status=inportb(MBASE+1);
while((status & 2)==2);
AORSEL0;
outportb(MBASE+1,DEFAULTRATE);
outportb(MBASE+6,rate);
AORSEL1;
do
     status=inportb(MBASE+1);
while((status & 2)==2);
pulse2=increments/256;
pulse1=increments-(pulse2*256);
AORSEL0; outportb(MBASE+1,pulse1);
AORSEL1;
do
     status=inportb(MBASE+1);
while((status & 2)==2);
AORSEL0; outportb(MBASE+1,pulse2);
AORSEL1;
do
     status=inportb(MBASE+1);
while((status & 2)==2);
AORSEL0; outportb(MBASE+1,pulse3);
delay(100);
if(increments!=MAXSTEPS)
     {
     AORSEL1;
     do
          status=inportb(MBASE+1);
     while((status & 4)==4);
     }
}

/*****************************************************************
************/

int round(double value)
{
double x, *iptr;

iptr=(double *) malloc(sizeof(double));
return( (x=modf(value,iptr)) > 0.5 ? ( (int) value)+1 : (int)
value);
```

```
}

/*****************************************************************
************/

void clear_plots(unsigned short int r1, unsigned short int r2,
float x1, float x2, float y1, float y2, unsigned int maxscale,
unsigned int minscale)
{
unsigned int i;
unsigned short int tick1=2, tick2=4;
char axislabel[4];


HM;
setviewport(33,172,233,322,1);
clearviewport();
setviewport(3,157,256,346,1);
for (i=0;i<=100;i+=10)
     {
     setcolor(15);
     line((i*x1)+30,165,(i*x1)+30,15);
     FG2;
     }

for (i=0;i<=r1;i+=15)
     {
     setcolor(15);
     line(30,165-(i*y1),230,165-(i*y1));
     FG2;
     }

setviewport(305,110,626,346,1);
clearviewport();
setviewport(267,92,626,346,1);
line(40,240,(int)((float)(maxscale-minscale)*x2)+40,240);
for (i=0;i<=(maxscale-minscale);i++)

line((int)((float)i*x2)+40,240,(int)((float)i*x2)+40,240-tick1);


for (i=0;i<=(maxscale-minscale);i+=10)
     {
        setcolor(15);
     line((int)((float)i*x2)+40,230,(int)((float)i*x2)+40,20);
     FG2;

line((int)((float)i*x2)+40,240,(int)((float)i*x2)+40,240-tick2);

     itoa(i+minscale,axislabel,10);
     outtextxy((int)((float)i*x2)+40-5,242,axislabel);
     }
```

```
for (i=0;i<=r2;i+=10)
     {
        setcolor(15);

line(40,230-(i*y2),40+(int)((float)(maxscale-minscale)*x2),230-(i
*y2));
     FG2;
     }

setviewport(290,30,600,70,1); clearviewport();
setviewport(0,0,639,349,1);
SM;
}

/*****************************************************************
************/
struct filedata *f_recall(void)
{
struct filedata *p, *first, *last;
struct ffblk fblk;
int complete;

if((p=(struct filedata *) malloc(sizeof(struct filedata)))==NULL)
exit(3);
first=p;
p->prev=NULL;
complete=findfirst("*.trh",&fblk,0);
if(complete!=0) return(NULL);
else
{
while(complete==0)
     {
     strcpy(p->fname,fblk.ff_name);
     if((p->next=(struct    filedata    *)    malloc(sizeof(struct
filedata)))==NULL) exit(3);
     last=p;
     p=p->next;
     p->prev=last;
     complete=findnext(&fblk);
     }

last->next=NULL;
return(first);
}
}

/*****************************************************************
************/

void print_plot(int x1, int y1, int x2, int y2)

{
```

```
FILE      *printer;
unsigned int   i, j, k, n1, n2, s, pc, bc;
unsigned char  prn_byte[640], bitvalue;
unsigned int   width, height;
unsigned int   prnheadpass, bytesperline;


if((printer=fopen("PRN","w"))==NULL) exit(5);
setviewport(0,0,639,349,1);
bc=getbkcolor();
width=(x2-x1)+1;
height=(y2-y1)+1;
(   (   h   e   i   g   h   t   %   8   )   >   0   )   ?
(prnheadpass=(int)(height/8)+1):(prnheadpass=(int)(height/8));
(   (   w   i   d   t   h   %   8   )   >   0   )   ?
(bytesperline=(int)(width/8)+1):(bytesperline=(int)(width/8));

n1=width % 256;
n2=(int) (width/256);
s=8;
fprintf(printer,"%c%c",'\033','@');
fprintf(printer,"%c%c%c",'\033','A',s);

for(i=0;i<prnheadpass;i++)
     {
     for(j=0;j<640;j++)
          prn_byte[j]=0;
     bitvalue=128;
     for(j=0;j<8;j++)
          {
          for(k=0;k<width;k++)
               {
               pc=getpixel(k+x1,(i*8)+j+y1);
               if(pc==PLOTTING || pc==GRID) prn_byte[k]|=bitvalue;

               }
          bitvalue/=2;
          }
        fprintf(printer,"%c%c%c%c%c",'\033','*','5',n1,n2);
     for(k=0;k<(bytesperline*8);k++)
          fprintf(printer,"%c",prn_byte[k]);
     fprintf(printer,"\n");
     }

fprintf(printer,"\n\n");
fprintf(printer,"%c%c",'\033','@');
fclose(printer);
}


^Z
```

APPENDIX C

Programme IMAGEPRN / C language
prints frame grabbed and processed digital images in dot matrix printers. (written by Carl Boland)

```
#include <conio.h>
#include <alloc.h>
#include <stdio.h>

#define    ESC       '\033'
#define    INIT           fprintf(printer,"%c%c",ESC,'@')
#define    LSPACE         fprintf(printer,"%c%c%c",ESC,'A',s)
#define    PLOTMODE fprintf(printer,"%c%c%c%c%c",ESC,'*','5',n1,n2)

#define  CUTOFF           0


main()
{

typedef struct {
     unsigned int colormaporigin;
     unsigned int colormaplength;
     unsigned char colormapentrysize;
     } colormapspec;

typedef struct {
     unsigned int xorigin;
     unsigned int yorigin;
     unsigned int width;
     unsigned int height;
     unsigned char pixelsize;
     unsigned char descriptor;
     } imagespec;

typedef struct  {
     unsigned char idfieldsize;
     unsigned char colormaptype;
     unsigned char imagetype;
     colormapspec clmpspec;
     imagespec imgspec;
     unsigned char *imageidfield;
     unsigned char *colormapdata;
     unsigned char imagedata;
     } targafile;
```

```
register int i, j, k;
unsigned char *p;
targafile tfile;
unsigned int prnheadpass;
FILE *input, *printer;
unsigned short  prn_byte[512];
unsigned char  n1, n2, s;
char filename[80];
unsigned char input_line[512];



clrscr();
cprintf("Enter Targa Filename: ");
cscanf("%s",filename);
input=fopen(filename,"rb");

/*****************************************************************
************/

fread(&tfile.idfieldsize,sizeof(unsigned char),1,input);
fread(&tfile.colormaptype,sizeof(unsigned char),1,input);
fread(&tfile.imagetype,sizeof(unsigned char),1,input);
fread(&tfile.clmpspec.colormaporigin,sizeof(unsigned int),1,input);

fread(&tfile.clmpspec.colormaplength,sizeof(unsigned int),1,input);

fread(&tfile.clmpspec.colormapentrysize,sizeof(unsigned
char),1,input);
fread(&tfile.imgspec.xorigin,sizeof(unsigned int),1,input);
fread(&tfile.imgspec.yorigin,sizeof(unsigned int),1,input);
fread(&tfile.imgspec.width,sizeof(unsigned int),1,input);
fread(&tfile.imgspec.height,sizeof(unsigned int),1,input);
fread(&tfile.imgspec.pixelsize,sizeof(unsigned char),1,input);
fread(&tfile.imgspec.descriptor,sizeof(unsigned char),1,input);

tfile.colormapdata=(unsigned    char    *)
calloc((tfile.clmpspec.colormaplength*tfile.clmpspec.colormapentr
ysize/8),sizeof(unsigned char));
p=tfile.colormapdata;
for(i=0;i<tfile.clmpspec.colormaplength;i++)
     for(j=0;j<(tfile.clmpspec.colormapentrysize)/8;j++)
          fread(p++,sizeof(unsigned char),1,input);

/*****************************************************************
************/


cprintf("\n\n\nID Field Size: %d\nColormap Type: %d\nImage Type:
%d\n\n",
     tfile.idfieldsize,tfile.colormaptype,tfile.imagetype);
```

```
cprintf("Colormap Origin: %d\nColormap Length: %d\nColormap Entry
Size: %d\n\n",

tfile.clmpspec.colormaporigin,tfile.clmpspec.colormaplength,tfile
.clmpspec.colormapentrysize);

cprintf("X-Origin: %d\nY-Origin: %d\nWidth: %d\nHeight: %d\nPixel
Size: %d\nDescriptor: %d\n\n",

tfile.imgspec.xorigin,tfile.imgspec.yorigin,tfile.imgspec.width,t
file.imgspec.height,tfile.imgspec.pixelsize,tfile.imgspec.descrip
tor);


n1=(unsigned char)(tfile.imgspec.width % 256);
n2=(unsigned char)(tfile.imgspec.width / 256);
s=8;

((tfile.imgspec.height%8)>0)?(prnheadpass=(unsigned
int)(tfile.imgspec.height/8,+1):(prnheadpass=(unsigned
int)tfile.imgspec.height/8);

printer=fopen("PRN","w");

INIT;
LSPACE;

for(i=0;i<prnheadpass;i++)
     {
     for(j=0;j<512;j++)
          prn_byte[j]=0;

     for(k=0;k<8;k++)
          {
          fread(input_line,sizeof(unsigned
char),tfile.imgspec.width,input);
             for(j=0;j<tfile.imgspec.width;j++)
               {
               if(k==7)   {if(input_line[j]>CUTOFF)
prn_byte[j]=(prn_byte[j]|1);  continue;}
               if(k==6)   {if(input_line[j]>CUTOFF)
prn_byte[j]=(prn_byte[j]|2);  continue;}
               if(k==5)   {if(input_line[j]>CUTOFF)
prn_byte[j]=(prn_byte[j]|4);  continue;}
               if(k==4)   {if(input_line[j]>CUTOFF)
prn_byte[j]=(prn_byte[j]|8);  continue;}
               if(k==3)   {if(input_line[j]>CUTOFF)
prn_byte[j]=(prn_byte[j]|16); continue;}
               if(k==2)   {if(input_line[j]>CUTOFF)
prn_byte[j]=(prn_byte[j]|32); continue;}
               if(k==1)   {if(input_line[j]>CUTOFF)
```

```
prn_byte[j]=(prn_byte[j]|64);  continue;}
                if(k==0)    {if(input_line[j]>CUTOFF)
prn_byte[j]=(prn_byte[j]|128); continue;}
                }
           }
           PLOTMODE;
           for(j=(tfile.imgspec.width-1);j>=0;j--)
                fprintf(printer,"%c",prn_byte[j]);
           fprintf(printer,"\n");

     }

INIT;

fclose(printer);
fclose(input);
clrscr();
}
```

APPENDIX D

Thermistor type - GB41P2 (Fenwell Electronics A1)

$$1/T = a + b \ln R + c (\ln R)^3$$

$a = 2.77271 * 10^{-3}$

$b = 2.5688 * 10^{-4}$

$c = 4.5 * 10^{-7}$

R = resistance in Kilohms

T = Temperature in Kelvin

APPENDIX E

Nag K., Rich N. and Keou'n K.M.W. Epifluorescence microscopic observation of dynamic changes during lateral phase transition of DPPC monolayers at the air water interface. Abs. No.361 Proceedings of 33 rd CFBS (Halifax) **1990.**

Nag K., Rich N. and Keough K.M.W. Observation of lateral phase transition in monolayers of Dipalmitoyl phosphatidylcholine. Abst.No. PP4 Congress of Canadian Association of Physicist. (St.John's) **1990.**

Nag K., Rich N. and Keough K.M.W. An epifluorescence microscopic surface balance for characterization of phospholipid monolayer architecture during pressure induced phase transitions. Abs.No. P3.1.11. 10 th International Biophysics Congress. (Vancouver) **1990**

Nag K. and Keough K.M.W. Dynamics of phospholipid domain formation in monolayers as studied by epifluorescence microscopy, Abs. No. P-Th-227. 20 th FEBS Meeting. (Budapest) **1990.**

Nag K., Boland C., Rich N.H. and Keough K.M.W. Design and construction of an epifluorescence microscopic surface balance for the study of lipid monolayer phase transition. Rev.Sci.Instr.(AIP) 61:3425 **1990.**